Positron-Emitting Radiopharmaceuticals

3

Piero A. Salvadori, Elena Filidei, and Assuero Giorgetti

Contents

Learning Objectives

- Provide an overview of radionuclides with relevant applications in PET.
- Define structure-activity relationships and how radiolabeling can induce molecular/biological perturbation.
- Describe routes of administration and their impact on biodistribution.
- Describe the impact of molecular size, polarity, and functional groups on distribution.
- Summarize key issues on handling positron-emitting radionuclides (shielding) and radiochemical synthesis.
- Explain main advantages and issues regarding ^{11}C-labeled radiopharmaceuticals.
- Provide basic information on ^{68}Ga-labeled radiopharmaceuticals and the ^{68}Ge/^{68}Ga generator.
- Provide basic information on the synthesis and use of ^{124}I-labeled radiopharmaceuticals.
- Provide information on the rationale for using positron-emitting radiopharmaceuticals in different pathophysiologic conditions according to the biologic/metabolic event targeted by different classes of imaging agents.

P. A. Salvadori (✉)
PET/Cyclotron Unit, CNR Institute of Clinical Physiology, Pisa, Italy
e-mail: salvador@ifc.cnr.it

E. Filidei · A. Giorgetti
Nuclear Medicine Unit, Fondazione CNR/Regione Toscana Gabriele Monasterio, Pisa, Italy

D. Volterrani et al. (eds.), *Nuclear Medicine Textbook*, https://doi.org/10.1007/978-3-319-95564-3_3

3.1 Section I: Positron-Emitting Radionuclides and Labeling Strategies

Imaging with positron emission tomography (PET) is based on the detection of the annihilation radiation. Annihilation radiation occurs when matter is converted to energy. This phenomenon occurs when a negatively charged electron (negatron) and a positively charged electron (positron, emitted in the course of decay of a positron-emitting radionuclide) come in contact. The resulting positron/negatron (matter) disappears and is replaced by two gamma photons (energy). While electrons are basic constituents of our physical world, positrons (or antielectrons) are very rare. They are produced by the decay of neutron-deficient nuclei, which are not naturally occurring.

The development of the cyclotron in the 1930s demonstrated that it is possible to generate new elements from a target with a selected composition of nuclei. The cyclotron is the equivalent of the alchemists' "philosophical stone," since it can transmute one element into a different one, thus facilitating separation of the new nucleus from the target matrix. It also allows the production of neutron-deficient nuclei, i.e., those prone to positron decay.

In the early 1940s, ^{11}C, ^{13}N, and ^{18}F (i.e., the major modern players for PET imaging) (Table 3.1) were the first radionuclides produced with a cyclotron in the form of simple compounds to be used as in vivo tracers. However, their short physical half-life and the poor detection capability for the high-energy 511 keV annihilation photons (scintillation/photomultiplier detectors were not invented until 1947) limited their clinical use.

Meanwhile, other radionuclides, such as ^{3}H, ^{14}C, and ^{131}I (and later on ^{99m}Tc), became more widely available, thus facilitating the use of radioactive compounds to trace biochemical processes in vivo. These tracer studies demonstrated that many biochemical processes occur in vivo at a very fast rate, so that the limitation of short physical half-life might not be as crucial as expected. In parallel, more efficient scintillation detectors and coincidence detection electronics were developed, which improved detection sensitivity and spatial resolution.

3.1.1 Positron-Emitting Radionuclides and Basic Chemistry

PET radiochemistry entails production of the β^+-emitting radionuclides and purification and incorporation of the β^+-emitting radionuclide in diagnostic radiopharmaceutical.

Three major features of the radionuclide depend on the methodology used: (1) radionuclide chemical form(s), (2) specific radioactivity, and (3) radionuclidic and/or radiochemical impurities. It is now possible to rely on a number of radiochemical building blocks, based on the "physiological" radionuclides (Table 3.2). Several radionuclides (Table 3.3) are currently being considered for further developments to address innovations in theragnostics (diagnostic and therapeutic use of the same construct).

Table 3.1 The "physiological" positron-emitting radionuclides

Radionuclide	Half-life (min)	Decay	Specific radioactivity (GBq/μmol)		Positron	
			Theoretical	Practical	E_{max} (keV)	Range (H_2O) mm
Oxygen-15	2.05	β^+ 100%	3.39×10^6	n.a.	1720	8.2
Nitrogen-13	10.0	β^+ 100%	6.96×10^5	<15	1190	5.4
Carbon-11	20.4	β^+ 99%	3.43×10^5	110–2600	970	4
Fluorine-18	109.7	β^+ 97%	6.34×10^4	18–740	635	2.4

Table 3.2 Nuclear reactions and most common chemical forms of positron-emitting radionuclides

Radionuclide	Nuclear reaction	Target composition	Particle energy (MeV)	Main chemical form(s)
Oxygen-15	$^{15}N(p,n)^{15}O$	$^{15}N_2$ (+O_2 trace)	10	$^{15}O_2$
	$^{14}N(d,n)^{15}O$	$^{15}N_2$ (+O_2 1–3%)	8	
		$^{15}N_2$ (+CO_2 1–3%)	8	$C^{15}O_2$
Nitrogen-13	$^{16}O(p,\alpha)^{13}N$	$H_2{}^{16}O$	11–18	$^{13}NO_2$ + $^{13}NO_3$
		$H_2{}^{16}O$ + ethanol	11–18	$^{13}NH_3$
Carbon-11	^{14}N $(p,\alpha)^{11}C$	$^{14}N_2$ (+O_2 trace)	10–13	$^{11}CO_2$ + ^{11}CO
		$^{14}N_2$ (+2–5% H_2)	10–13	$^{11}CH_4$
Fluorine-18	$^{18}O(p,n)^{18}F$	$H_2{}^{18}O$	7–18	$H^{18}F$
	$^{20}Ne(d,\alpha)^{18}F$	^{20}Ne + 0.5–1% $^{19}F_2$	8–14	$^{18}F_2$ ($+^{19}F_2$)

Formalism adopted to describe nuclear reactions: A(x,y)B, where *A*, *target nuclide*; *B*, *produced nuclide*; *x*, *bombarding particle*; *y*, *emitted particle(s)*

Table 3.3 Radionuclides "of interest" for PET other than ^{11}C, ^{13}N, ^{15}O, and ^{18}F

Radionuclide	Half-life	β decay mode	Theoretical specific radioactivity (GBq/μmol)	Principal emissions (keV)		Source
				E_{max} β+	EC main peaks	
Rubidium-82	1.3 min	β+ 96%	5.4×10^6	3350 2580	776	Generator $^{82}Sr/^{82}Rb$
Copper-62	9.8 min	β+ 98%	7.1×10^5	2930	1172	Generator $^{62}Zn/^{62}Cu$
Technetium-94m	52 min	β+ 70%	1.3×10^5	2500	871	Cyclotron $^{94}Mo(p,n)^{94m}Tc$
Gallium-68	68 min	β+ 89%	1.0×10^5	1900	1077	Generator $^{68}Ge/^{68}Ga$
Iodine-120	1.4 h	β+ 56%	8.3×10^4	4000	1523 640	Cyclotron $^{120}Te(p,n)^{120}I$
Copper-61	3.3 h	β+ 62%	3.5×10^4	1150 1200	940 560	Cyclotron $^{61}Ni(p,n)^{61}Cu$
Copper-64	12.7 h	β+ 18% β− 37%	9.1×10^3	657	1346	Cyclotron $^{64}Ni(p,n)^{64}Cu$
Yttrium-86	14.7 h	β+ 34%	7.9×10^3	1220 1578	1077 628–443	Cyclotron $^{86}Sr(p,n)\ ^{86}Y$
Zirconium-89	78.4 h	β+ 23%	1.5×10^3	902	909	Cyclotron $^{89}Y(p,n)^{89}Zr$
Iodine-124	4.2 d	β+ 23%	1.2×10^3	1532 2135	603 1691	Cyclotron $^{124}Te(p,n)^{124}I$

β+, positron; EC, electron capture; d, days; h, hours; min, minutes

^{68}Ga opened the way for PET generator products ($^{68}Ge/^{68}Ga$ generators). In addition to other properties of radionuclides used for PET, Table 3.1 reports for each radionuclide their theoretical and practical specific activity (SA), i.e., the activity associated to the number of atoms or molecules of interest; SA is expressed as Bq/mol, more commonly as GBq/μmol for practical reasons. SA is primarily related to the isotopic dilution of the radionuclide by isotopes of the same element, and it is influenced by chemical factors (e.g., abundance, natural occurrence, and distribution of other isotopes) associated both with radionuclide production and with their handling. SA may refer to a radiolabeled precursor as well as to a final product, and it declines with time elapsed after production—due to radionuclide decay.

Any radiolabeled product used in vivo should have a specific activity suitable to the intended scope, i.e., consistent with the target concentration in vivo; due consideration should also be paid to toxicity or biological activity of the radiolabeled compound, especially concerning high-potency agonists or antagonists.

A few radionuclides can be employed clinically in their elemental form, such as sodium [^{18}F]fluoride, sodium [^{124}I] iodide, or [^{15}O]oxygen. For most applications they are bound to a molecular frame that confers to the radiopharmaceutical the intended function in vivo. The chemical form of the radionuclide and its features as a chemical element influence the chemical reactions through which this "precursor" is incorporated into any given radiopharmaceutical. For instance, ^{18}F can be produced either as fluoride salt ([^{18}F]NaF) or as elemental fluorine ([^{18}F]F_2). These two chemical forms, or precursors, have completely different chemistries (see further below in this chapter).

By definition, radionuclides maintain the chemical feature of the element they belong to. Therefore, while the chemistry of C, O, N, and F is based on the formation of covalent bonds, alternative bonds may be considered for other elements. For instance, metals can form nonstoichiometric compounds called coordination complexes, in which they constitute the core of the complex and stably bind suitable chelating groups (ligands) in their coordination sphere. These coordinate covalent bonds are the basis for technetium chemistry as well as for β+-emitting metals, such as ^{68}Ga, ^{89}Zr, and ^{64}Cu. In order to form stable coordination complexes, a strict relationship must exist between the element (ionic radius, electronic configuration) and the ligand(s) (size of the molecule, number and nature of the coordinating groups in the molecule).

Key Learning Points

- Positron-emitting radionuclides are employed for diagnostic imaging applications based on the emission of two 511 keV monochromatic photons following the positron-negatron annihilation event.
- Cyclotrons are used to produce chemical forms containing positron-emitting radionuclides.
- Radiolabeled chemical forms (radioactive precursors) can be used to prepare more complex radiolabeled molecules.
- Specific activity indicates the radioactivity per number of atoms or molecules of the element or radiolabeled compound under consideration.

3.1.2 Substrate Characteristics and Radiolabeling Strategies

The clinical development of PET scanners began in earnest in 1976 with the demonstration that the glucose analog 2-[^{18}F]fluoro-2-deoxy-D-glucose ([^{18}F]FDG) was safe and effective for imaging glucose utilization in the human brain. [^{18}F]FDG was conceived as an in vivo extension of Sokoloff's inspiring experiments on measurement of glucose metabolic rate using 2-deoxy-D-[^{14}C]glucose and tissue autoradiography.

The introduction of the ^{18}F atom in position 2 of the glucose molecule, replacing the naturally occurring hydroxyl group, is the key point for the synthesis of [^{18}F]FDG (Fig. 3.1). To achieve this a synthesis pathway was designed, which utilized a labeling-prone substrate (or "cold precursor").

The design of a radiolabeling strategy (Fig. 3.2) goes beyond the chemistry issues and must consider the intended use of the tracer. Fundamental requirements in the radiochemistry process for the synthesis of PET radiotracers are:

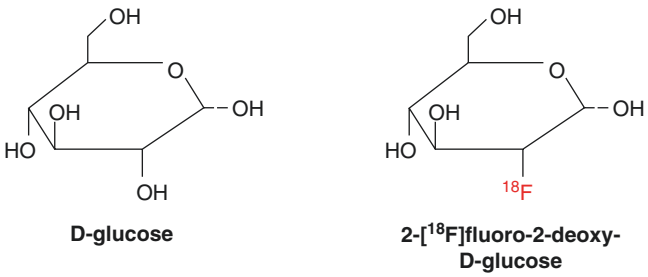

Fig. 3.1 A priori molecular design in radiotracer development: 2-[^{18}F]fluoro-2-deoxy-D-glucose ([^{18}F]FDG)

- To select fast reactions and introduce the short-lived radionuclide as late as possible in the synthetic pathway (possibly as the last step), in order to limit loss of activity due to physical decay.
- To design the substrate (cold precursor) in such a way so as to promote selectivity and region-specificity (i.e., directing the reaction toward the desired product and at the same time avoiding/limiting side products).
- To avoid the presence of interfering/competing chemical groups that may inhibit or affect the radiolabeling reaction. Usually, protective groups are used to eliminate interferences and to direct the radionuclide toward a specific target portion in the molecule.

Some labeling approaches have become "classic solutions," such as the introduction of suitable "leaving groups" in substrates conceived for fluorine nucleophilic substitutions or the use of alkylating agents able to carry ^{11}C or ^{18}F atoms.

The introduction of "foreign" elements, groups, and molecular fragments into a biologically active molecule may affect its biological behavior and acceptance. [^{18}F]FDG was a clear example of how substituting a fluoride atom for a hydroxyl group in the glucose molecule transformed a fuel molecule into a cell-trapped substrate. This is still true for many other fluorinated analogs of bioactive molecules.

The quest for new PET radiotracers is continuously growing and extending to many different substrates, in particular proteinaceous substrates. Therefore, molecular design must consider conformational analysis of ad hoc functionalized peptides, proteins, and nanostructured and composite materials prior to start a radiolabeling project.

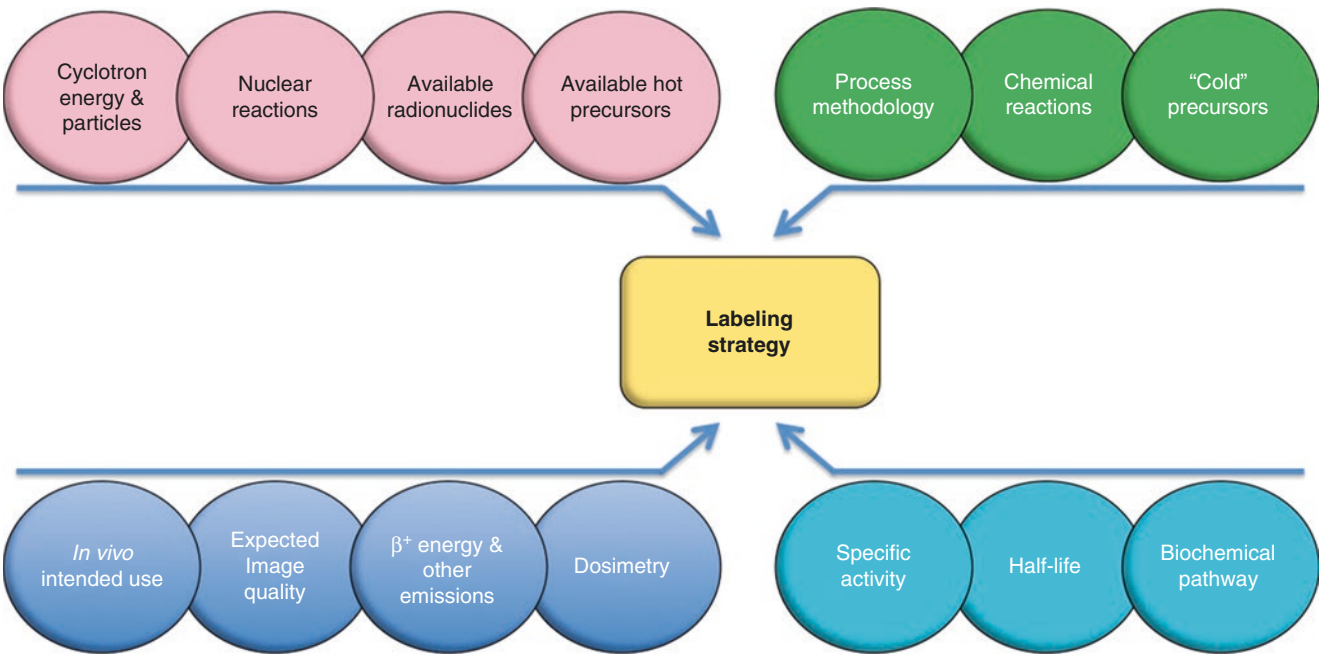

Fig. 3.2 Key points to be analyzed during the design of a radiolabeling strategy

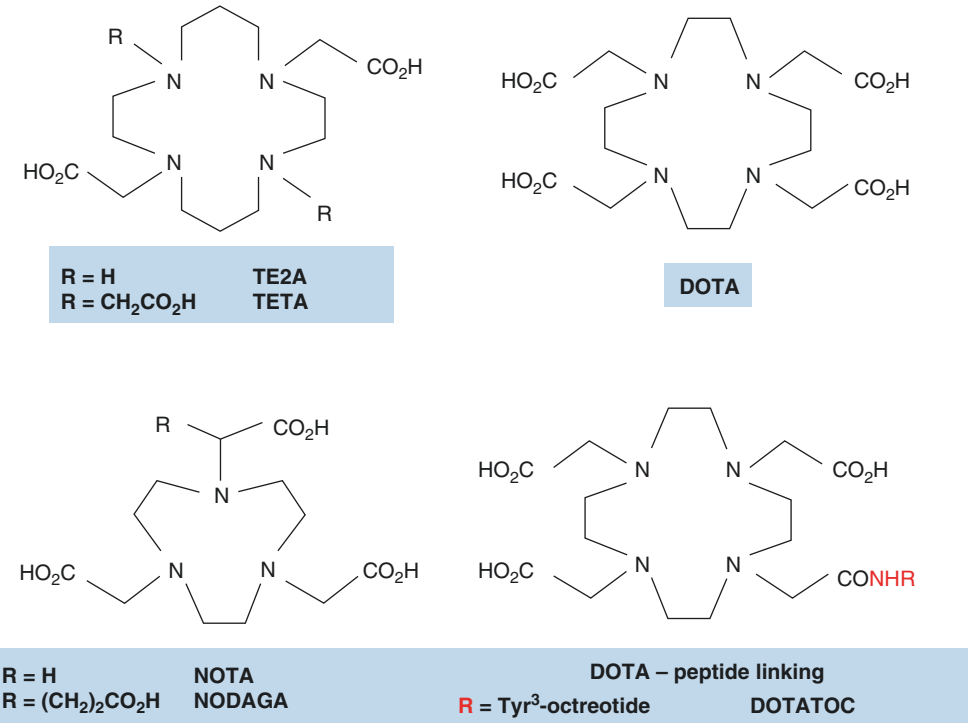

Fig. 3.3 Chelating cores used with positron-emitting radiometals. One of the groups external to the ring may be used as a linker to a protein or peptide

In general, complexes or chelates of positron-emitting radiometals cannot be easily bound directly to a biologically active molecule. Therefore, introduction of a suitable chelating core in the molecular is required for labeling a biologically active substrate with a radiometal (Fig. 3.3).

These bridging groups, usually called prosthetic groups, are "bifunctional," i.e., they have chemical affinity for the substrate on one side and for the radionuclide on the other side. They are also used for nonmetallic radionuclides when chemistry hurdles have to be overcome between radioactive precursor chemistry and substrate.

Key Learning Points

- Fast reactions and ad hoc precursors are required to prepare PET radiotracers.
- The nature and position of the radionuclide (label) may influence the biochemical acceptance and metabolic fate of the radiolabeled tracer.
- Bifunctional reagents may help in achieving binding of the radiolabel to the biologically active vector.

3.1.3 Radiopharmaceuticals and Biological Systems

As with single-photon radiopharmaceuticals (see Chap. 2), there are multiple routes of administration, including oral, intravenous, intra-arterial, subcutaneous, and inhalation. PET radiopharmaceuticals are most frequently administered intravenously, while less frequently performed procedures are based on inhalation of radioactive gases, such as [^{11}C]CO, [^{11}C]CO_2, [^{15}O]CO, and [^{15}O]O_2.

The blood is both the vehicle distributing the radiopharmaceutical throughout the body and the first biochemical environment the radiotracer is exposed to. The molecular/biochemical characteristics of the radiopharmaceutical determine its residence in circulating blood as well as its metabolic fate (Fig. 3.4). Interactions with the blood components (proteins and blood cells) must also be considered to ensure that the radiopharmaceutical is not degraded or transformed. The vascular phase is important in data analysis, as the delivery of the tracer (input function) is a key parameter in data analysis.

Molecular size, polarity, and the presence of active permeation mechanisms affect the ability of a radiopharmaceutical to cross the vascular endothelium and diffuse into the interstitial space. [^{18}F]FDG enters the brain by a facilitated diffusion process mediated by glucose transporter-1 (GLUT-1). Many organs have highly specialized endothelia (such as the blood-brain barrier); therefore, each tracer must comply with specific requirements that should be considered a priori when designing the molecule.

Classic parameters commonly used in drug design (LogP, LogS, PSA, etc.) are considered during the design phase of the tracer as necessary (although not always sufficient) characteristics (Table 3.4). PET tracers generally undergo specific molecular interactions to reach a specific target tissue/organ. When quantifying the radioactivity distribution, it is

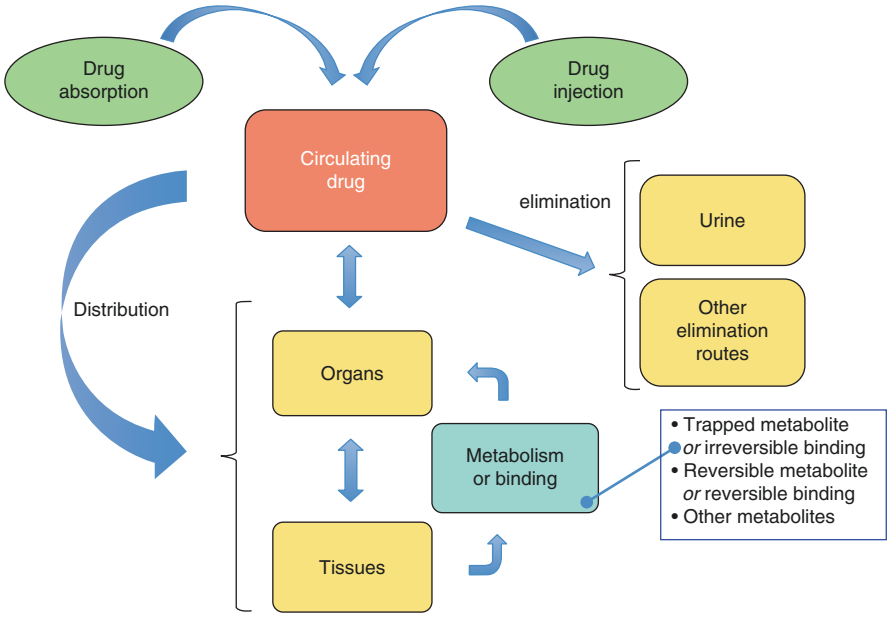

Fig. 3.4 Diagrammatic representation of the molecular characteristics of the tracer that influence its kinetic and metabolic fate in vivo

Table 3.4 Molecular characteristics and early tests for their assessment

Molecular properties		Characteristics	Description
Intrinsic molecular properties	MW	Molecular size/weight	MW influences diffusion coefficient in physiological membranes
	clog *P*	Lipophilicity[a]	Calculated[b] log *P*
	log *S*	Solubility	Predicted solubility (calculated from molecular parameters)
	PSA	Polar surface area	Metric (Å^2) used to predict the ability of a drug to permeate cellular barriers
	Ha	H-bond acceptors	Number of groups that are H-bond acceptor
	Hd	H-bond donors	Number of groups that are H-bond donor
Experimental properties (physicochemical)	log *P*	Lipophilicity	Logarithm of the molecule partition coefficient between an organic solvent[c] and water (neutral species)
	Δ log *P*	Hydrogen bonding	(N-octanol/water log *P*)-(hexane/water log *P*)
	log D_{pH}	Lipophilicity/ ionization	logarithm of the distribution coefficient between an organic solvent[c] and a buffer (usually pH = 7.4)
	S	Solubility	Speciation done in water and/or biological fluids
	pKa	Acid-base	Negative logarithm of the ionization constant in water
	CHI	Chromatographic hydrophobicity index	Parameter derived from analytical tests (HPLC) on the candidate substance
Experimental properties (in vitro biological)	Plasma stability	Metabolic stability	Plasma and blood contain hydrolases, in particular proteases and esterases, with hydrolytic activity on ester and/or amide bonds
	Blood stability		
	F%	Free drug fraction	Binding to plasma protein may deeply influence (bio)availability of the drug at the target
	Hepatocytes	Biotransformation metabolic stability	Hepatocytes contain all drug-metabolizing enzymes and closely mimic the in vivo situation. Liver microsomal preparation contains all CYP isozymes' other metabolic enzymes, such as FMO and UGT Oxidative and conjugation metabolism
	Liver microsomes		
	EC_{50}/IC_{50}	Binding affinity	EC_{50} = concentration of a drug that gives half-maximal response IC_{50} = concentration of an inhibitor where the response (or binding) is reduced by half
	Caco-2	Biomembrane permeability	Cell model, derived from cells of human colon adenocarcinoma, expressing efflux transporters (and variable influx transporters)
	MDCK	Biomembrane permeability	Madin-Darby canine kidney cell model. Polarized cells with low expression of ABC transporters

[a]Lipophilicity or hydrophobicity affects drug absorption, bioavailability, hydrophobic drug interactions
[b]Calculation based on molecular structure and chemical groups present in the molecule
[c]Octanol is typically used; other solvents may be used to explore particular hydrogen-bonding (neutral/donor/acceptor, e.g., hexane/chloroform/propylen glycol dipelargonate) characteristics of the molecule

important to distinguish the chemical form carrying the radionuclide. Transformations that may occur from blood to final excretion must be known. This is mandatory when employing a modeling approach for quantitative estimates of the regional concentration of a selected radiolabeled species. Blood sampling and radiochemical analysis may be necessary to identify metabolites derived from the original radiopharmaceutical.

On the other hand, in vivo biotransformation per se can be the target of the investigation with a PET tracer. For instance, tissue ischemia leads to alteration of the local redox capacity and pH; certain PET tracers may respond to these alterations by changing their initial chemical nature and thus causing local accumulation of radioactivity. Hypoxic myocardium or hypoxic tumors are the typical targets for this imaging approach. Tracers that accumulate in hypoxic tissues are based on redox-sensitive elements (such as copper in ^{67}Cu-PTSM) or on redox-sensitive molecular groups (such as the 2-nitroimidazole moiety of ^{18}F-FMISO). Tracers whose stability is pH-dependent, such as ^{68}Ga-citrate or pHLIPs (pH (low) insertion peptides), are labeled with either ^{18}F or ^{68}Ga. Nevertheless, the mechanism of local accumulation of both redox- and pH-sensitive tracers is not fully elucidated.

The majority of PET tracers are designed to either (1) fit a specific binding pocket of a target molecule or (2) enter a biochemical pathway. Therefore, molecular structure and impact of the labeling moiety (radionuclide and prosthetic group if present) must be carefully evaluated for designing suitable tracers.

Receptor and enzymes, the target of several PET ligands/substrates, constitute the most typical applications pursued to exploit the selectivity and specificity of the lock-and-key mechanism. The receptor ligand (or the enzyme substrate) fits a specific binding site and, doing so, determines the biochemical response. A wide variety of receptor systems have been assessed with PET tracers (Table 3.5).

PET ligands can facilitate the early development phases of a drug compound to evaluate pharmacokinetics in humans. Localization of these radiolabeled agents demonstrates the proof-of-principle, saving time in the development of new drugs. The high-specific radioactivity of PET tracers plays a key role in this application, as they can be administered and traced back even at the low concentrations of ligands at their signaling sites. In the specific case of receptor ligands, reversibility of binding and affinity of the PET ligand with the target must be considered, to make sure the tracer will reflect the true behavior of the receptor under physiological conditions and the intended use (e.g., for mapping the total receptor population, mapping receptor modulation, etc.).

There are two main strategies to assess an enzymatic process: (1) suicide substrate, thereby the tracer interacts with the binding site in an irreversible way, and (2) "normal" substrates, thereby the tracer interacts with the enzyme according to the expected pathway. An example of the first type of substrate is [^{11}C]-L-deprenyl-D_2, used to investigate astrocytosis in neurodegenerative diseases. This ligand binds selectively and irreversibly to monoamine oxidase-B (MAO-B) in the brain and acts as a suicide inhibitor through the formation of a covalent bond with the enzyme moiety, thus allowing a regional mapping of enzyme density sites.

[^{18}F]FDG is a paradigmatic example of the second type of substrate/enzyme interaction. [^{18}F]FDG is a substrate of the enzyme hexokinase that transforms it into the phosphorylated product, [^{18}F]FDG-6-P. In turn, [^{18}F]FDG-6-P, which is not fit to be a substrate of the enzyme glucose-6-phosphate isomerase, remains trapped into the cell. Indeed, the phosphorylation rate and the transport/extraction are not the same for [^{18}F]FDG and glucose, and adequate corrections must be employed to measure local glucose metabolic rates using PET-derived data on [^{18}F]FDG extraction rates. To this purpose, a "lumped constant" has been calculated from head-to-head experiments, e.g., comparing [^{18}F]FDG with [^{3}H] glucose or [^{14}C]glucose (biochemically identical to native glucose). In this regard, it should be considered that the lumped constant may vary among different tissues, among different regions of the brain, and also within the same tissue/organ during disease versus physiologic conditions. The example of [^{18}F]FDG as a metabolically trapped substrate has opened the way to the development of other PET tracers (Fig. 3.5).

An additional target of PET tracers is the assessment of molecular transport and pool measurements. Cellular homeostasis and function are largely based on mechanisms regulating the transit of molecules across membranes and their intracellular concentration. Solute carrier proteins, ion channel-linked receptors, G-protein-linked receptors, and enzyme-linked receptors have been exploited to develop PET tracers for molecular imaging. For example, many transport systems for amino acids (AAs) (e.g., system L, system A/N, etc.) are enhanced in neoplastic cells. [^{11}C] Methyl-L-methionine has been used to image-enhanced AA transport and protein metabolism in brain tumors, thus overcoming the limitations of the [^{18}F]FDG PET scan due to the high background associated with the physiologically high uptake of [^{18}F]FDG in the brain. The development of ^{18}F-labeled AAs, with improved logistic and scan time, has considerably expanded the clinical applications of this approach, targeting different tumors via the associated AA transport systems.

Transporters also regulate the efflux of xenobiotics and toxic substances from the intracellular to the extracellular space. The ATP-binding cassette (ABC) family, and particularly glycoprotein-P (PgP) in its isoform I (MDR1/ABC1 or multidrug resistance pump), can be targeted with PET tracers for selecting patients for chemotherapy and for treatment adjustment. PET tracers for either PgP substrates (e.g., [^{11}C]

Table 3.5 Radiotracers for neurotransporter and receptor systems

Radiotracer	Traced system		Clinical application[a]
^{18}F-FDOPA	Dopamine synthesis	Dopamine	Parkinson's disease (DA) Insulinomas (DA)
^{18}F-fluoromethyltyrosine (^{18}F-FMT)			Brain tumors (DA, RT)
[^{11}C]SCH23390	D1 receptor antagonist		Parkinsonian syndromes (RT) Schizophrenia (RT) CNS drug development
[^{11}C]NNC-112			
[^{11}C]*N*-methylspiperone	D2/3 and $5HT_{2A}$ receptor densities		
[^{11}C]raclopride	D2/D3 receptors (antagonist)		
[^{11}C]-(+)-PHNO	D2/D3 receptors (agonist)		
^{18}F-fallypride	Extrapyramidal D2 receptor (reversible)		Psychosis in AD (RT) Impulse control disorders in PD CNS drug development
[^{11}C]WIN-35428	Dopamine transporter		Narcolepsy (RT) Drug abuse (RT)
[^{11}C]cocaine			
^{18}F-FECNT			Parkinson's disease (DA) Psychiatric symptoms in PD (RT) Dementia (Lewy bodies) (RT)
^{18}F-FP-β-CIT			
^{124}I-nor-β-CIT			
[^{11}C]hydroxytriptan ([^{11}C]5-HTP)	Serotonin synthesis precursor	Serotonin	Neuroendocrine tumors (DA) Dysphoria and social anxiety disorders (RT)
[^{11}C]WAY-100635	$5HT_{1A}$ receptor antagonist		Depression Functional recovery poststroke (RT)
^{18}F-altanserin	$5HT_{2A}$ receptor antagonist		
^{18}F-setoperone	$5HT_{2A}$ receptor antagonist		
4-^{18}F-ADAM	Serotonin transporter		Behavioral disorders (RT) Depression (RT) CNS drug development
[^{11}C]AFM			
[^{11}C]MADAM			
[^{11}C]dihydrotetrabenazine ([^{11}C]DTBZ)	Vesicular monoamine transporter	Monoamine	Depression (CA, RT) Therapy monitoring (RT)
[^{11}C]L-deprenyl-D_2	Irreversible inhibitor of MAO-B		
pF-[^{18}F]deprenyl			
[^{11}C]chlogyline	Irreversible inhibitor of MAO-A		
[^{11}C]carfentanil	μ-OR agonist	Opioid receptor (OR)	Schizophrenia (RT) Dependencies (RT) Expectation and reward brain systems (RT) Mood transitions (RT)
[^{11}C]LY-2795050	κ-OR antagonist		
^{18}F-(-)cyclofoxy	μ/κ-OR antagonist		
[^{11}C]methylnaltrindole	δ-OR antagonist		
[^{11}C] or ^{18}F-diprenorphine	μ,κ,δ-OR antagonist		
^{18}F-FE-PEO	OR full agonist		
[^{11}C]buprenorphine	OR mixed agonist/antagonist		
^{18}F-FPEB	mGluR subtype 5 (mGluR5)	Metabotropic glutamate receptor (mGluR)	Alcohol addiction (RT)
[^{11}C]ABP688			Focal cortical dysplasia (RT)
[^{11}C]ITMM	mGluR subtype 1 (mGluR1)		Neuropsychiatric disorders (schizophrenia, bipolar disorder, addiction) (RT)
^{18}F-FIMX			

[a]Principal use: DA, clinical use as diagnostic agent; RT, clinical research tool; AD, Alzheimer's disease; PD, Parkinson's disease

daunorubicin) or PgP inhibitors (e.g., [^{11}C]verapamil) have been tested to assess MDR expression and quantification in patients with malignancies.

The 18 kDa translocator protein (TSPO) is minimally expressed in normal healthy glial cells but is overexpressed in response to brain injuries and inflammation due to microglia activation; TSPO substrates have been radiolabeled for evaluating neuroinflammation as well as some cancers and peripheral inflammation. Examples of the tracers depicting molecular transport are summarized in Table 3.6.

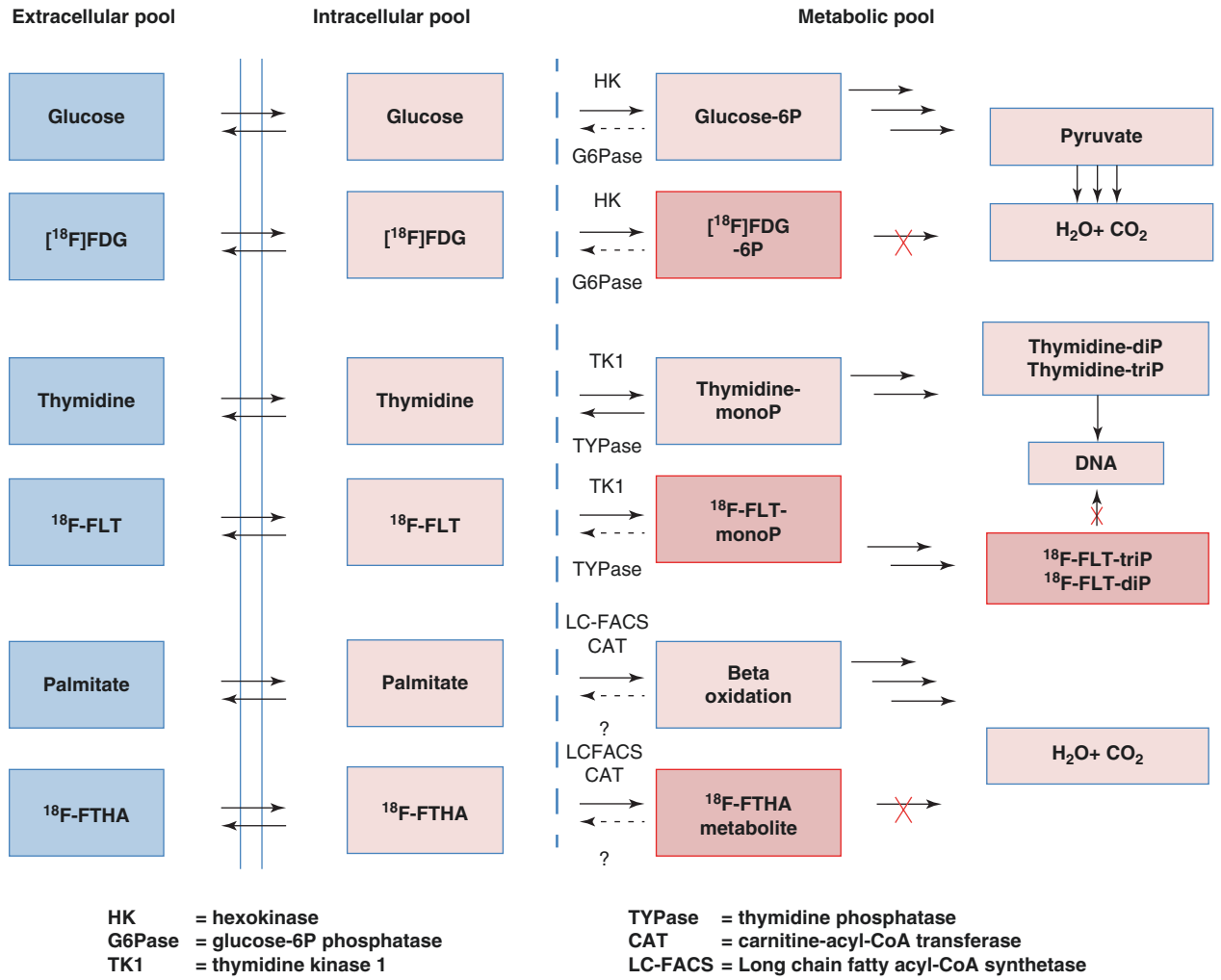

Fig. 3.5 Examples of PET tracers that exploit the metabolic trapping principle (FTHA also enters triglyceride synthesis)

Table 3.6 Examples of molecular characteristics and interactions used to investigate biological processes in vivo

Radiotracer	Mechanism of uptake	Biochemical process	Clinical applications
[^{15}O]water	Freely diffusible substrate	Myocardial blood flow and perfusion	Regional perfusion (cardiology, oncology)
[^{13}N]ammonia	Facilitated diffusion; intracellularly trapped as glutamine		Myocardial perfusion, BBB transport
^{18}F-flurpiridaz	NADH-ubiquinone oxidoreductase inhibitor of mitochondrial complex-1 (MC-1)		Myocardial perfusion
^{82}Rb-chloride	Internalized as monovalent cation and substrate of Na/K-ATPase		Myocardial perfusion
[^{18}F]FDG	GLUT-facilitated transport. Trapped intracellularly, after hexokinase phosphorylation, with direct relationship to glucose metabolic rate	Regional metabolism	Oncology Neurology Cardiology Infection Inflammation
[^{11}C]choline	Upregulated choline transport and phosphorylation in tumors. Substrate of choline kinase, the phosphorylated [^{11}C]choline is essentially trapped within cells		Prostate cancer Cholinergic system[a]
^{18}F-FTHA [^{11}C]palmitate [^{11}C]acetate	Facilitated transport by monocarboxylate transporter family. Substrates of intracellular acetyl-CoA synthetases. FTHA remains intracellularly trapped due to β-oxidation interruption by sulfur-for-methylene substitution along the chain		Oxidative metabolism Nonalcoholic steatohepatitis and fatty liver disease

(continued)

Table 3.6 (continued)

Radiotracer	Mechanism of uptake	Biochemical process	Clinical applications
^{18}F-FMISO	All are based on the 2-nitroimidazole moiety. The tracer passively diffuses through membranes and then is reduced by nitroreductase and forms covalent bonds intracellularly under reduced O_2 levels	Regional hypoxia	Tumor oxygenation in oncology (pre-radiation therapy)
^{18}F-FAZA			
^{18}F-FETNIM			
^{64}Cu/^{62}Cu-ATSM	The tracer passively diffuses through membranes; the complex undergoes thiol-mediated intracellular reduction. Cu(I) separates from complex and binds to intracellular proteins (Cu pathway)		Tumor oxygenation in oncology Myocardial ischemia/ hypoxia
^{68}Ga-PSMA (and ^{18}F-PSMA)	Targeting glutamate carboxypeptidase II or prostate-specific membrane antigen (PSMA)	Upregulated protein function and expression	Prostate cancer
[^{11}C]methyl-L-methionine ([^{11}C]MET)	System L (Na^+-independent transport of neutral AA)	Enhanced amino acid transport	Brain tumors
[^{11}C]α-1-methyltryptophan ([^{11}C]AMT)			Biomarker of epileptogenic process
^{18}F-fluoroethyltyrosine (^{18}F-FET)			Prostate cancer
^{18}F-fluciclovine (^{18}F-FACBC)	ASCT2 (Na^+-dependent exchangers for Ala-Ser-Cys-Asp-Gln)		Prostate cancer
^{18}F-cis-4-fluoro-L-proline	System A (Na^+-dependent transport of neutral AA) and $B^{0,+}$ (Na^+-independent transport of cystine and neutral and dibasic AA)		Preclinical: brain neurodegeneration and radionecrosis
^{18}F-propyl-L-glutamate	System X_{c-} (cystine/glutamate antiporter)		Preclinical: glutathione-based drug resistance
[^{11}C]PK11195	Candidate ligands to 18 kDa translocator protein	Upregulated protein Function and expression	Neuroinflammation (Microglia activation)
[^{11}C]DPA-713			
^{18}F-GE-180			
[^{11}C]verapamil	P-glycoprotein inhibitor		Multidrug resistance
[^{11}C]loperamide	P-glycoprotein substrate		
^{18}F-fluoropaclitaxel			
[^{11}C]-6-bromo-methylpurine	Multidrug resistance protein substrate		
[^{11}C]dantrolene	Breast cancer resistance protein		

Most of the tracers described here are still under development. The molecular level of interaction requires due consideration of inter-individual differences, disease genotype, and phenotypic manifestation

[a]High specific radioactivity required

Besides transmembrane transport, it is also important to investigate what is happening inside the cells, including activity of specific genes. Reporter genes can be a substrate (transformed into a product that is metabolically trapped intracellularly or acting as a suicide substrate) of an enzyme encoded by the reported gene. Alternatively, a radiolabeled ligand acting as the reporter probe can be used to bind to the receptor encoded by the reporter gene. The major limitation of this approach is immunogenicity associated with the use of the therapeutic transgene, in particular those based on viral and nonhuman sources.

Key Learning Points

- Bloodstream drives the distribution of radiotracers throughout the body and may influence pharmacokinetic parameters.
- Radiolabeled compounds may be transformed (in the blood or tissues/organs) and thus give rise to radiolabeled metabolites, which may confound image interpretation.
- Radiotracer molecular structures are specifically designed to interact with specific tissue targets (e.g., receptor or enzymatic binding sites) or characteristics (e.g., pH, redox activity).
- Key cellular functions can be explored with radiotracers (e.g., transmembrane transport, gene or protein expression).

3.1.4 Production Flowchart and Related Issues

Successful production of a suitable PET tracer moves through a number of steps:

- Production (at a cyclotron or a generator) of the radionuclide in the necessary amount, suitable chemical form and quality
- Availability (cost, stability, quality) of the cold precursor(s)
- Reproducibility of the radiolabeling reaction(s)
- Efficient purification procedure
- Formulation for administration and dispensing of the final product (vials, syringes)
- Effective quality controls (e.g., chemical, radiochemical, radionuclidic purity, sterility, and bacterial endotoxins)

Full compliance of the process with the pharmaceutical standards required for human administration may require the adoption of challenging solutions to cope with the short time frame and with the need for adequate shielding of the high-energy radiation associated with positron emission. Pharmaceutical grade standards must be maintained throughout the process for equipment and environment (see Chap. 40 of this book "Radiopharmacy/radiochemistry for positron-emitting radiopharmaceuticals, including Quality Assurance and process validation principles").

"Closed systems" based on automation of radiochemistry and radiopharmacy procedures successfully address this challenge.

Key Learning Points

- PET tracer production must be well planned and optimized in all steps to cope with the radionuclide short half-lives.
- Radiotracers are to be considered as medicinal products, and appropriate quality standards must be maintained during the product's entire life cycle.

3.1.5 Basic of Automation and Synthesis Devices

Automation plays a major role in radiopharmaceutical chemistry. In the late 1970s, most radiochemistry expertise was focused on protein radioiodination and on technetium radiochemistry/radiopharmacy. This technology was adapted to start remote processing of cyclotron-produced radiogases and, by using flow-through chemistry, the production of the earliest PET radiolabeling precursors (Table 3.7).

The passage from complicated switching boards, manually controlled by the operator who had to visually control metering instruments and devices inside the hot cell via a lead glass, to sequencers and computers has been driving the process. Automation technology progress has been paralleled by miniaturization of the components (valves, switches, sensors, and metering instruments) and electronics for input/output interfaces.

3.1.5.1 Automation of Radiopharmaceutical Synthesis

A key point in the synthesis of a PET tracer is to keep the whole process under control. The operator must know how

Table 3.7 Earliest radiolabeling precursors used for positron-emitting radiopharmaceuticals

Target material	Nuclear reaction	Product	Conversion method	Final product	Use of final product
$^{14}N_2$ (+O_2 trace)	$^{14}N(p,\alpha)^{11}C$	$[^{11}C]CO_2$ + $[^{11}C]CO$	Oxidation (CuO/750 °C)	$[^{11}C]CO_2$	PET tracer[a]
					Labeling precursor
			Reduction (Zn/400 °C)	$[^{11}C]CO$	PET tracer[b]
					Labeling precursor
$^{14}N_2$ (+1% H_2)		$H[^{11}C]CN$	In-target production	$H[^{11}C]CN$	Labeling precursor
$^{14}N_2$ (+5% H_2)		$[^{11}C]CH_4$	Catalytic (NH_3 + Pt/1000 °C)	$H[^{11}C]CN$	
			In-target production	$[^{11}C]CH_4$	
$H_2{}^{18}O$	$^{18}O(p,n)^{18}F$	$H^{18}F$	$CsCO_3$/calcination	$Cs^{18}F$	
^{20}Ne (+0.5–1% $^{19}F_2$)	$^{20}Ne(d,\alpha)$ ^{18}F	$[^{18}F]F_2$	$CH_3CO_2NH_3$	$CH_3CO_2{}^{18}F$	
			XeF_2	$[^{18}F]XeF_2$	
$^{14}N_2$ (+2% O_2)	$^{14}N(d,n)^{15}O$	$[^{15}O]O_2$	In-target production	$[^{15}O]O_2$	PET tracer[c]
			Reduction (H_2 + Pd/150 °C)	$[^{15}O]H_2O$	PET tracer[d]
$^{15}N_2$ (+1% H_2)	$^{15}N(p,n)^{15}O$	$[^{15}O]H_2O$	In-target production		
$^{14}N_2$ (+0.1% CO)	$^{14}N(d,n)^{15}O$	$[^{15}O]CO_2$ + $[^{15}O]CO$	Oxidation (MnO_2-CuO)	$[^{15}O]CO$	PET tracer[e]
			Purification (charcoal/soda lime)	$[^{15}O]CO_2$	PET tracer[f]

[a]Clearance rate, gas exchange, blood flow
[b]Blood volume, splenic red blood cell mass
[c]Oxidative metabolism; oxygen extraction ratio (in combination with $[^{15}O]H_2O$ or $[^{15}O]CO_2$ and $[^{15}O]CO$)
[d]Blood flow/perfusion
[e]Blood pool
[f]Blood flow/perfusion

the process is progressing, and have the possibility to interact with the system should something go wrong. To achieve this, the level of radioactivity (at start, in-process, and in the final product collect vial) is measured and monitored as a sensitive and meaningful indicator of process performance. Many additional process parameters, such as reactor temperature, pressure, pH, etc., may need continuous monitoring to ensure a timely and a well-controlled process.

The fluidics of the system must be suitable to handle the very small volumes used in radiopharmaceutical chemistry (usually microliter to milliliter) and the extremely low concentrations (often at picomoles) of high-specific activity PET products. Efficient transfer of the product(s), as a solution or in a gas phase, from a collect vial on to a reactor, a purification column, or to the final product vial requires novel devices.

In current systems the controlling device (electronics, valve actuators, syringe motors) is separated from the fluidics, the latter being gathered into a cassette to be loaded onto the synthesizer (Fig. 3.6). Advantages of this approach include (1) cleaning of fluidics is not necessary because a new cassette is used for each synthesis, (2) mis-connections are avoided, and (2) errors by the operator (especially in loading reagents and mounting the components) are avoided. Cassettes are available as kits in which all reagents and purification supports and ancillary components (e.g., sterilizing filters) are provided and certified by the manufacturer. Besides facilitating the quick setup of the system, this is a convenient simplification in the phase of suppliers/raw materials validation and acceptance, as key parts of process validation and radiopharmaceutical quality systems according to good manufacturing practice. A further advantage is that the cassettes are produced and certified as sterile and pyrogen-free.

In general, the cassette kit is specific for the production of a selected radiopharmaceutical and is replaced after the process is completed before starting a new synthesis. This step is sometimes critical, due to residual activity in fluidics and components. Specific technical solutions in the design of hot cells (shielded repository), remote-controlled manipulators, and cassette self-cleaning are often adopted to circumvent this drawback.

In cassette-based chemistry, microfluidics is emerging as a new approach, since we deal with high-specific radioactivity products, which requires small volumes of reagents. Most of the microfluidic radiochemistry technology derives from

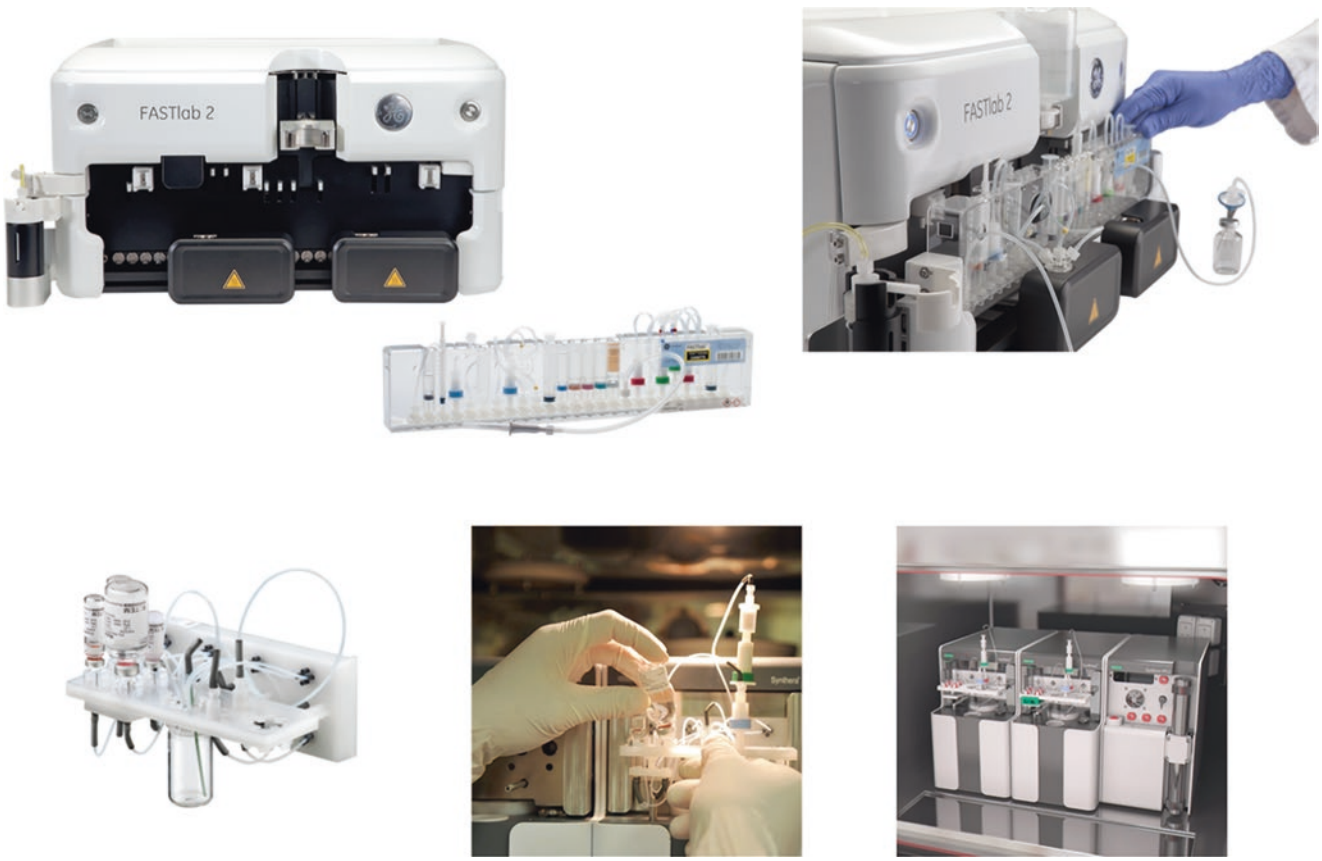

Fig. 3.6 Modern approach to automatic synthesizers based on cassette-like fluidics (tailored on the radiotracer process) and exploiting a separate, multipurpose hardware

microelectronics manufacturing developments that have permitted miniaturization, at the micron scale. The result is a chip-like "microcassette" in which microliter scale processes can be performed.

Furthermore, microfluidic technology involves higher surface-to-volume ratios of flow-chemistry microreactors than "normal" vessel radiochemistry. In these microreactors with tens of micron diameter and length of few centimeters, reagents come quicker and more efficiently in contact, while temperature (energy) is precisely and efficiently transferred to the reactants. Furthermore, flows of reactants can be accurately controlled, from laminar to highly turbulent, and used as an additional condition in the process setup.

In general, higher yields and faster reaction rates (timescale can be changed from minutes to seconds) than common vessel chemistry are achieved, and it is possible to repeat the reaction several times, as one single batch of reagents and precursors in the milliliter scale is sufficient for many runs. In principle, it should be possible to replace the bulky production of a single radiopharmaceutical (to be dispensed to several patients) with a "dose-on-demand" approach (selecting on the spot from a list of available radiopharmaceuticals).

Key Learning Points

- Automation and miniaturization are key enabling technologies in radiopharmaceutical chemistry.
- Remote-controlled radiochemical platforms inside shielded hoods (hot cells) are used to prepare and process the radiopharmaceuticals.
- Radiotracer-specific pre-loaded cassettes (hardware and reagents as a kit) are used on general purpose radiochemical platforms.

3.1.6 ^{18}F-Labeled Radiopharmaceuticals

The majority of PET radiopharmaceuticals employed in clinical practice are based on ^{18}F. The short positron range in tissues results in better image quality than with other PET radionuclides, and its physical half-life allows not only more complex synthetic strategies but also the delivery of radioactive products to off-site satellite PET centers.

The stability of the C–F bond prevents fluorine leakage from the labeled molecule, and the small ionic radius produces minor molecular alteration, much less pronounced than those produced by other halogens such as iodine.

Fluorine-18 can be produced as molecular fluorine ([^{18}F]F_2) and aqueous solution of fluoride salts (e.g., [^{18}F]KF). These two molecular forms usually originate from different nuclear reactions and have completely different chemistry. The extremely high reactivity of molecular fluorine, at some point during the radionuclide production process [^{18}F]F_2, requires the addition of F_2 as a carrier, to allow its efficient recovery from the target. Therefore, carrier-added [^{18}F]F_2 has a lower specific radioactivity than the no-carrier-added [^{18}F]fluoride. Moreover, the [^{18}F]fluoride targetry is simpler, and the nuclear reaction yields higher than those of [^{18}F]F_2.

3.1.6.1 Electrophilic Fluorinations

[^{18}F]F_2 was the first radionuclidic chemical for cyclotron-produced ^{18}F. Therefore, the earliest reaction pathways using fluorine-18 for labeling molecules of biological interest were the electrophilic reactions based formally on F^+ as the reactive intermediate. In this regard, it should be noted that the F–F complex has a positive charge; therefore, it is electron-avid (i.e., electrophilic). Since the F–F bond is rather weak, elemental fluorine tends to resume its electronegative charge by avidly attracting electrons. Pure F_2 reacts so explosively with many substrates that it needs to be diluted with inert noble gases and used at low temperature. Even in these conditions, it exhibits very high chemical reactivity, thus interacting very quickly and in a rather nonselective manner with the electron-rich portion(s) of the molecule yielding electrophilic substitutions and additions (Fig. 3.7). Notably, the reaction of [^{18}F]F_2 (diluted to 0.1% in neon gas) with *O*-tetraacethylglucal as cold precursor was the initial way to synthesize [^{18}F]FDG.

In general, F_2 reactivity is so strong that it is very difficult to limit side products/reactions and avoid substrate oxidative degradation. A number of "tamed" derivatives of [^{18}F]F_2 have therefore been prepared in the quest for better electrophilic radiolabeling agents (Table 3.8). These derivatives are still used with electron-rich substrates via electrophilic substitution, in particular demetalation of organometallic reagents (e.g., organotin and organomercury derivatives). The most common application of electrophilic ^{18}F-fluorination is the synthesis of ^{18}F-FDOPA, through regioselective electrophilic demetalation of an organotin substrate (although a nucleophilic alternative is being developed).

3.1.6.2 Nucleophilic Fluorinations

The ^{18}O(p,n)^{18}F nuclear reaction is well known. Nevertheless, early production strategies produced ^{18}F-fluoride ion aqueous solutions (in which the nucleophilic reactivity is quenched), limiting initial diffusion of nucleophilic fluorination in PET radiochemistry laboratories. The development of cryptands and phase-transfer reagents, able to bind ionic species in the aqueous phase and transfer them into an organic phase (the preferred medium for most of the organic reactions), paved the way to a revolution in radiofluorination.

The relevance of this approach emerged with the synthesis of [^{18}F]FDG, by a nucleophilic route, based on the displacement of a triflate leaving group by an "activated" nucleophilic fluoride. Activation was obtained with a crown

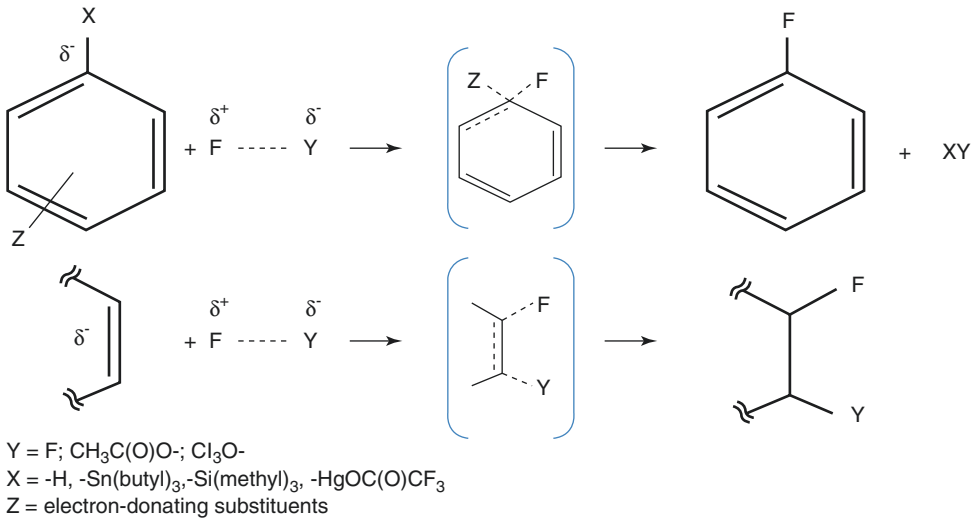

Fig. 3.7 General principles of electrophilic substitution (upper row) and electrophilic addition (lower row)

Table 3.8 Direct and derived radiolabeling agents for electrophilic fluorination (examples)

Cyclotron-produced precursor	Conversion	New radiolabeling reagent	Applications
$[^{18}F]F_2$	No conversion (direct reaction)	n.a.	$[^{18}F]$FDG (electrophilic addition), ^{18}F-FDOPA (electrophilic demetallation), 4-^{18}F-fluoromethyltyrosine (fluorodemercuriation), 2-^{18}F-fluoro-L-tyrosine (fluorodestannylation)
	$[^{18}F]F_2$ (gas) on solid ammonium acetate	$CH_3CO_2{}^{18}F$	$[^{18}F]$FDG 5-$[^{18}F]$fluorouracil 4-^{18}F-fluoroantipyrine ^{18}F-RGD-peptides
	$[^{18}F]F_2$ on Xe at high temperature	$[^{18}F]XeF_2$	$[^{18}F]$FDG
	$[^{18}F]F_2$ on 1,4-disubstituted 1,4-diazabicyclo[2.2.2]octane	$[^{18}F]$selectfluor bis(triflate)	Preparation of fluoroaromatics and difluoroalkylarenes
	$[^{18}F]F_2$ on N-substituted pyridines	$[^{18}F]$*N*-fluoro-pyridine (or pyridinium)	Fluorination of electron-rich "cold substrates" (organometallic)
	$[^{18}F]F_2$ on sulfonamides	^{18}F-labeled *N*-fluoro-alkylsulfonamides ^{18}F-labeled *N*-fluoro-benzenesulfonamides	
	$[^{18}F]F_2$ on $KClO_3$	$[^{18}F]FClO_3$	Preparation of 2-deoxy-2-fluoro-D-hexoses by fluorination in water
$H^{18}F$ (anhydrous)	Exchange labeling in freon	$[^{18}F]$diethylaminosulfur trifluoride ($[^{18}F]$DAST)	Conversion of alcohols into fluorides
$[^{18}F]$fluoride	(Post-target method) microwave discharge on $[^{18}F]$methyl fluoride/F_2	$[^{18}F]F_2$	High specific activity molecular $[^{18}F]$fluorine
	$[^{18}F]$fluoride/crown ether complex in solution	^{18}F-labeled Pd(IV) fluoride/aryl complex	Fluorination of arene moiety

Arenes = substituted benzene rings (aromatic rings)

amino polyether (Kryptofix® or $K_{2.2.2}$) having the ability to complex the potassium, used as counterion to the fluoride and thus leaving the fluoride "naked" and more prone to reaction. At the same time, the bulky organic complex between the crown ether and the potassium had enough "organic" character to carry along the fluoride in organic phase ($[^{18}F]KF/K_{2.2.2}$). The synthesis of $[^{18}F]$FDG with this new method was faster (30 min versus 120 min) and more efficient than the older electrophilic route, in which 50% of the activity was lost due to the reaction stoichiometry that included the separation of two fluorinated isomers (Fig. 3.8).

Thus, the use of activated ^{18}F-fluoride and nucleophilic substitution (Fig. 3.9) has quickly become a common synthesis strategy to prepare a variety of new tracers. The cold

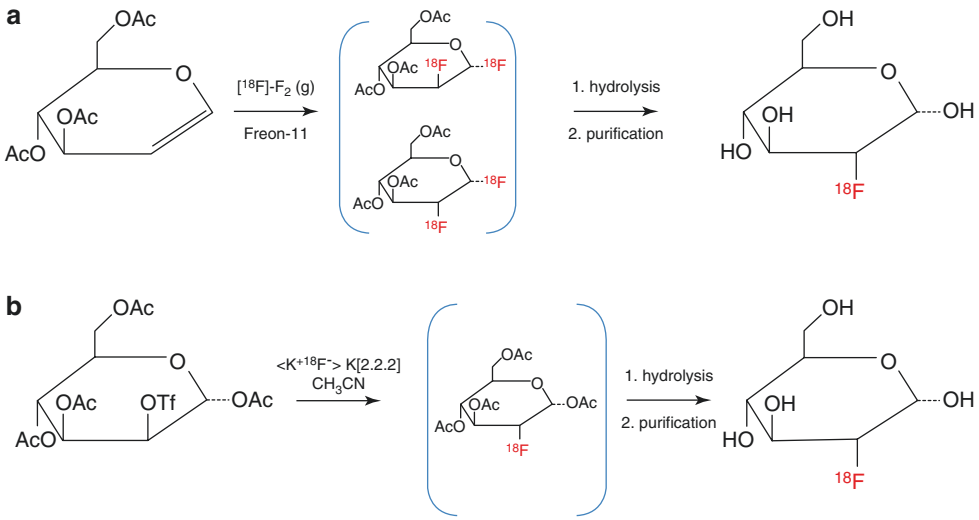

Fig. 3.8 (**a**) The original [^{18}F]FDG synthesis based on the electrophilic route. (**b**) The improved version exploiting the nucleophilic reaction with fluoride

	Yield	Synthesis time	Specific activity
method a)	8-10%	120 min	carrier-added
method b)	>50%	30 min	no carrier-added

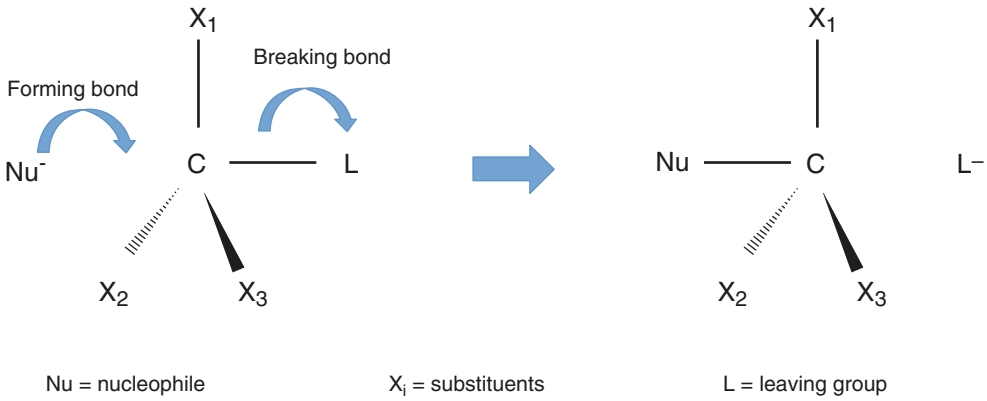

Fig. 3.9 General principle of a reaction proceeding via nucleophilic substitution

precursor to be labeled could be designed, often adopting complex chemistry to make radiolabeling straightforward, in general completed in no more than two steps.

3.1.6.3 Prosthetic Groups and Large Molecule Radiofluorination

The efficiency of the nucleophilic radiofluorination triggered a generation of "second-line" reagents. These are radiolabeled molecules exhibiting a peculiar reactivity, different from fluorine/fluoride, that have the function to carry on board the radiolabel and are used as a radiolabeled reagent (or synthon) in the synthesis with a cold precursor (Table 3.9). Usually the entire labeled molecule is incorporated into the final product. A classic example is the ^{18}F-fluoromethylation of a nor-methyl substrate. In practice, with these reagents, radiolabeling with fluorine-18 is limited not only to the formation of a C–F bond but can take advantage of a much wider chemistry.

Classic biologically active, organic molecules (e.g., Lipinski-like) are not the sole targets for radiofluorination. Neither [^{18}F]F_2 nor activated ^{18}F-fluoride have favorable chances to directly interact with these substrates; however, these molecules can be radiolabeled with ad hoc synthons and ad hoc "prosthetic" chemical groups (Fig. 3.10).

Once the prosthetic group is introduced in the molecular frame by direct functionalization of the peptide final product or during its synthesis, radiolabeling can be performed keeping in mind that with any biological molecules (large molecules in particular) reaction conditions may play a key role in maintaining the integrity of the biological activity. For example, the use of organic solvents and/or excessive temperatures may alter the biological properties of the peptide. A new strategy potentially circumventing this limitation encompasses the use of orthogonal chemistry. This approach exploits chemistries and groups that are not encountered in biomolecules or involved in biological processes and there-

Table 3.9 Fluorinated reagents and prosthetic groups

Cyclotron-produced precursor	Fluoride activation strategy	Synthon	Typical labeling target(s) in the substrate	End-product
[^{18}F]fluoride	$K_2CO_3/K_{2.2.2}$ (or TBAH)	[^{18}F]fluorobromomethane	Amines, thiols, alcohols[a]	Fluoromethylation
		[^{18}F]fluoroethyltosylate		Fluoro-ethylation
		p-[^{18}F]fluoroiodobenzene *p*-[^{18}F] fluoroaryl-tributylstannane *p*-[^{18}F]fluoroarylboronic acids	Alkynes, aromatic rings	Pd-mediated cross-coupling reactions
		p-[^{18}F]fluorobenzaldehyde 2-[^{18}F]fluoro-2-deoxyglucose[b]	*N*-hydroxylamine or Hydrazine derivatives	Oximes[c] or hydrazones[c]
		4-([^{18}F]fluoromethyl)phenyl isothiacyanate 4-[^{18}F]fluorobenzoic acid *N*-succinimidyl 4-([^{18}F] fluoromethyl) benzoate	Amines[a] (e.g., terminal amino groups and ε-NH_2 of lysines)[a]	Amide bond formation with protein, peptides, and antibodies
		N-(4-[^{18}F]fluorophenyl) maleimide [^{18}F]fluorophenacyl bromide	Thiols[a] (e.g., cysteine)	Protein, peptides, and antibodies
		ω-[^{18}F]fluoroalkyne ω-[^{18}F]fluoroazides	Azide-containing substrates[d] Alkyne-containing substrates[d]	Triazole[c] formation

Synthon = molecular fragment that will be incorporated into the final compound
[a]Off-target multiple labeling is possible. Protective groups may be needed
[b]As open-chain anomer (aldehyde)
[c]Bio-orthogonal bond. This bond is not degraded in vivo by common biochemical processes
[d]"Click chemistry": cycloaddition azide-alkyne. May be mediated by catalysts (e.g., copper) or facilitated by intramolecular strains in a substrate (e.g., cyclooctyne)

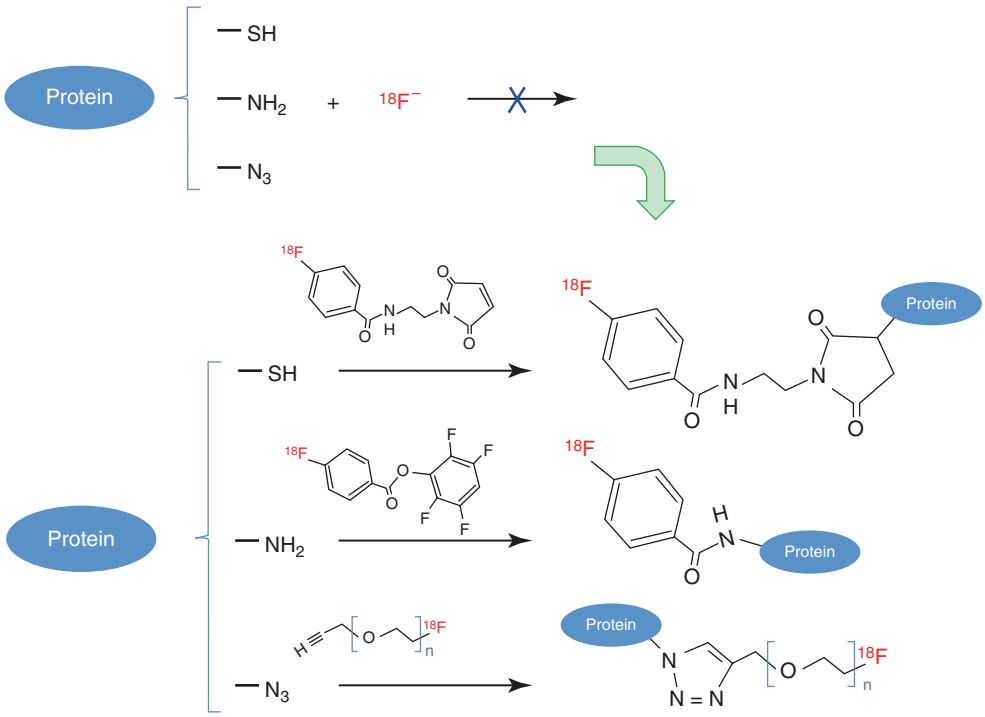

Fig. 3.10 Radiofluorination of protein substrates

fore can be applied without interference or competition by existing groups and withstand biodegradation.

Key Learning Points

- The majority of PET radiopharmaceuticals are based on ^{18}F.
- Two alternatives chemical methods are available to prepare radiofluorinated compounds: nucleophilic route (based on ^{18}F-fluoride as precursor) or electrophilic route (based on $[^{18}F]F_2$ as precursor).
- Nucleophilic labeling is simpler, more efficient, and widely used.
- Nucleophilic-based radiofluorinations can achieve better specific activity than the electrophilic reaction.
- Depending on the chemistry of the process, the radiofluorinated precursor can be converted into derived reagents having better reactivity with selected substrates (cold precursors).
- Selected functional groups (prosthetic groups) may be introduced into the molecular frame to allow direct radiolabeling with radioactive fluorine.

3.1.7 ^{11}C-Labeled Radiopharmaceuticals

Carbon-11 is regarded as an ideal radionuclide for labeling molecules of biological interest but with the major disadvantage of its 20.3-min physical half-life. From the chemical point of view, substitution of native ^{12}C with the positron emitter ^{11}C leaves the biological characteristics unchanged; nevertheless, the short time window for PET imaging permits only those applications in which the PET study addresses a fast biokinetic process. In these conditions, the short physical half-life may even be an advantage, as repeat tests can be performed in the same subject (e.g., test/retest applications).

The production of carbon-11 in a gas target takes advantage of hot atom chemistry and target gas composition to direct the product of the nuclear reaction toward different chemical forms, mostly $[^{11}C]CO/CO_2$ and $[^{11}C]CH_4$. These are currently the building blocks that are available to synthesize ^{11}C-labeled compounds.

Direct use of $[^{11}C]CO_2$ in carboxylation reactions was the simplest approach to produce organic compounds, such as carboxylic acids and their derivatives. However, carbon-11 radiochemistry has expanded to a high number of labeling agents, thus increasing the efficacy and flexibility of ^{11}C-labeling reactions (Table 3.10). Although the list of

Table 3.10 Basic ^{11}C-synthons and carbon chemistry employed per product categories

Cyclotron-produced precursor	Synthons derived from precursor	Typical use	End-product(s)
$[^{11}C]CO_2$	Neat[a]	Formation of carboxylates by direct reaction with Grignard reagents and organolithiums; these compounds can be functionalized to carboxyamides and amines (by reduction of amides)	Carboxylic acids Amides Carbamates Oxazolidinones Substituted ureas Alkyl carbonates
	$[^{11}C]$formaldehyde	Electrophilic aromatic substitutions and ring-closure reactions, Mannich-like alkylation reactions[b]	
	$[^{11}C]$phosgene		
	$[^{11}C]$methyl iodide	Alkylations	N-, O-, S-methylderivatives;
$[^{11}C]CH_4$	$[^{11}C]$methyl iodide		
	$[^{11}C]$methyl triflate		
	$[^{11}C]$cyanidric acid and $[^{11}C]$cyanate	Nucleophilic additions and substitutions	Amides, Amines, Amino acids, Hydantoins, nucleosides Ureas
$[^{11}C]CO$	Neat[c]	Carbonylation reactions ketones, -amides, -ureas, -carboxylic acids, and -esters. Selenium-mediated carbonylation; transition metal catalyzed insertion and reductive elimination of C–C, C–N, and C–O bonds	Ketones, Alcohols, Carboxylic amides, Aminocarbonylations

[a]Specific radioactivity may vary
[b]Complementary to alkylations obtained with methyl iodide
[c]CO trapping efficiency and solubilization in the reaction media are challenging

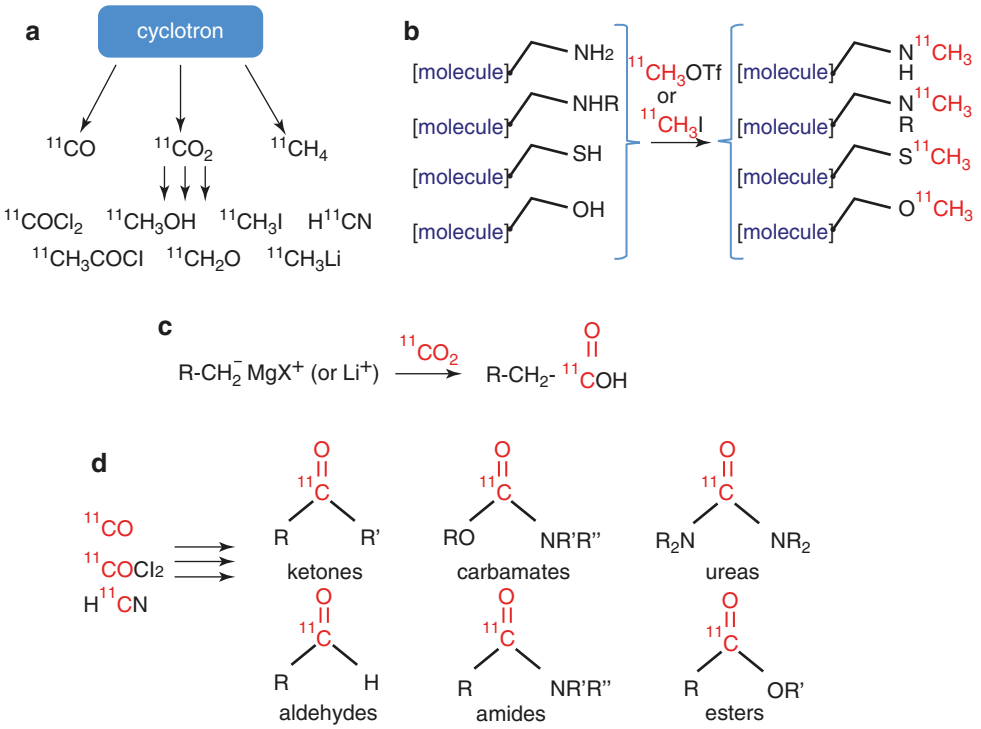

Fig. 3.11 (**a**) Precursors for labeling with ^{11}C and (**b**–**d**) general application in carbon chemistry

^{11}C-labeled "building-blocks" may appear limited (Fig. 3.11a), the variety of biological molecules that can be labeled is extremely ample.

3.1.7.1 ^{11}C-Methylation Reactions

Alkylation reactions proceed quickly and efficiently, with very good selectivity. ^{11}C-Methyl iodide has been an early target in carbon-11 radiochemistry; later, this methylation agent has been joined by the cognate compound ^{11}C-methyl triflate. Both compounds can currently rely on very efficient and dedicated synthesizers, in which the most crucial point is keeping high the specific radioactivity and the conversion of the precursor radiogas into the desired methylation agent. Methylation is a one-step reaction that is performed directly on the cold precursor (Fig. 3.11b). To this purpose, the molecule is designed in such a way that it carries an alkylation-prone group (including either an N, O, or S heteroatom) that is usually the desmethyl (nor-methyl) analog of the final, target product.

The substrate is always present in much larger concentration than the labeling agent, thus increasing both the reaction rate and reaction selectivity, in practice eliminating the possibility of multiple additions to the same molecule. The reaction is quite frequently carried out in a liquid phase, but it has also been developed on solid supports and even in microfluidic apparatuses. In general, the alkylating agent is prepared and distilled directly into the vessel containing the substrate to be labeled in a suitable organic solvent (e.g., DMSO, DMF, acetone), which has to be tested for in the final product. More recently, the use of ^{11}C-methyl iodide has been expanded to the formation of carbon–carbon bonds, by using palladium-mediated reactions even if the transition to a production-sustainable procedure still depends on the palladium complex.

3.1.7.2 Emerging ^{11}C-Labeling Reactions

Carboxylation reactions of organometallic reagents (Fig. 3.11c), currently included under the more general term of CO_2-fixation reactions, have constituted the first approach to ^{11}C-labeling, as they made use of the $[^{11}C]CO_2$ directly coming from the cyclotron target. Strong anionic-like reagents, such as Grignard reagents or organolithiums, must be used to overcome the chemical inertness of CO_2. A full spectrum of carboxylic acids and fatty acids (FA) have been prepared following this route; in particular, [^{11}C]acetate and 1-[^{11}C]palmitate are widely used as tracers to assess oxidative metabolism and FA consumption/storage in the heart and liver. The synthesis is very flexible, and many other FAs (oleate, arachidonate, heptadecanoate, docohexaenoate, acetoacetate, etc.) have been labeled in different positions and with different purposes (e.g., neurotransmission in the brain) (Fig. 3.12). These reactions require extremely dry conditions and are generally carried out under an inert atmosphere (N_2 or Ar). Furthermore, careful attention must be paid to avoid contamination by atmospheric CO_2 (which is readily absorbed by the very reactive reagents) in order to maintain high and reliable specific radioactivity.

Direct formation of ^{11}C-labeled compounds by $[^{11}C]CO_2$-fixation has been more recently carried out using strong organic bases, as in the synthesis of ^{11}C-labeled carbamates that, like urea, are stable in vivo.

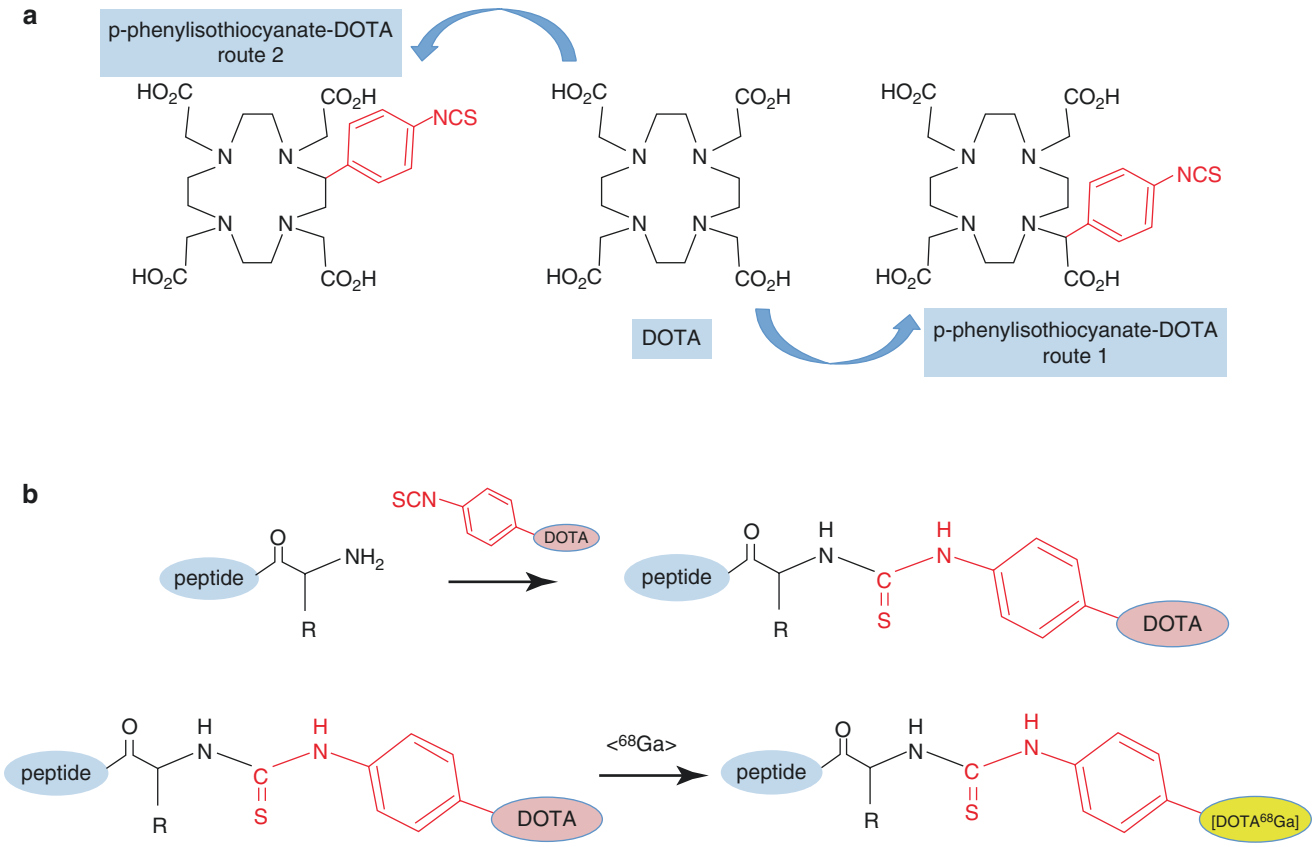

Fig. 3.12 Example of a prosthetic group (**a**) used to label peptides with radiometals (**b**)

Other radioactive precursors have been used for the preparation of ^{11}C-carbonyl compounds, such as [^{11}C]phosgene and [^{11}C]isocyanates, but seldom have found their way in the preparation of products applied for clinical use.

The precursor [^{11}C]KCN has been more frequently used in nucleophilic substitutions of aliphatic substrates (such as halogenated compounds and tosylates) to yield ^{11}C-labeled amides, carboxylic acids, and amino acids, such as [^{11}C]glutamine used for metabolic imaging of tumors and [^{11}C]leucine used for tracing amino acid transport.

Finally, direct introduction of [^{11}C]CO—easily available from the carbon-11 target at the cyclotron—into substrates has also been pursued. The main limitation of this approach is the very poor solubility of carbon monoxide and the difficulties in trapping efficiently the precursor. Recent developments in the rhodium- and palladium-mediated CO insertion reaction may provide more viable solutions.

All the new radiolabeling pathways mentioned above contribute to the development of novel ^{11}C-labeled radiopharmaceuticals (Fig. 3.11d), although mostly for research purposes rather than for clinical applications, targeting relevant enzymatic (e.g., FAAH, LAT1, MAO-A, and -B) and receptor systems (κ-opioid, D3, and 5-HT1A).

Key Learning Points

- Simple ^{11}C-radiolabeled chemical species obtained at the cyclotron can be used as building blocks to prepare more complex molecules.
- Most of the ^{11}C-labeled radiotracers with clinical applications are obtained via a methylation reaction (onto O, N, or S heteroatoms in the molecule) of selected desmethyl precursors.
- Other organic chemistry reactions are being developed to extend the number of ^{11}C-radiolabeled compounds (e.g., carboxylation, carbonylation).
- Short half-life limits the use of ^{11}C-radiotracers to in-house applications, where clinical investigation prevails over routine use.

3.1.8 ^{68}Ga-Labeled and Radiometal-Based Radiopharmaceuticals

Gallium-68 can be obtained from a generator or also directly from cyclotron bombardment. The ^{68}Ge/^{68}Ga generator has been known since 1964, but drawbacks in generator performance (such as low elution yield, ^{68}Ge breakthrough, and

interference from metallic impurities) have limited its application. In aqueous solution, gallium has a 3^+ oxidation state and can exist as free hydrated ion only at acidic pH. The development of suitable gallium chemistry was not an easy task: mimicking Fe^{3+}, $^{68}Ga^{3+}$ produces a very stable complex with transferrin in vivo. Therefore, the synthesis of ligands ensuring the formation of Ga-complexes exhibiting high thermodynamic and kinetic stability was a necessary step to overcome the Ga-transferrin complex formation in vivo, both directly (larger stability constant) or via ligand exchange (higher kinetic stability).

A crucial step forward was the observation that macrocyclic chelators (DOTA, NOTA, etc.) (Fig. 3.3) produce stable complexes with metals in the 3^+ oxidation state, including gallium. A major breakthrough was the elaboration of these macrocycles as prosthetic groups linked to peptides of biological interest (Fig. 3.12).

3.1.8.1 ^{68}Ga-Labeling

The "lead" compound of ^{68}Ga-radiopharmaceuticals is ^{68}Ga-DOTA-TOC (Fig. 3.3). This compound has high affinity for the somatostatin (SST) receptors (particularly subtype 2) and is clinically employed for PET imaging of neuroendocrine tumors (NET). ^{68}Ga-DOTA-TOC PET yields much better imaging results than ^{111}In-DTPA-TOC SPECT, therefore becoming a reliable PET screening agent to select patients for therapy with ^{90}Y-DOTA-SST analogs. The promising results obtained in early clinical trials constitute an important impulse toward developing new SST analogs by following two directions: (1) finding new and better chelators and (2) developing potent and selective peptide vectors to which a suitable chelating prosthetic group can be linked. In particular, total peptide chemistry (manual or automatic) could facilitate the insertion of modified amino acids or amino acid-like intermediates carrying the chelating group. Whenever necessary, e.g., when active conformation exists for the molecule, in silico calculations may be performed to evaluate any structural perturbation following prosthetic group insertion.

Commercial availability of more efficient and reliable ^{68}Ge/^{68}Ga generators has further promoted the use of gallium-68 in nuclear medicine departments (especially those without a cyclotron), and many ^{68}Ga-labeled radiopharmaceuticals are currently available for either clinical use or research purposes (Table 3.11).

The most notable family of novel PET ^{68}Ga-radiopharmaceuticals is a group of ligands that bind with strong affinity and avidity to the prostate-specific membrane antigen (PSMA), a transmembrane glycoprotein with enzymatic activity (glutamate carboxypeptidase II) that is highly specific for either normal prostate tissue and (especially) of prostate carcinoma. This property makes PSMA an enticing target for the imaging and therapy of prostate cancers. Several small molecular weight ^{68}Ga-PSMA ligands have been produced, including ^{68}Ga-PSMA-11, ^{68}Ga-PSMA-617, and ^{68}Ga-PSMA-I&T that appear as the most promising for imaging prostatic cancer. The current trend is to consider these radiopharmaceuticals not only for their high diagnostic potential in detecting early recurrences of prostate cancer but also within an integrated scenario of theranostics thereby their uptake in cancel lesions can predict the efficacy of therapy with, e.g., ^{177}Lu-PSMA-ligands.

3.1.8.2 Other Radiometals

Success of the new methodologies developed for labeling bioactive peptides with ^{68}Ga has triggered more attention on

Table 3.11 ^{68}Ga-based radiotracers obtained via direct or bifunctional labeling

^{68}Ga-labeling strategy	Acronym	Short description	Target use
Direct labeling	^{68}Ga-EDTA	^{68}Ga-ethylenediaminetetraacetic acid	BBB integrity Renal function
	^{68}Ga-Cit	^{68}Ga-citrate	Hypoxia Inflammation
	^{68}Ga-MAA	^{68}Ga-human serum albumin macroaggregates	Perfusion
Labeling with bifunctional agents	^{68}Ga-DOTA-TOC	^{68}Ga-DOTA-Tyr^3-octreotide	Somatostatin analogs used in neuroendocrine tumor detection (NET)
	^{68}Ga-DOTA-TATE	^{68}Ga-DOTA-Tyr^3,Thr^8-octreotide	
	^{68}Ga-DOTA-NOC	^{68}Ga-DOTA-NaI-octreotide	
	^{68}Ga-NOTA-RGD	^{68}Ga-NOTA-[arginyl-glycyl-aspartic seq.]	RGD motif targeting $\alpha_v\beta_3$ integrins
	^{68}Ga-NOTA-GSA	^{68}Ga-NOTA-glycosyl human serum albumin	Liver function
	^{68}Ga-DOTA-hEGF	^{68}Ga-Human epidermal GF	EGFR expression
	^{68}Ga-DOTA-MG0	^{68}Ga-DOTA-minigastrin	Cholecystokinin-2 gastrin receptor (in NET)
	^{68}Ga-DOTA-BZH3	^{68}Ga-DOTA-bombesin derivative	Gastrin-releasing peptide receptor
	^{68}Ga-NOTA-BBN2	^{68}Ga-NOTA-bombesin derivative	

other radiometals as candidates for labeling both existing and new molecules, so to expand the range of available tracers and their use can.

The relatively short physical half-life of ^{68}Ga (about 68 min) results in a short useful imaging window for radiopharmaceuticals labeled with this radionuclide. Unfortunately, there are few radionuclides having an acceptable half-life and decay mode with reasonable positron emission abundance. Furthermore, nuclear chemistry constraints (targetry technology and production protocols) and nuclide-specific chemistry play important roles in selecting a radionuclide for labeling compounds of biological interest.

Copper-64 (half-life 12.7 h) is considered an acceptable, although not optimal, candidate; in fact, its positron energy/range is similar to that of ^{18}F, but its positron abundance is only 19%. ^{64}Cu-ATSM has been used mainly for detecting hypoxic areas, such as those present in many tumors or myocardial ischemia. On the other hand, the radionuclide per se in the simple chemical form ^{64}Cu-chloride is emerging not only because of its potential for imaging in oncology but also because of its potential for antitumor therapy due to its emission of β^- particles—within the scenario of theragnostics. Furthermore, its ability to form stable complexes and its 12.7 h half-life have renewed attention on the possibility to transfer the experience gained with ^{68}Ga-labeling to ^{64}Cu-labeling, for instance, using peptides functionalized with a prosthetic group containing a TETA or TE2A chelating core. Thus, ^{64}Cu has been chelated to different peptides and proteins, such as the integrin-targeting peptide containing the RGD sequence (or Arg-Gly-Asp) and antibodies (e.g., ^{64}Cu-DOTA-Cetuximab). Theranostics is the common denominator in this rapidly expanding field, thereby imaging and therapy using the same antibody construct as the tumor-targeting carrier molecule (e.g., an anti-EGFR antibody), labeled with ^{64}Cu for immune-PET and with ^{177}Lu for radioimmunotherapy, respectively.

Zirconium-89 (with physical half-life 78.4 h and 22.7% abundance β^+ emission) is an additional promising radionuclide. Its quite long physical half-life allows PET imaging on multiple days after administration, thus ensuring a longitudinal follow-up of the biodistribution pattern of labeled therapeutic antibodies (mAbs) or other compounds.

The critical issue in the use of ^{89}Zr is to identify good chelators able not only to allow the preparation of ^{89}Zr-complexes in good yield but also, and most importantly, to ensure that they can withstand the long exposure to the in vivo environment so to prevent release of free ^{89}Zr (bone being the target tissue). This task is not simple due to the characteristics of the coordination core of Zr. While many "classic" coordination cores used for other radiometals proved inefficient, the best results have so far been obtained using the core of siderophore, i.e., desferrioxamine; most of the bifunctional chelators currently under investigation follow this route. Table 3.12 summarizes some examples of radiometal-labeled products that are under development, particularly for oncology applications.

Table 3.12 Examples of radiolabeling of biological molecules with radiometals

Radionuclide	Biological vector	Biochemical target
Zirconium-89	Anti-PSMA	Prostate cancer
	Cetuximab	EGFR expression
	Rituximab	CD20 expression
	Trastuzumab	HER2 expression
	Nanocolloidal albumin	Sentinel lymph node
	Bevacizumab	Ovarian cancer
Copper-64	Trastuzumab	HER2 expression
	DOTA-NT-Cy5.5	Neurotensin receptor
	DOTA-alendronate	Mammary microcalcifications
	DOTA-patritumab	HER3/ERBB3 solid tumors
	CBTE2A-galectin-3 peptide	Breast carcinoma
	DOTA-AE105	Urokinase plasminogen activator receptor

Direct radiolabeling of large molecules (such as antibodies or other proteins) is complicated by the variety of groups that may be present in such macromolecules and by the high risk of altering the active conformation or the active site(s). Usually, exposed functional groups (such as ε-amino groups of lysine or thiol groups of cysteine residues) are targeted by bifunctional agents with chemical selectivity/affinity for these groups. Nevertheless, newer reactions (such as orthogonal chemistry ligation via click chemistry) are being tested to expand the radiolabeling perspectives. An interesting feature of click chemistry is the possibility to pretreat the protein with the click-prone reagent and to perform the click reaction in aqueous media with the preformed complex, or even in vivo, following a two-step administration.

Key Learning Points

- Developments of gallium chemistry and ^{68}Ge/^{68}Ga generator technology have boosted the interest over ^{68}Ga as a clinically significant radionuclide.
- ^{68}Ga needs good chelating groups, such as macrocycles containing nitrogen atoms, for acceptable in vivo stability.
- Macrocycles can be chemically linked to biologically active compounds (e.g., peptides) to yield ^{68}Ga-labeled substrates.
- ^{68}Ga-DOTA-TOC (octreotide) targeting somatostatin receptors and ^{68}Ga-PSMA ligands targeting prostate-specific membrane antigen sites are the most common ^{68}Ga-radiotracers in clinical use.

- Other radiometals (such as ^{64}Cu and ^{89}Zr) are being assessed as additional radiotracers based on chelation chemistry and peptide (protein) radiolabeling.
- ^{64}Cu and ^{89}Zr have longer half-life than ^{68}Ga and might be used to trace longer kinetics.

3.1.9 Miscellanea

3.1.9.1 ^{124}I-Labeled Radiopharmaceuticals

Iodine-124 has a physical half-life of 4.2 days and a 23% abundance β^+ emission. Although these features are suboptimal for imaging, ^{124}I can be used for theragnostic applications. After having acquired all relevant pharmacokinetic data that may be necessary to build up an accurate treatment plan, the same substrate that has been used for imaging (labeled with ^{124}I) can then be used at higher activities for treatment (e.g., labeled with ^{131}I or with other suitable radionuclide emitting β^- particles).

In principle, all the know-how developed and consolidated over the years on other radioisotopes of iodine (^{123}I, ^{125}I, ^{131}I) can be quickly transferred on to ^{124}I. Iodine-124 is available as sodium iodide, and, as such, it can be used for nucleophilic substitutions or, in combination with the use of an oxidizing agent, for electrophilic substitutions. Classic oxidizing agents commonly used for radioiodination, such as chloramine-T or Iodogen®, have been successfully used to prepare ^{124}I-labeled radiopharmaceuticals. Well-established prosthetic groups, such as the Bolton-Hunter reagent, and newer bifunctional compounds have been used when direct labeling was not possible due to the lack of radioiodination-prone moiety (e.g., tyrosine or histidine residues in peptides) or when it was necessary to carefully target the introduction of the radiolabel via the prosthetic group.

Small molecules, peptides, and proteins have been labeled and tested—with variable results in terms of clinical use. Table 3.13 lists the most widely used ^{124}I-radiopharmaceuticals as well as the radiolabeling route adopted.

3.1.9.2 Radiopharmaceuticals Labeled with Very Short-Lived Radionuclides

The radionuclides with half-lives shorter than carbon-11 normally require that their production source is next to the PET examination room; therefore, logistical problems are frequently encountered, and there is a declining trend regarding their clinical use, especially when reasonable imaging alternatives become available (e.g., ultrasonography or MRI).

The shorter the half-life, the narrower is the variety of tracers that may be used as precursors and transformed into the final radiopharmaceutical; for half-lives below the 10 min half-life of ^{13}N, only flow-through chemistry can be used. Although some attempts have been undertaken to produce ^{13}N-labeled amino acids, the only clinically viable ^{13}N-labeled product is [^{13}N]ammonia, which can be produced either in-target or by Devarda's alloy treatment of irradiated pure water (reduction of the cyclotron-produced nitrite/nitrate aqueous solution). In both cases, processing lasts only few minutes and ends in a calibrated syringe of the injectable solution. Accurate quantitation of myocardial blood flow and efficient test/retest measurements with low background due to the quick decay justify the use of [^{13}N] ammonia PET.

The use of radiogases labeled with oxygen-15 ($t_{1/2}$ 2.03 min, β^+ abundance 100%) was adopted in the early phases of development PET imaging, particularly for studies on cerebral blood flow, perfusion, and oxygen metabolism, during which a combination of different tracers was used, i.e., [^{15}O]water (for measuring flow), [^{15}O]CO (for measuring blood volume), and [^{15}O]O_2 (for measuring oxygen extraction). Alternative methods have currently largely replaced the use of these tracers (which also involved a relevant radiation exposure burden), and only few research centers are still using this approach, in particular to measure regional blood flow (mostly in the brain and/or myocardium).

The ultrashort-lived rubidium-82 ($t_{1/2}$ 76 s, β^+ abundance 100%) is produced by the ^{82}Sr/^{82}Rb generator, which is commercially available and meets all the requirements in terms of efficacy and safety. Given the extremely short half-life of the radionuclide (a potassium analog), the entire generator, equipped with shielding, pumps, eluting solution, and any

Table 3.13 Biologically active substrates under development for theranostic applications as radioiodinated agents

Radioiodination method	Short description	Acronym	Biochemical target
Oxidative radioiodination	Antibody fragment	^{124}I-mini-Ab F16SIP	Treatment of NSCC
	5-iodo-2′-deoxyuridine	^{124}I-IUDR	Tumor cell proliferation
Iododestannilation	EGFR inhibitor	^{124}I-ML08	EGFR expression
	EGFR kinase activity	^{124}I-IPQA	
	Cyclin-dependent kinase 4/6 inhibitors	^{124}I-labeled CKIA	Tumor cell proliferation
Isotopic exchange with iodide	2-nitromisonidazole moiety	^{124}I-IAZA	Tumor hypoxia
		^{124}I-IAZG	
	Epinephrine analog	^{124}I-MIBG	Adrenergic activity (NET)

other formulating accessories, is connected to the patient through an i.v. line, and the eluate is directly administered to the patient. Although blood flow measurements obtained with this method are not identical to those obtained with [^{13}N]ammonia, this system has the advantage to allow PET myocardial blood flow measurements without the need of an on-site cyclotron; furthermore, measurements can be repeated under different pathophysiologic conditions (e.g., at rest and during a pharmacologic stress test) in the same imaging session.

Key Learning Points

- ^{124}I is being considered for theragnostic application both as diagnostic/therapeutic use by dose escalation and in "sister imaging" before therapy with ^{131}I-labeled compounds.
- ^{124}I is not optimal from the imaging and dosimetric point of view.
- ^{124}I relatively long half-life and the consolidated knowledge on radioiodination reactions may find application in protein/peptide radiolabeling.
- The very short half-life radionuclide ^{13}N has its optimal application in PET quantitation of regional myocardial blood flow but can be used only on-site.
- Ultrashort-lived ^{82}Rb (from long-lived ^{82}Sr generator) can be used in clinical settings as a commercial medical device.

3.1.10 What Might Be Next

Over 4000 compounds have been reported in the literature radiolabeled with one of the many existing positron-emitting radionuclides. Yet, the number of imaging agents actually reaching the stage of clinical practice is very limited. Although the regulatory burden is often a recurrent theme as "the" attrition factor in reaching out a more widespread application of new PET tracers, addressing the multifaceted, variable disease manifestations and at the same time the intrinsic, profound molecular characteristics of the tracers remains a hard challenge. On the other hand, molecular complexity is now seen as an opportunity. In fact, an emerging trend in radiolabeling is to develop nanostructured materials and elaborate these complex constructs as multi-probe tracers, e.g., optical/MRI/PET constructs that could combine the in vitro biochemistry at cellular level with the in vivo findings.

3.2 Section II: Positron-Emitting Radiopharmaceuticals for Clinical Use

3.2.1 Sodium ^{18}F-Fluoride

The microelement fluorine is a normal constituent of the hydroxyapatite crystals forming the mineral matrix of the bone. Sodium ^{18}F-fluoride is one of the first radiopharmaceuticals approved by the US Food and Drug Administration (in 1972) for clinical use as a bone-seeking agent. Technical difficulties in imaging the 511 keV annihilation photons with the instrumentation available at that time subsequently led to its withdrawal in 1984 from the approval list, and ^{18}F-fluoride was replaced by diphosphonates labeled with ^{99m}Tc, emitting γ-rays with optimal energy for imaging with standard gamma cameras. The development of clinical PET scanners has revived interest in the clinical use of sodium ^{18}F-fluoride as a PET bone-scanning agent with much greater diagnostic performance than gamma camera imaging with ^{99m}Tc-diphosphonates.

Upon its i.v. administration, ^{18}F-fluoride undergoes a high and rapid bone uptake which is combined with a fast, biexponential blood clearance; these kinetic features result in high bone-to-background ratios reached within a short time, so that imaging can be acquired as early as 1 h (or less) after administration. The intensity and extent of ^{18}F-fluoride uptake throughout the skeleton reflects blood flow and bone remodeling.

The mechanism of uptake in the bone is based on an ion exchange process thereby each fluoride ion exchanges for an hydroxyl ion on the surface of the newly formed hydroxyapatite crystals, followed by chemisorption into the crystalline matrix with prolonged retention (until subsequent remodeling of the bone). About 20% of injected activity is excreted through the urinary tract within 2 h after administration.

Although the normal biodistribution of ^{18}F-fluoride is rather uniform, the axial skeleton has a higher uptake than the appendicular skeleton, and the bone around joints displays higher uptake than the shafts of long bones. Increased ^{18}F-fluoride uptake can be observed in both sclerotic and lytic metastases.

Key Learning Points

- Sodium ^{18}F-fluoride is a PET bone-seeking radiotracer.
- It follows the metabolic pathway of fluorine being incorporated into the hydroxyapatite crystals that form the mineral matrix of the bone.
- It can be used to image bone remodeling, such as in both sclerotic and lytic tumor metastases.

3.2.2 Flow/Perfusion Agents

As mentioned in Section I of this chapter, the simplest PET-based approach to image blood flow and tissue perfusion of various organs is based on the administration of ^{15}O-labeled small molecules that undergo virtually unrestricted diffusion, such as water ($[^{15}O]H_2O$; see here below) or radioactive gases as $[^{15}O]O_2$ by itself, ^{15}O-labeled carbon monoxide ($[^{15}O]CO$), and ^{15}O-labeled carbon dioxide ($[^{15}O]CO_2$). Since the physical half-life of ^{15}O is about 2 min, an important advantage of using these ^{15}O-labeled agents is the possibility to perform repeated measurements at short intervals during a single imaging session (e.g., every 15 min). This feature enables to investigate the pathophysiology of blood flow/perfusion in different conditions, for instance, at rest and under stress when evaluating myocardial perfusion or during sensorial deprivation then again during activation tests when evaluating brain perfusion.

The very short physical half-life of PET tracers labeled with ^{15}O or with other cyclotron-produced short-lived radionuclides (e.g., ^{11}C) that are not available locally through the use of radionuclide parent/daughter generators constitutes an important limitation to a wider utilization of the ^{15}O-labeled PET tracers. Among the tracers mentioned above, $[^{15}O]H_2O$ remains the preferred PET agent for quantitative perfusion imaging.

3.2.2.1 $[^{15}O]H_2O$

In principle, $[^{15}O]H_2O$ is an ideal radiotracer for quantitative flow measurements with PET, particularly myocardial blood flow. In fact, this tracer diffuses freely across the myocardiocyte membrane, with an extraction rate close to 100% at each pass, not affected by metabolic factors. Since the physical half-life of ^{15}O is 2.06 min, its utilization requires the availability of an on-site cyclotron. As a freely diffusible tracer, $[^{15}O]H_2O$ concentration in the blood pool is high, thus determining suboptimal imaging due to a low myocardial-to-background signal. This requires subtraction of the blood pool activity from the original image by the inhalation of $[^{15}O]CO$, which binds irreversibly to hemoglobin so that the blood pool activity can be digitally subtracted to visualize myocardium. $[^{15}O]H_2O$ has been validated and extensively used for quantitation of myocardial blood flow and coronary flow reserve. Digital subtraction techniques and parametric imaging produced by automated software packages have been implemented to display perfusion at the voxel level in the form of parametric imaging depicting absolute quantitative flow values, thus facilitating the use of $[^{15}O]H_2O$ in clinical practice—provided of course that an in-house cyclotron is available.

3.2.2.2 ^{82}Rb-Chloride

Rubidium-82 is a potassium analog taken up by the myocardium through active transport mediated by the Na^+/K^+ ATPase-pump. Although the physical half-life of ^{82}Rb is extremely short (1.25 min), this radiotracer is produced by on-site by the $^{82}Sr/^{82}Rb$ generator (^{82}Sr decaying with a physical half-life of 25.55 days). The positron range of ^{82}Rb (8.6 mm) and its relatively low extraction fraction (about 65% at each pass) are suboptimal as compared to other PET tracers for myocardial perfusion. In addition, ^{82}Rb extraction can be decreased by severe acidosis, hypoxia, and ischemia. Thus, uptake of ^{82}Rb in the myocardium varies as a function of the combined effect of blood flow, metabolism, and myocardial cell integrity.

3.2.2.3 $[^{13}N]$Ammonia

Ammonia labeled with ^{13}N (physical half-life 9.96 min) is used for quantitative assessment of myocardial perfusion. The favorable positron range (2.53 mm) and an 80% extraction fraction at each pass allow acquisition of intermediate-to-high-quality images. The uptake of $[^{13}N]$ammonia is nonlinearly correlated with regional myocardial blood flow, as doubling the flow leads to a 70–80% increase in tracer uptake. Furthermore, inhibition of glutamine synthetase with L-methionine reduces metabolic trapping of $[^{13}N]$ammonia, suggesting that the glutamic acid-glutamine reaction is primarily responsible for ammonia trapping into the myocardium. $[^{13}N]$Ammonia circulates in the blood in the ionic form $[^{13}N]NH^{4+}$ that is converted back to $[^{13}N]NH_3$ upon entering the extravascular space. Since $[^{13}NH_3]$ is lipophilic, it can freely diffuse across the sarcolemma. Into the myocardial cell, $[^{13}N]NH_3$ is metabolically trapped by conversion to ^{13}N-glutamine. In healthy subjects, myocardial retention of $[^{13}N]NH_3$ is heterogeneous, with higher uptake in the interventricular septum than in the lateral wall. Furthermore, high uptake in the liver can interfere with evaluation of the inferior wall. Although the lung uptake of $[^{13}N]$ammonia is usually low, it may increase in patients with left ventricular dysfunction or with chronic pulmonary disease as well as in smokers.

Although the relatively short half-life of ^{13}N requires access to a cyclotron for radiotracer production, it has the advantage to permit rest-stress assessment of myocardial blood flow in the same session. Similar to SPECT, PET perfusion images can be graded visually and perfusion defects reported in terms of their extent, severity, and location. However, cardiac PET with radiotracers such as $[^{13}N]$ammonia offers the unique opportunity to estimate absolute myocardial blood flow and coronary reserve. This type of quantitation requires dynamic acquisitions and compartmental analysis of radiotracer kinetics.

3.2.2.4 ^{18}F-Flurpiridaz

^{18}F-Flurpiridaz is an analog of the insecticide pyridaben, an inhibitor of NADH-ubiquinone oxidoreductase, also known as mitochondrial complex-1 (MC-1, a component of the electron transport chain). ^{18}F-Flurpiridaz inhibits MC-1 by competing for binding with ubiquinone without affecting the viability of myocardial cells. Uptake of this radiotracer in the myocar-

dium is rapid, followed by slow washout. In a phase II clinical trial, cardiac PET with ^{18}F-flurpiridaz showed superior image quality and higher diagnostic accuracy than SPECT imaging. Absolute myocardial blood flow and coronary reserve may be measured with ^{18}F-flurpiridaz, yielding values in a similar range as those measured with other radiotracers.

3.2.2.5 Novel ^{18}F-Labeled Myocardial Perfusion Agents

^{18}F-Fluoro-dihydrorotenone (^{18}F-FDHR) is derived from rotenone, a neutral lipophilic compound that binds to MC-1 in the electron transport chain. The myocardial retention of this tracer is higher and less affected by flow than that of ^{201}Tl and better correlated with flow both at 1 and 15 min after injection.

^{18}F-p-Fluorobenzyl triphenyl phosphonium (^{18}F-FBnTP, a lipophilic cation) is taken up by myocardiocytes by passive diffusion and accumulates mainly in the mitochondria. This radiotracer (which is excreted mainly by renal clearance) accumulates in the myocardium within 5 min after administration and is efficiently retained up to 90 min. Activity in the blood pool and in the lungs decreases over time, leading to favorable uptake ratios and high-quality images at later time points after administration. Nonetheless, no clinical investigations with ^{18}F-FBnTP have been reported yet. Due to accumulation in the mitochondria as a function of the mitochondrial membrane potential, this tracer has also been defined as a "PET voltage sensor," and its potential as an imaging marker of apoptosis has also been suggested.

^{18}F-4-Fluorophenyl triphenyl phosphonium (^{18}F-FTPP) is an additional lipophilic cationic tracer that accumulates in the mitochondria as function of their transmembrane potential. Early clinical investigations with this tracer yield myocardial blood flow values comparable with those obtained with [^{13}N]ammonia PET.

Key Learning Points

- PET perfusion imaging is the unique technique that allows noninvasive absolute quantification of regional blood flow and flow reserve.
- PET perfusion radiotracers ($^{15}OH_2O$; ^{82}Rb; $^{13}NH_3$) have short half-lives that permit repeated measures of blood flow in the same session and under stressors stimuli.
- With the exception of ^{82}Rb, the availability of these radiotracers is limited by the need for on-site cyclotron.
- ^{18}F-Flurpiridaz is a promising agent with higher extraction, higher image resolution, and longer half-life than previously employed blood flow radiotracers and is currently undergoing clinical validation.

3.2.3 Energy Substrates

3.2.3.1 2-Deoxy-2-[^{18}F]fluoro-D-glucose

Replacing the hydroxyl group on position 2 of glucose with a hydrogen atom yields a glucose analog, 2-deoxy-D-glucose, that is taken up by cells through the glucose transporters (GLUTs) in a competitive manner with glucose. Once inside the cells, 2-deoxy-D-glucose is phosphorylated by hexokinase to form 2-deoxy-D-glucose-6-phosphate, which—unlike glucose-6-phosphate—cannot progress through the glycolytic pathway. Therefore, 2-deoxy-D-glucose-6-phosphate accumulates within the cell and is not metabolized further. As an antagonist of glucose metabolism, 2-deoxy-D-glucose has been investigated as a possible therapeutic agent in conditions of high glucose metabolic demand, as typically observed in tumor tissues.

The radiolabeled counterpart of 2-deoxy-D-glucose is 2-deoxy-2-[^{18}F]fluoro-D-glucose (or [^{18}F]FDG), which is obtained by substituting the hydroxyl group at the C-2 position of the native glucose molecule with the positron emitter ^{18}F (Fig. 3.13). [^{18}F]FDG shares with 2-deoxy-D-glucose the same transmembrane transport and intracellular metabolism characteristics that lead to virtually irreversible intracellular accumulation (Fig. 3.14).

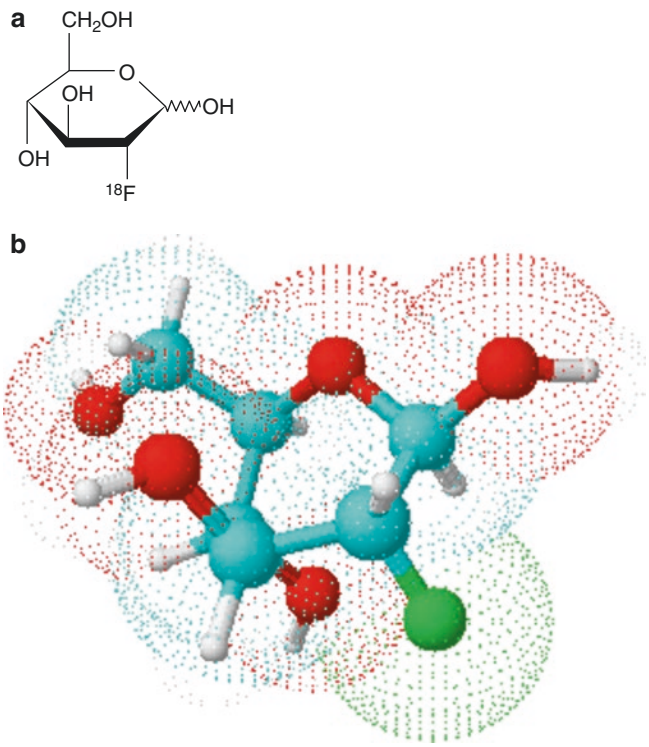

Fig. 3.13 Chemical structure (**a**) and tridimensional molecular representation of (**b**) of [^{18}F]FDG. Color codes for constituting elements: *green*, ^{18}F; *red*, O; *gray*, H; *light blue*, C (*reproduced with permission from: Volterrani D, Erba PA, Mariani G, eds. Fondamenti di medicina nucleare – Tecniche e applicazioni. Milan: Springer; 2010*)

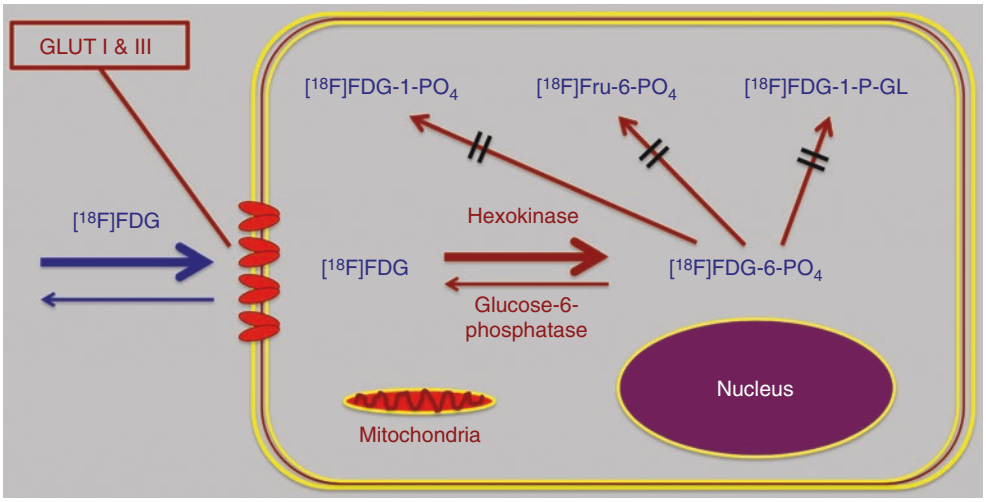

Fig. 3.14 After entering cells through the same mechanism as native glucose (GLUT system), [^{18}F]FDG is converted to [^{18}F]FDG-6-PO$_4$ by the enzyme hexokinase, in the same manner as native glucose. The reverse enzyme glucose-6-phosphatase (which would revert [^{18}F]FDG-6-PO$_4$ back to [^{18}F]FDG, freely diffusible outside the cell) operates at very low levels and almost exclusively in hepatocytes. [^{18}F]FDG-6-PO$_4$ is not a substrate for any of the metabolic routes that glucose-6-PO$_4$ normally undergoes, therefore remaining trapped inside cells (*modified from: Volterrani D, Erba PA, Mariani G, eds. Fondamenti di medicina nucleare – Tecniche e applicazioni. Milan: Springer; 2010*)

Based on the concept that glucose is the sole energy substrate for neurons, [^{18}F]FDG was initially used in humans to map glucose metabolism in the brain. Exploring brain metabolism either under physiologic conditions or in patients with different abnormalities of the central nervous system has remained for some years the exclusive utilization of [^{18}F]FDG in humans, also because early PET technology limited size of the gantry to accommodate the head only of the subject undergoing a PET scan. Current indications for PET with [^{18}F]FDG still include, among others, characterization of patients with various neurological disorders (dementing disorders, epilepsy, movement disorders, and neuro-oncology), in addition to indications in oncology and detection of viable ischemic myocardium.

The current predominant use of [^{18}F]FDG in oncology stems from studies performed in 1924, when Warburg et al. reported that cancer cells have an increased glucose metabolism, based on the observation that, even under aerobic conditions, these cells produce large amounts of lactic acid from the degradation and oxidation of glucose. This increased glycolytic activity is called *Warburg effect* and can be traced using PET imaging. Soon after the development of [^{18}F]FDG as a PET imaging agent, Som et al. pioneered studies demonstrating that this tracer can accumulate in various spontaneous and transplanted tumors in animals. The first study with the use of [^{18}F]FDG PET in patients with cancer was published by DiChiro and colleagues in 1982, showing that [^{18}F]FDG uptake was higher in high-grade gliomas than in low-grade gliomas. This investigation opened the avenue for all subsequent studies with the use of [^{18}F]FDG PET for imaging various types of cancers.

Upon systemic i.v. injection, [^{18}F]FDG rapidly distributes in the body fluids and is taken up by various tissues through glucose transporters and trapped intracellularly. Similarly as for glucose, [^{18}F]FDG distributes to tumor tissue proportionally to regional blood flow, and it is transported into the cell by facilitated diffusion mediated by specific membrane glucose transporters (GLUT family). Overexpression of GLUT-1 has been shown to be closely related to [^{18}F]FDG uptake in human cancers and is also supposed to be an intrinsic marker of hypoxia. In this regard, vascular growth in tumor tissue is frequently insufficient to meet the local metabolic demand. The consequent chronic hypoxia causes the release of specific biochemical mediators, like the hypoxia-inducible factor-1a (HIF-1a), which is considered to support tumor growth by inducing angiogenesis via the expression of vascular endothelial growth factor (VEGF). Recent studies suggest that GLUT-1 overexpression is linked to the HIF-1a production and that hypoxic conditions correspond to a higher [^{18}F]FDG uptake; moreover, tumor hypoxia activates the anaerobic glycolytic pathway. Once into the cell, [^{18}F]FDG is phosphorylated by mitochondrial hexokinase to form [^{18}F]FDG-6-phosphate. The elevated glycolysis of cancer cells is associated with an increased hexokinase production and activity. Moreover, in cancer cells [^{18}F]FDG-6-phosphate cannot be dephosphorylated or progress through other metabolic pathways as glucose-6-phosphate would do, because of its nature of a modified molecule of glucose. As a result, [^{18}F]

FDG-6-phosphate is trapped into the cell (see Fig. 3.14). Although [^{18}F]FDG-6-phosphate may be converted back to [^{18}F]FDG, the enzyme glucose-6-phosphatase is either at very low levels or absent in most cancers. The overexpression of GLUT transporters combined with the increased hexokinase activity and trapping of the molecule results in an increased accumulation of [^{18}F]FDG in cancer cells that is significantly higher than in benign tissues. Biodistribution of [^{18}F]FDG can be affected by several physiologic factors, the most important being blood glucose levels that can reduce radiotracer uptake through competition. Therefore, before performing a PET scan with [^{18}F]FDG, patients should fast to reduce competition with plasma glucose. This requirement is especially important in diabetic patients, in whom high glucose levels can be present that can interfere with imaging quality and results.

PET images are qualitatively interpreted in terms of the presence, distribution, and intensity of radiotracer uptake into the suspected cancer mass. Intensity of radiopharmaceutical uptake relative to the normal tissue has been used to differentiate benign from malignant lesions. Strategies have been developed for qualitative classification of regional [^{18}F]FDG accumulation, such as the intensity of uptake compared to liver uptake. Alternatively, [^{18}F]FDG uptake is semi-quantitatively assessed using the standardized uptake value (SUV) according to the following formula:

SUV = Activity (Bq g^{-1})/[injected activity (Bq)/patient weight (g)]

Although compartmental modeling approaches, originally proposed by Patlack and Sokoloff, allow absolute quantification of tumor glucose metabolism (in terms of moles of glucose/mass of tissue per time unit), technical complexity limits their use in the clinical practice.

[^{18}F]FDG is the PET probe most commonly employed in nuclear medicine. More than 90% of oncologic PET scans use [^{18}F]FDG, since glucose metabolism is increased in most lung, colorectal, pancreatic, esophageal, stomach, head and neck, cervical, ovarian, and breast cancers, as well as melanoma and most types of lymphoma. A 2009 survey of the National Oncologic PET Registry of the United States included results from nearly 41,000 [^{18}F]FDG PET scans performed in more than 34,000 patients at 1368 centers. Thirty-five percent of the scans were for initial staging, 36% for restaging after treatment, and 29% for evaluation of disease recurrence. The [^{18}F]FDG PET findings resulted in change in patient management in 38.0% of the cases. However, despite being an outstanding radiotracer with many advantages for use in oncology, [^{18}F]FDG is not a specific radiotracer for oncology, since it cannot distinguish a high metabolic rate associated with cancer from increased glucose metabolism related to other causes, such as infection/inflammation. This can cause false positive results on PET imaging when evaluating patients with cancer. Moreover, several malignancies with low glucose metabolic rate (such as early prostate cancer) or well-differentiated cancers or tumors with a predominant mucinous component may not display high [^{18}F]FDG uptake. Therefore, there is great interest in developing novel PET probes to target more specific biomarkers of cancer proliferation.

On the other hand, evaluation of patients with suspected infection/inflammation constitutes per se a current indication for PET with [^{18}F]FDG.

Finally, although the primary energy substrate for cardiomyocytes is fatty acid, these cells also utilize glucose as a metabolic substrate. In the assessment of myocardial viability, ischemic myocardium, which has downregulated contractile function, utilizes more glucose than surrounding tissue, with an adequate oxygen supply. When comparing the metabolic pattern of myocardium to the distribution of perfusion, viable ischemic regions demonstrate a relative increase in [^{18}F]FDG compared to perfusion and compared to surrounding tissue. Specific preparation protocols have been described to optimize the diagnostic yield of the investigation—mostly based on glucose load inducing raised insulin levels.

3.2.3.2 Free Fatty Acids

The transport rate of free fatty acids (FFAs) in the brain, heart, and tumors is regulated by the FFA concentration in blood. Although FFAs can freely diffuse across cell membranes, specific transporters, such as FATP1 and FATP6, facilitate their transmembrane transport. Inside the cells, FFAs are either metabolized to triglycerides and sterols or transported into the mitochondria for energy production through β-oxidation. Carnitine palmityl-transferase I and II (CPT I–II) transport fatty Acyl-CoA from the cell cytosol into mitochondria, and oxidation generates acetyl-CoA for the Krebs cycle to produce energy (ATP). In the cytosol of normal cells, acetyl-CoA is converted to malonyl-CoA by acetyl-CoA carboxylase inhibitors reducing the CPT activity and transport of FFAs into the mitochondria. In tumor tissue, although FFA synthesis is increased to match the energy demand linked to the enhanced proliferation rate, the mitochondrial oxidation pathway is altered, and energy production is shifted toward glucose utilization. This phenomenon favors FFA utilization for production of phospholipids and sterols.

FFA consumption can be investigated with PET imaging by tracing acetate metabolism through the use of *[^{11}C]acetate* (Fig. 3.15). Acetate is transported into the normal cell by the monocarboxylate transporter; once inside the cell, [^{11}C]acetate can enter the Krebs cycle, to be rapidly converted to tricarboxylic acids intermediates and eventually to [^{11}C]CO_2, which can be found in the exhaled air. In this regard, [^{11}C]acetate washout has been intensively studied as an index of

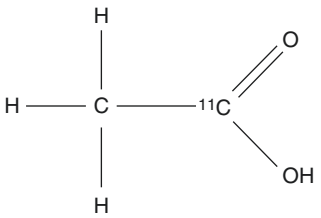

Fig. 3.15 Chemical structure of [^{11}C]acetate

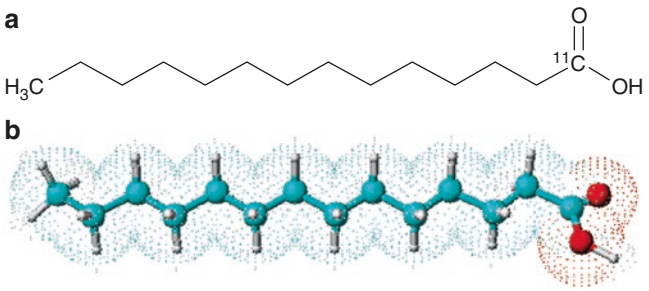

Fig. 3.16 Chemical structure (**a**) and tridimensional molecular representation (**b**) of [^{11}C]palmitate. Color codes for constituting elements: *light blue*, C; *red*, O (*reproduced with permission from: Volterrani D, Erba PA, Mariani G, eds. Fondamenti di medicina nucleare – Tecniche e applicazioni. Milan: Springer; 2010*)

the Krebs cycle activity. Since [^{11}C]acetate has a high first-pass extraction, it is particularly suitable to assess myocardial blood flow.

There is however another possible metabolic pathway for [^{11}C]acetate, i.e., conversion to acetyl-CoA by acetyl-CoA synthase (present both in the cytosol and mitochondria) and FFA synthase. Fatty acid synthase is expressed predominantly in hepatocytes, but is also present in the white adipose, endometrial, and intestinal tissues and is overexpressed in several malignancies including prostate and lung cancers. Since overexpression of the enzyme is associated with tumor aggressiveness and poor prognosis, [^{11}C]acetate has been used clinically for PET imaging in patients with prostate, renal, brain, or hepatocellular tumors or other cancers with low GLUT expression and [^{18}F]FDG uptake. However, important discrepancies have been reported on the clinical usefulness of PET with [^{11}C]acetate, probably due to the use of non-standardized imaging protocols. A recently published meta-analysis of [^{11}C]acetate PET in prostate cancer concluded that further high-quality studies are needed to assess its usefulness in clinical practice.

The fatty acid analog *14-(R,S)-^{18}F-fluoro-6-thia-heptadecanoic acid* (^{18}F-FTHA) can be used to assess fatty acid metabolism. ^{18}F-FTHA is a long-chain FFA that is taken up by tissues to enter mitochondria or to be incorporated into complex lipids. In mitochondria, ^{18}F-FTHA undergoes the initial steps of β-oxidation, but it then remains trapped because further oxidation is blocked by its sulfur heteroatom. Because of this property, ^{18}F-FTHA has provided good target-to-background signal on PET images and appears promising in the investigation of tumor fatty acid metabolism. Unfortunately, tracer kinetics is not completely elucidated, and the existing information is mostly limited to the heart, skeletal muscle, and liver, mainly derived from studies in small animals.

[^{11}C]Palmitate (Fig. 3.16) may in principle be preferable to ^{18}F-FTHA to trace FFA metabolism, because it is indistinguishable from endogenous palmitate and therefore reflects the rapid and somewhat complex metabolism of fatty acids. Unfortunately, this property is also a major obstacle to derive accurate estimates of [^{11}C]palmitate kinetics. In fact, upon i.v. injection [^{11}C]palmitate undergoes rapid oxidation, storage, or even redistribution as radiolabeled triglycerides. This results in the formation of several different ^{11}C-labeled metabolites, which must be identified and subtracted from blood activity in order to obtain a correct input function. Therefore, dynamic studies with [^{11}C]palmitate require frequent blood sampling and cumbersome identification and measurements of ^{11}C-metabolites, which may be estimated directly or through indirect assessment based on the appearance of [^{11}C]CO_2 in the blood. As a consequence, the use of [^{11}C]palmitate in humans is restricted to clinical investigations.

Key Learning Points

- [^{18}F]FDG is a glucose analog that follows the glycolytic pathway, accumulates into the cells, and is not metabolized further.
- [^{18}F]FDG can be used to characterize neurological disorders, to assess myocardial viability, and to identify sites of inflammation/infection.
- The predominant use of [^{18}F]FDG is in oncology to trace the increased glycolytic activity of tumor masses (Warburg effect). PET imaging allows diagnosis, staging of the disease, and response to therapy.
- Free fatty acid consumption and utilization can be investigated in vivo with PET using [^{11}C]acetate, ^{18}F-fluorothiaheptanoic acid, and [^{11}C]palmitate.
- [^{11}C]Acetate is most frequently employed in clinical studies to assess the increased lipid metabolism in tumor and to evaluate myocardial blood flow. Its use is confined to PET centers with on-site cyclotron facilities.

3.2.4 Substrates for Phospholipid Synthesis

Choline is necessary for the synthesis of phospholipids in cell membranes, as well as for methyl metabolism, cholinergic neurotransmission, transmembrane signaling, and lipid-cholesterol transport and metabolism. The biochemical process explored with choline-based PET tracers is membrane synthesis. After entering into cells through the activity of specific transporters, choline is phosphorylated by the enzyme choline kinase (CK). Phosphorylcholine is further incorporated into phosphatidylcholine (lecithin) that is a major phospholipid of all membranes. Through choline dehydrogenase and betaine aldehyde dehydrogenase, phosphorylcholine is metabolized into betaine and finally, through the enzyme choline acetyltransferase, into acetylcholine.

Since cell membranes duplicate at the same rate as the rate of cell duplication, tumor cells incorporate choline rapidly to meet the need of rapid synthesis of cell membranes. The levels of choline and phosphorylcholine are increased in a variety of tumor cells, mirroring enhanced activation of choline uptake and phosphorylation. In slowly proliferating tumors, high phospholipid metabolite levels are related to alterations in choline transport, incorporation, and utilization. Interestingly, malignant transformation is associated with an increase in the cellular transport and phosphorylation of choline, as well as in increased expression of CK.

Choline can be directly labeled with ^{11}C (yielding *[^{11}C] choline*, which is biochemically indistinguishable from native choline), or alternatively ^{18}F can be used to label suitable choline analogs. The successful use of [^{11}C]choline (Fig. 3.17) as a PET tracer for the detection of prostate cancer was reported in 1998, leading to clinical investigations in patients with other malignancies as well, including brain tumors, lung cancer, esophageal cancer, colon cancer, bladder cancer, and other types of cancers. Physiologic uptake of [^{11}C]choline is observed in all glands (pituitary, salivary glands, pancreas), as well as in the liver, kidney, bowel, and stomach. As with all ^{11}C-labeled tracers, the short physical half-life of ^{11}C (20 min) limits the use of [^{11}C]choline to PET centers that have an on-site cyclotron facility. To overcome these limitations, analogs of choline labeled with ^{18}F have been developed, such as *^{18}F-fluoro-ethylcholine* (Fig. 3.18) and *^{18}F-fluoro-methylcholine* (Fig. 3.19); these two tracers have similar biodistribution patterns, with higher urinary excretion than [^{11}C]choline. In particular, ^{18}F-fluoro-methylcholine mirrors metabolic processing of native choline more closely than ^{18}F-fluoro-ethylcholine and is therefore the PET imaging agent commercially available.

[^{11}C]choline and ^{18}F-fluoro-methylcholine are part of the current armamentarium for the detection of prostate cancer

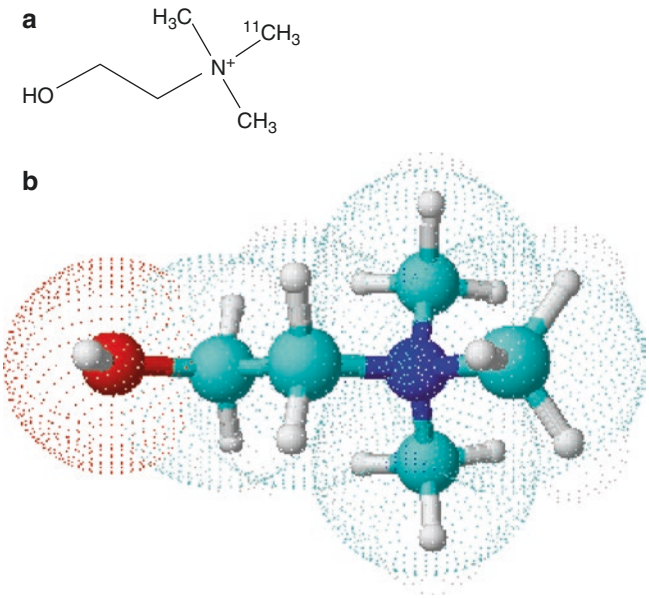

Fig. 3.17 Chemical structure (**a**) and tridimensional molecular representation (**b**) of [^{11}C]choline. Color codes of constituting elements: *red*, O; *gray*, H; *light blue*, C; *deep blue*, N (*reproduced with permission from: Volterrani D, Erba PA, Mariani G, eds. Fondamenti di medicina nucleare – Tecniche e applicazioni. Milan: Springer; 2010*)

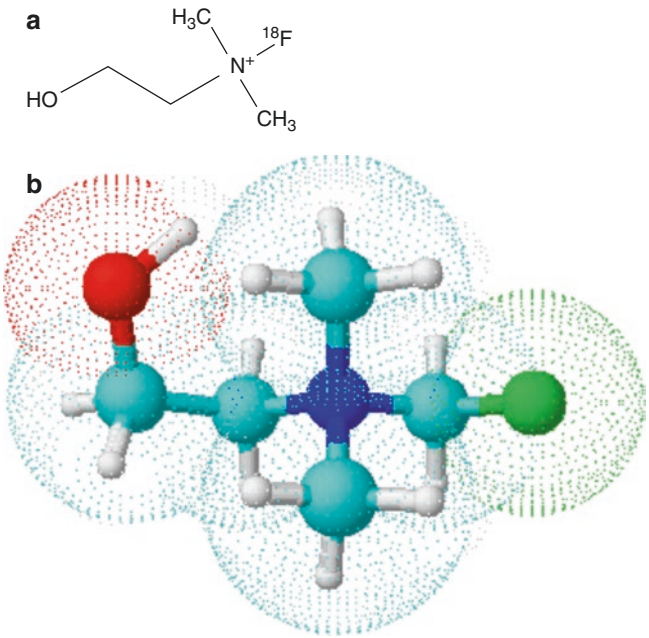

Fig. 3.18 Chemical structure (**a**) and tridimensional molecular representation (**b**) of ^{18}F-fluoro-ethylcholine. Color codes of constituting elements: *red*, O; *gray*, H; *light blue*, C; *deep blue*, N; *green*, ^{18}F (*reproduced with permission from: Volterrani D, Erba PA, Mariani G, eds. Fondamenti di medicina nucleare – Tecniche e applicazioni. Milan: Springer; 2010*)

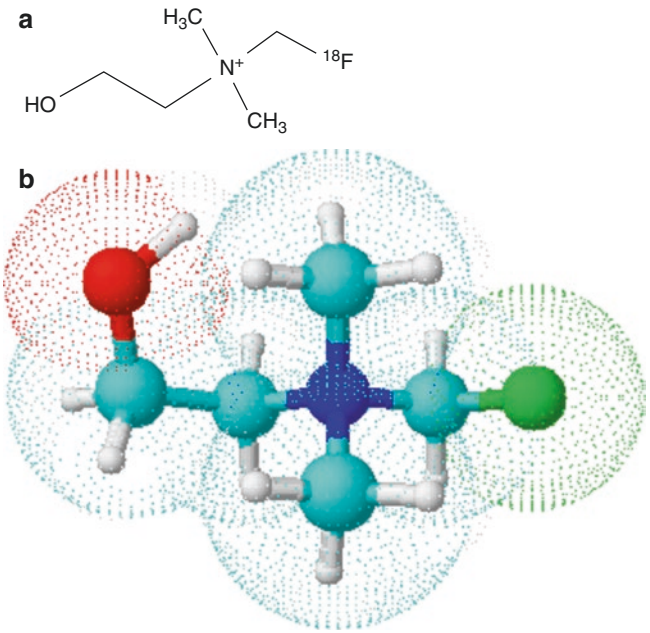

Fig. 3.19 Chemical structure (**a**) and tridimensional molecular representation (**b**) of ^{18}F-fluoro-methylcholine. Color codes of constituting elements: *red*, O; *gray*, H; *light blue*, C; *deep blue*, N; *green*, ^{18}F (*reproduced with permission from: Volterrani D, Erba PA, Mariani G, eds. Fondamenti di medicina nucleare – Tecniche e applicazioni. Milan: Springer; 2010*)

and, to a lesser degree, for brain, bladder, and non-small cell lung cancers. In particular, early prostate cancer cells frequently display low expression of the GLUT transport system and low glucose consumption, thus resulting in frequent false negative results on [^{18}F]FDG PET. Instead, PET with choline radiotracers is particularly effective in patients with prostate cancer, high Gleason scores (8–10), and high or increasing level of the prostate-specific antigen (PSA). PET with ^{18}F-fluoro-methylcholine is currently used mostly to monitor the recurrence of prostate cancer after treatment with radical prostatectomy, radiotherapy, or hormonal therapy alone, as it yields useful information for patient management.

Key Learning Points

- Because of their enhanced proliferation, tumor cells utilize greater amounts than normal cells of substrates for the synthesis of cell membranes.
- Phospholipids are essential components of cell membranes.
- Phospholipid precursors enter cells through the action of specific transporters, after which they are usually phosphorylated by specific kinases.
- Choline is one of the main precursors for the synthesis of phospholipids in cell membranes, as well as for methyl metabolism, cholinergic neurotransmission, transmembrane signaling, and lipid-cholesterol transport and metabolism.
- In patients with malignancies, choline-based radiopharmaceuticals are utilized to explore with PET imaging the biochemical process of membrane synthesis.
- [^{11}C]Choline is biochemically indistinguishable from native choline and has been widely used for PET imaging, mainly in patients with prostate cancer among other malignancies that do not overexpress the GLUT system.
- The logistic limitations of ^{11}C linked to its short physical half-life (20 min, which restrict its use to centers with an in-house cyclotron) have been overcome with the use of ^{18}F-labeled choline analogs, such as ^{18}F-fluoro-ethylcholine and ^{18}F-fluoro-methylcholine.

3.2.5 Substrates for Protein Synthesis

As the basic building blocks of proteins, amino acids have many physiologic roles, primarily for the synthesis of structural proteins during cell replication, but also interacting with energy substrates, and finally as precursors of bioactive molecules (hormones, mediators of cell-to-cell interaction, etc.). In cancer cells the levels of protein synthesis are increased for survival, replication, and invasion. As a consequence, amino acid transport across plasma membranes by specific transporters is upregulated. Therefore, molecular imaging of amino acid metabolism is an attractive target, especially for malignancies where PET imaging with [^{18}F]FDG has certain limitations.

In the past, the most widely used amino acid for tumor imaging with PET was *[^{11}C]methionine* (Fig. 3.20). Although the mechanism of uptake in tumor cells is not completely elucidated, it probably reflects substrate transport across the tumor cell membrane and does not seem to be affected by hypoxia. [^{11}C]Methionine has been used mostly for investigating brain tumors, where the use of [^{18}F]FDG may be problematic because of the physiologically high uptake in the normal brain gray matter. Instead, background uptake of this radiotracer in the normal brain is very low, and non-tumor conditions, such as edema and fibro-necrosis, do not exhibit significant uptake. However, despite the high target-to-background ratio, [^{11}C]methionine cannot be used for differentiating benign from malignant cancers. Whereas, [^{11}C]methionine has advantages in assessing whether there is

tumor recurrence versus posttreatment fibrosis/necrosis even in patients with low-grade brain cancers, in whom [^{18}F]FDG is not very helpful. The reported sensitivities and specificities in the evaluation of the remnant or the relapse of the disease are 87% and 89%, respectively.

*O-(2-^{18}F-fluoroethyl)-*L*-tyrosine* (^{18}F-FET; see Fig. 3.21) was developed in the 1990s to provide an ^{18}F-labeled amino acid PET tracer with a longer physical half-life than the ^{11}C-compounds, more suitable for routine clinical applications also in nuclear medicine centers without an in-house cyclotron. The exact transport mechanisms of ^{18}F-FET (which is currently the most widely used amino acid tracer for brain tumor imaging) are not fully clarified. ^{18}F-FET belongs to the class of amino acids transported across the cell membrane via specific L-amino acid transporters, a system that is especially active at the blood-brain barrier. Another possible mechanism is a Na^+-dependent activity associated to transmembrane transport. Cancers typically exhibit higher ^{18}F-FET uptake than nonneoplastic lesions, which may be helpful in differential diagnosis. A meta-analysis of 13 ^{18}F-FET PET studies with a total of 462 patients yielded a pooled 82% sensitivity and 76% specificity for the diagnosis of primary brain tumors (gliomas). However, diagnostic applications in non-oncological diseases with increased uptake of ^{18}F-FET have been described, including brain abscesses, epilepsy, demyelinating processes, and in tissue adjacent to cerebral ischemia or hematomas. Thus, ^{18}F-FET PET may be helpful in the preliminary assessment of equivocal brain lesions, but histological evaluation remains necessary under most circumstances to provide a definite diagnosis.

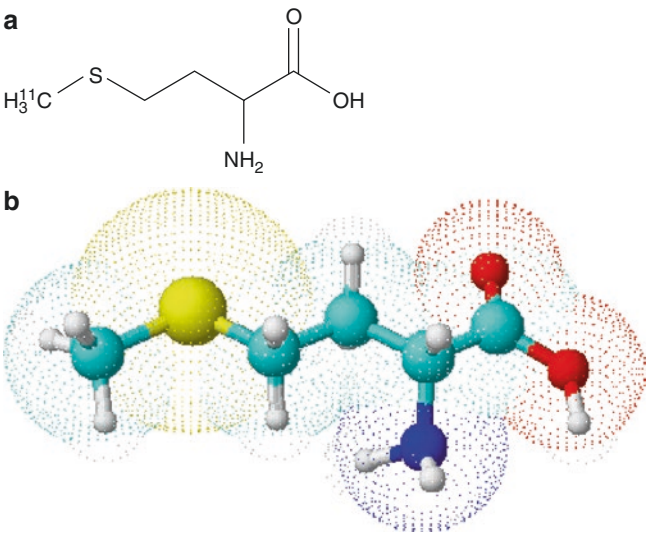

Fig. 3.20 Chemical structure (**a**) and tridimensional molecular representation (**b**) of [^{11}C]methionine. Color codes of constituting elements: *red*, O; *gray*, H; *light blue*, C; *deep blue*, N; *yellow*, S (*reproduced with permission from: Volterrani D, Erba PA, Mariani G, eds. Fondamenti di medicina nucleare – Tecniche e applicazioni. Milan: Springer; 2010*)

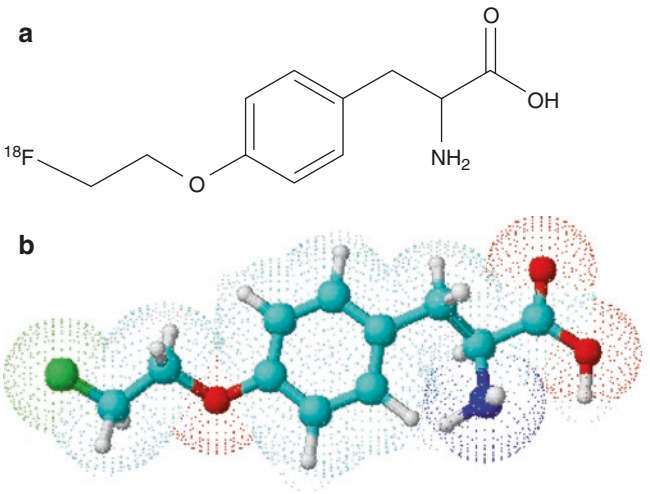

Fig. 3.21 Chemical structure (**a**) and tridimensional molecular representation (**b**) of *O*-(2-^{18}F-fluoroethyl)-L-tyrosine. Color codes of constituting elements: *red*, O; *gray*, H; *light blue*, C; *deep blue*, N; *green*, ^{18}F (*reproduced with permission from: Volterrani D, Erba PA, Mariani G, eds. Fondamenti di medicina nucleare – Tecniche e applicazioni. Milan: Springer; 2010*)

Furthermore, PET with ^{18}F-FET is useful to assess response of brain tumors to therapy at an early stage of treatment with high accuracy, as well as to detect tumor recurrence during the follow-up. Such assessments can be problematic even when high-resolution MR morphological imaging is available.

The synthetic amino acid *anti-1-amino-3-^{18}F-fluorocyclobutanecarboxylic acid* (^{18}F-FACBC or ^{18}F-fluciclovine; see Fig. 3.22) is also transported through the L-amino acid transporters (LAT) as well as by the system of alanine-serine-cysteine transporters (ASCT), which is primarily involved in the transmembrane transport of glutamine. In many cancers, including prostate cancer, a metabolic shift occurs when glutamine is used as an alternative energy source instead of glucose. This metabolic shift is associated with overexpression of the amino acid transporters (LAT1

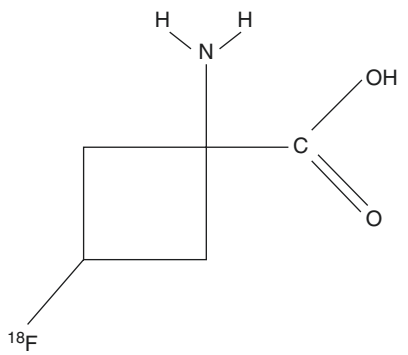

Fig. 3.22 Chemical structure of *Anti*-1-amino-3-^{18}F-fluorocyclobutanecarboxylic acid (also known as ^{18}F-FACBC, or ^{18}F-fluciclovine)

and ASCT2) and with a more aggressive pattern of growth of prostate cancer. ^{18}F-fluciclovine can be used to trace in vivo the increased activity of membrane transporters and for identifying high-risk patients. Furthermore, the biodistribution of ^{18}F-fluciclovine is advantageous versus [^{18}F]FDG, because low urinary excretion helps images interpretation of the PET images in the pelvis and abdomen. The higher diagnostic performance of ^{18}F-fluciclovine versus conventional imaging, especially for recurrent prostate cancer, has been demonstrated by different clinical studies, whereas a relatively low specificity limits the potential role of the radiotracer in the primary diagnosis of prostate cancer.

The amino acid dihydroxyphenylalanine (DOPA) contains two hydroxyl groups on the third and fourth positions of the phenol ring; for PET imaging, it can be labeled with either ^{11}C to yield the [^{11}C]DOPA tracer or with ^{18}F to yield *3,4-dihydroxy-6-^{18}F-fluoro-phenylalanine* (or ^{18}F-DOPA; see Fig. 3.23). L-DOPA is the precursor of the neurotransmitters dopamine, norepinephrine, and epinephrine (altogether known as catecholamines). Therefore, PET with ^{18}F-DOPA is used for functional imaging of pathologies in which enhanced intracellular transport and decarboxylation of DOPA are the diagnostic targets, allowing visualization of sympathetic cells. ^{18}F-DOPA enters cells through the amino acid transport systems (LAT1) for large neutral amino acids, which are present in nearly all cells. The enzyme aromatic amino acid decarboxylase (AADC) metabolizes ^{18}F-DOPA to 6-^{18}F-fluorodopamine, which in turn can be stored in secretory vesicles by the vesicular monoamine transporter (VMAT), thus remaining effectively trapped inside the cell. Alternatively, 6-^{18}F-fluorodopamine can be degraded by other enzymes, such as monoamine oxidase (MAO), yielding breakdown products that are rapidly cleared from the cell.

In order to prevent early decarboxylation of ^{18}F-DOPA to 6-^{18}F-fluorodopamine in extracerebral tissues and thus improve image quality, it is possible to administer carbidopa [L-α-hydrazino-α-methyl-β-(3,4-dihydroxyphenyl) propionic acid], an AADC inhibitor. This enhances striatal uptake by increasing the ^{18}F-DOPA concentration in the plasma and decreasing renal excretion. Carbidopa is used also to enhance ^{18}F-DOPA uptake by tumor cells when imaging patients with neuroendocrine tumors (NETs). Physiological uptake/accumulation of ^{18}F-DOPA occurs in the basal ganglia, liver, pancreas, adrenal glands, gallbladder, biliary tract, kidneys, ureters, and urinary bladder.

PET/CT with ^{18}F-DOPA PET/CT is used clinically mainly to assess the extent of degeneration of presynaptic dopaminergic neurons (as in Parkinson's disease), to image brain tumors, and to image well-differentiated NETs, such as medullary thyroid cancer, pheochromocytoma, paraganglioma, and congenital hyperinsulinemic hypoglycemia.

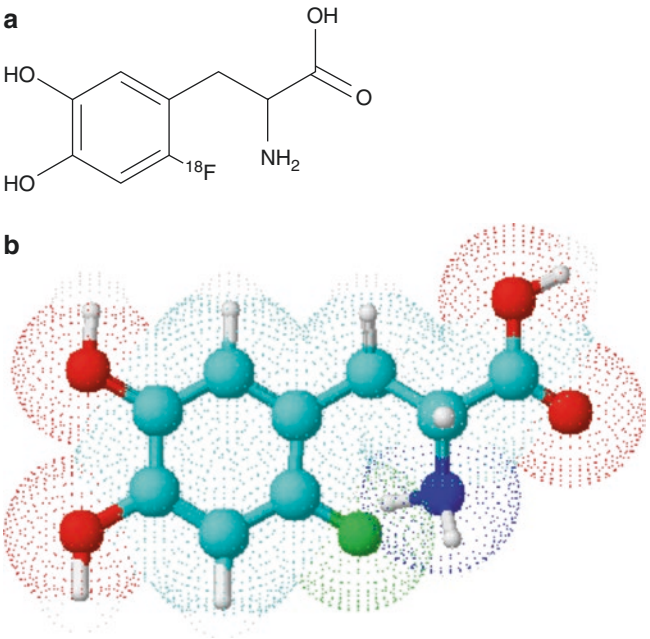

Fig. 3.23 Chemical structure (**a**) and tridimensional molecular representation (**b**) of 3,4-dihydroxy-6-^{18}F-fluoro-phenylalanine (or ^{18}F-DOPA). Color codes of constituting elements: *red*, O; *gray*, H; *light blue*, C; *deep blue*, N; *green*, ^{18}F (*reproduced with permission from: Volterrani D, Erba PA, Mariani G, eds. Fondamenti di medicina nucleare – Tecniche e applicazioni. Milan: Springer; 2010*)

Key Learning Points

- Phospholipid synthesis and turnover can be investigated with PET using [^{11}C]choline, ^{18}F-fluoroethylcholine, and ^{18}F-fluoro-methylcholine.
- PET with positron-labeled choline tracers is particularly effective in tumors with low metabolic rate and mostly used to monitor the recurrence of prostate cancer after treatment with radical prostatectomy, radiotherapy, or hormonal therapy.
- [^{11}C]Methionine is the most widely used amino acid for tumor imaging with PET, particularly for brain cancers. It is supposed to reflect substrate transport across the tumor cell membrane and does not seem to be affected by hypoxia.
- ^{18}F-fluoro-ethyl-tyrosine is an amino acid transported across the cell membrane via specific L-amino acid transporters that has high diagnostic accuracy for the diagnosis of primary brain tumors (gliomas) and their recurrence after treatment.
- ^{18}F-DOPA is a precursor of neurotransmitters (catecholamines), and it is mainly used to assess the extent of degeneration of presynaptic dopaminergic neurons (as in Parkinson's disease), to image brain tumors, and to image well-differentiated neuroendocrine tumors.

3.2.6 Substrates for DNA Synthesis

Cell proliferation as a biological target is particularly appealing in cancer imaging, as it is a characteristic feature of tumor development and growth. The nucleoside thymidine is utilized for DNA synthesis by proliferating cells during the S-phase of the cell cycle; unlike other nucleosides, thymidine is not incorporated into RNA. There are two main pathways leading to DNA synthesis. The "salvage pathway" recycles nucleoside precursors from outside the cell, while the de novo endogenous pathway methylates deoxyuridine monophosphate to form thymidine monophosphate through the action of thymidylate synthetase. The "salvage" pathway is more specific for DNA synthesis than the de novo pathway, because precursors of the latter are also utilized for RNA synthesis.

[^{11}C]Thymidine (Fig. 3.24) has initially been used for PET imaging of cell proliferation in vivo. However, this radiotracer is suboptimal for PET imaging because its rapid catabolism results in the release and recirculation of labeled metabolites in the blood; therefore, arterial blood sampling, analysis of plasma metabolites, and complex compartmental modeling are required for image interpretation and quantitation.

The radiolabeled thymidine analog *^{18}F-fluoro-3′-deoxy-3-L-fluorothymidine* (^{18}F-FLT; see Fig. 3.25) is more suitable for clinical use, both because of the longer physical half-life of the radionuclide and because it is more resistant to phosphorylase-mediated degradation in vivo. ^{18}F-FLT is taken up by cells through the same mechanisms as native thymidine. Transmembrane transport is facilitated by nucleoside transporters, especially the human equilibrative nucleoside transporter 1 (hENT1), whose expression may be upregulated in tumor cells. ^{18}F-FLT follows the salvage pathway of DNA synthesis and, like thymidine, undergoes phosphorylation by thymidine kinase 1 (TK1), to form ^{18}F-FLT-monophosphate. In quiescent cells, TK1 activity is virtually absent, while it is increased in proliferating cells, particularly in the S-phase of the cell cycle. ^{18}F-FLT-monophosphate may be phosphorylated into ^{18}F-FLT-diphosphate and ^{18}F-FLT-triphosphate. At this point of the pathway to DNA synthesis, ^{18}F-FLT metabolism differs from that of native thymidine, as ^{18}F-FLT-triphosphate is not incorporated into DNA and thus remains trapped in the cytosol. The rate-limiting step for intracellular ^{18}F-FLT accumulation is initial phosphorylation by TK1. Phosphorylated ^{18}F-FLT can be dephosphorylated by the enzyme 5′-deoxynucleotidase, although this reaction occurs at a slow rate. Thus, the accumulation of ^{18}F-FLT-monophosphate, diphosphate, and triphosphate nucleotides forms the basis for PET imaging. ^{18}F-FLT is catabolized in the liver with the production of ^{18}F-FLT-glucuronide, which is released in the blood and excreted through the urinary system. Therefore, ^{18}F-FLT-glucuronide is the only metabolite in blood to be considered for kinetic modeling. In addition to TK1 activity, uptake and retention of ^{18}F-FLT are influenced also by the balance between the salvage pathway and de novo DNA synthesis.

The intensity of ^{18}F-FLT uptake correlates with the extent Ki-67 expression, a histopathologic marker of cell proliferation. In various cancers (such as lung, breast, colon cancers as well as lymphomas), ^{18}F-FLT uptake has been demonstrated to be more tumor-specific than [^{18}F]FDG uptake with regard to inflammatory lesions, even though some ^{18}F-FLT uptake can be detected also in some inflammatory tissues involving proliferating immune cells. Interest is growing also in the use of this tracer to assess response to antitumor

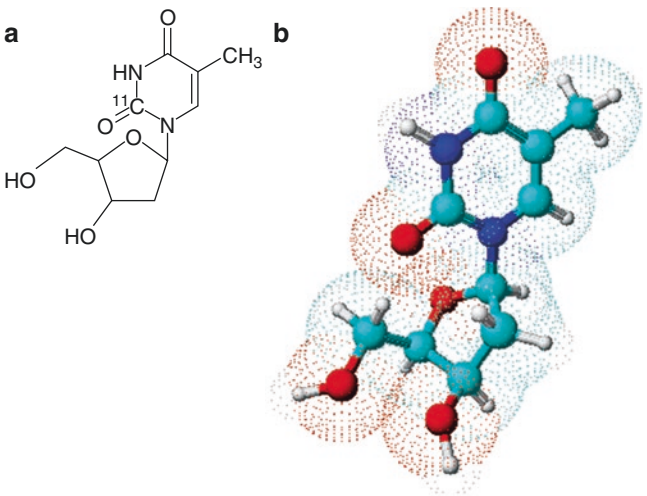

Fig. 3.24 Chemical structure (**a**) and tridimensional molecular representation (**b**) of [^{11}C]thymidine. Color codes of constituting elements: *red*, O; *gray*, H; *light blue*, C; *deep blue*, N (*reproduced with permission from: Volterrani D, Erba PA, Mariani G, eds. Fondamenti di medicina nucleare – Tecniche e applicazioni. Milan: Springer; 2010*)

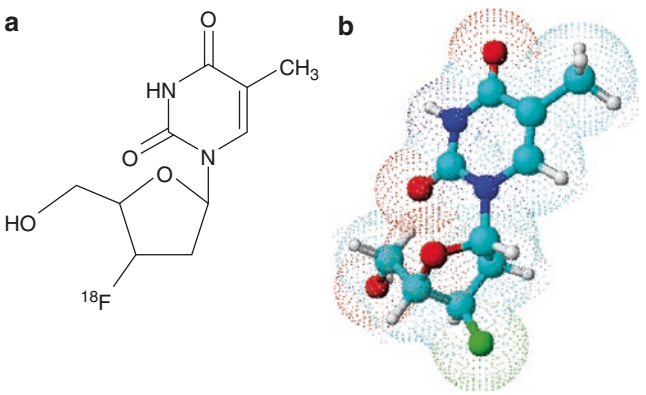

Fig. 3.25 Chemical structure (**a**) and tridimensional molecular representation (**b**) of ^{18}F-fluoro-3′-deoxy-3-L-fluorothymidine (^{18}F-FLT). Color codes of constituting elements: *red*, O; *gray*, H; *light blue*, C; *deep blue*, N; *green*, ^{18}F (*reproduced with permission from: Volterrani D, Erba PA, Mariani G, eds. Fondamenti di medicina nucleare – Tecniche e applicazioni. Milan: Springer; 2010*)

therapy. Since ^{18}F-FLT uptake in the cancer mass is considered to trace the degree of DNA synthesis and cell proliferation, effective treatment should reduce tracer uptake. This rationale has been demonstrated to hold true, as several publications have reported that the extent of ^{18}F-FLT uptake reflects the effects of anticancer therapies and is related to changes in proliferation rates as determined by ex vivo analyses. ^{18}F-FLT uptake has potential as an imaging biomarker for response assessment.

Key Learning Points

- [^{11}C]Thymidine and ^{18}F-FLT are taken up by cells through the same mechanisms as native thymidine and can be used to study DNA synthesis and cell proliferation in vivo.
- The rate-limiting step for intracellular ^{18}F-FLT accumulation is phosphorylation by thymidine kinase 1, whose activity is increased in proliferating cells.
- The intensity of ^{18}F-FLT uptake correlates with the extent Ki-67 expression, a histopathologic marker of cell proliferation.
- ^{18}F-FLT uptake has a high potential as an imaging biomarker for response assessment.

3.2.7 Positron-Emitting Agents Based on Ligand-Acceptor Interaction

3.2.7.1 Somatostatin Receptor-Based Agents

Somatostatin receptors, which are structurally related membrane glycoproteins, are expressed in various normal tissues, including the central nervous system (CNS), anterior pituitary, thyroid, pancreas, gastrointestinal tract, spleen, and adrenals. Five different subtypes of somatostatin receptors (SSTR1–SSTR5) have been characterized, expressed with variable density on tumor cell surface among various types of tumors. Expression of SSTR1 and SSTR2 are predominant in gastro-entero-pancreatic neuroendocrine tumors (GEP-NETs).

Several ^{68}Ga-labeled somatostatin analogs have been evaluated for PET imaging of neuroendocrine tumors, based on the use of a suitable chelator for binding the radiometal, i.e., 1,4,7,10-tetraazacyclododecane-*N*,*N*′,*N*″,*N*‴-tetraacetic acid (or DOTA). ^{68}Ga-[DOTA^0,Tyr^3]octreotide (*^{68}Ga-DOTA-TOC*) is the first ^{68}Ga-labeled somatostatin analog developed for clinical use in cancer patients. Other ^{68}Ga-labeled somatostatin analogs have been developed, with either increased sensitivity or more favorable affinity profile, such as ^{68}Ga-[DOTA,1-Nal^3] octreotide (*^{68}Ga-DOTA-NOC*) and ^{68}Ga-[DOTA^0,Tyr^3]octreotate (*^{68}Ga-DOTA-TATE*; see Fig. 3.26). These PET radiopharmaceuticals provide excellent image quality with better spatial resolution (3–5 mm) and diagnostic performance than the γ-emitting analogs (e.g., ^{111}In-DTPA-pentetreotide), particularly if the tumor lesions are embedded in organs with high physiologic uptake (e.g., the liver) and in case of small lesions (<1.5 cm). These molecular probes differ in their affinity profile for the somatostatin receptor subtypes. In particular, the affinity of ^{68}Ga-DOTA-TATE for the SSTR2 subtype is approximately tenfold higher than that of ^{68}Ga-DOTA-TOC. Whereas, ^{68}Ga-DOTA-NOC has high affinity for the SST2, SSTR3, and SSTR5 subtypes.

^{68}Ga-labeled somatostatin analogs have mostly been used for imaging of thoracic and GEP-NETs. They can be used also for imaging of focal congenital hyperinsulinism, breast cancer, medulloblastoma, supratentorial primitive neuroectodermal tumors, meningioma, neuroblastoma, pheochromocytoma/paraganglioma, and potentially in all solid tumors that express somatostatin receptors.

3.2.7.2 Estrogen and Androgen Receptor-Based Agents

^{18}F-Fluoroestradiol (^{18}F-FES) binds to the estrogen receptors and thus allows in vivo mapping of the estrogen receptor status of tumor lesions. This is particularly interesting in breast cancer patients, where ^{18}F-FES has been used to predict response to hormonal therapy.

The androgen analog *16-β-^{18}F-fluoro-5α-dihydrotestosterone* (^{18}F-FDHT) binds with high affinity to the androgen receptor, and promising results have been obtained using this agent for PET imaging in patients with prostate cancer. Assessment of the androgen receptor status could provide important information for patient selection and to predict response to therapy.

3.2.7.3 PSMA-Based Agents

The prostate-specific membrane antigen (PSMA) is a type II integral membrane glycoprotein (100–120 kDa), with an intracellular component, a transmembrane component, and a large extracellular domain, that was first detected in a human prostatic carcinoma cell line. PSMA is a homologue of *N*-acetyl-L-aspartyl-L-glutamate peptidase I, an enzymatic protein which is physiologically active in the central nervous system, where it cleaves the neurotransmitter *N*-acetyl-L-aspartyl-L-glutamate into *N*-acetylaspartate and glutamate. In malignant tissue, it has been suggested that PSMA is involved in angiogenesis, as increased PSMA is overexpressed in the stroma adjacent to neovasculature of solid tumors. Due to its selective overexpression in 90–100% of prostate cancer lesions, PSMA is a reliable tissue marker for prostate cancer and is considered an ideal target for theranostic applications. Increased PSMA expression is correlated with increased tumor grade, advanced pathological stage, aneuploidy, and biochemical recurrence. Most importantly, PSMA is overexpressed when prostate cancer lesions become

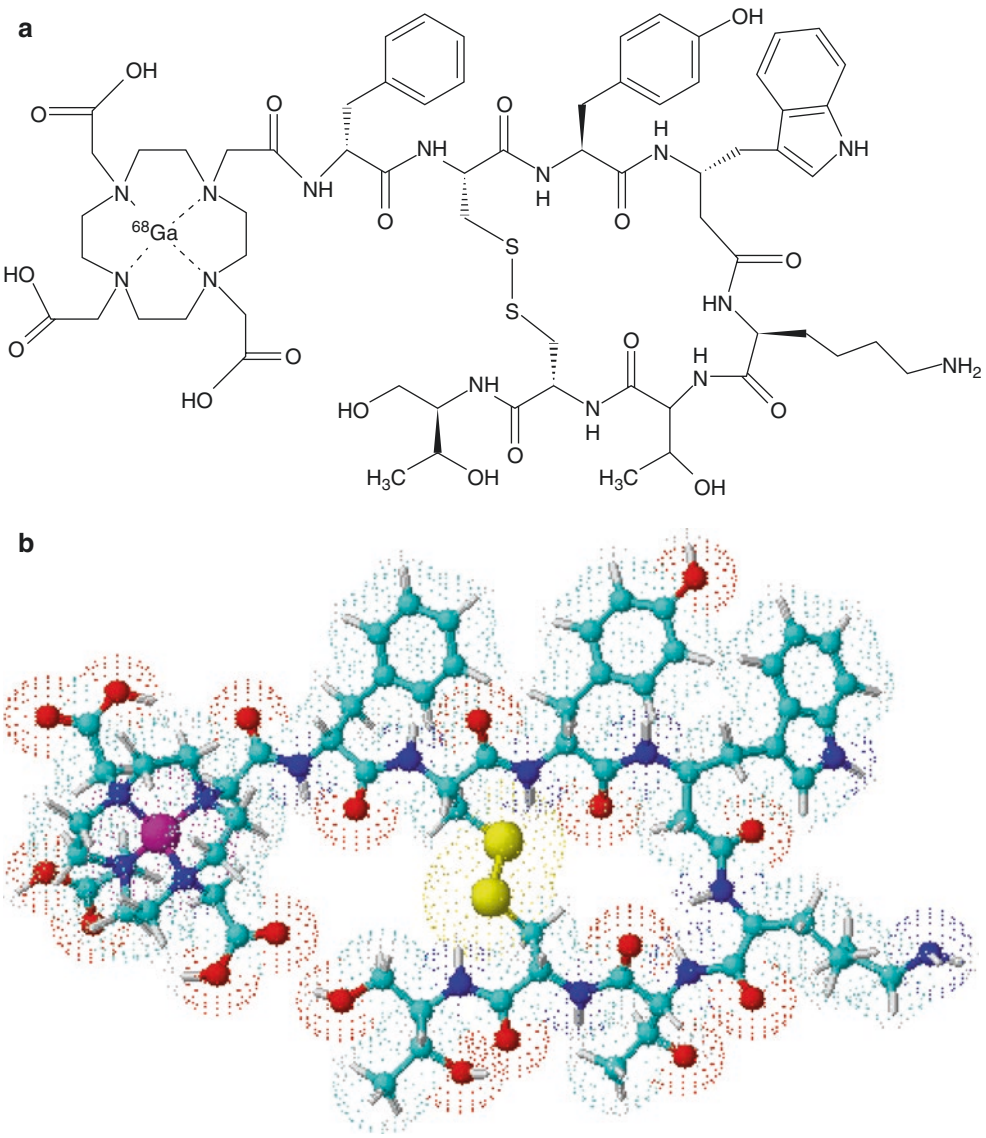

Fig. 3.26 Chemical structure (**a**) and tridimensional molecular representation (**b**) of ^{68}Ga-[DOTA^{0},Tyr^{3}] octreotate (^{68}Ga-DOTA-TATE). Color codes of constituting elements: *red*, O; *gray*, H; *light blue*, C; *deep blue*, N; *yellow*, S; *fuchsia*, ^{68}Ga (*reproduced with permission from: Volterrani D, Erba PA, Mariani G, eds. Fondamenti di medicina nucleare – Tecniche e applicazioni. Milan: Springer; 2010*)

androgen-independent. This feature makes PSMA particularly valuable, since it has potential as an early indicator of tumor progression after androgen-deprivation therapy. Moreover, PSMA expression is a prognostic factor for disease recurrence.

Although its denomination suggests a high degree of prostate specificity, PSMA is also expressed in several normal tissues (such as the salivary glands, proximal renal tubules, epididymis, ovary, the luminal side of the ileum-jejunum, and astrocytes in the CNS), as well as in the neovasculature of tumors other than prostate cancer, including bladder, pancreas, lung, and kidney cancers.

Antibody-based PSMA PET agents targeting the extracellular domain of PSMA include ^{64}Cu- and ^{89}Zr-labeled PSMA antibodies and antibody fragments, as well as ^{64}Cu-labeled aptamers. More recently, small high-affinity ligands acting as PSMA antagonists have been labeled with ^{68}Ga, ^{18}F, ^{11}C, ^{64}Cu, and ^{86}Y. One of these ligands, *^{68}Ga-Glu-urea-Lys(Ahx)-HBED-CC* (also known as *^{68}Ga-PSMA-11*), is currently the most extensively validated PSMA-based PET probe for clinical use in prostate cancer patients. HBED-CC stands for *N*,*N*′-Bis(2-hydroxy-5-(ethylene-beta-carboxy)benzyl)ethylenediamine *N*,*N*′-diacetic acid, a highly effective chelator for labeling various compounds with radiometals such as ^{68}Ga (among others). ^{68}Ga-PSMA-11 has a strong binding affinity to PSMA and is efficiently internalized into prostate cancer cells. Excellent contrast on the images is seen in 1 h postinjection, even in patients with low PSA levels.

Further modifications of PSMA-11 have resulted in the production of a novel small PSMA-ligand, *^{68}Ga-PSMA-617*, that has a significantly higher binding affinity to PSMA associated with a highly efficient internalization into prostate cancer cells. In addition to ^{68}Ga, PSMA-617 can be labeled

with ^{111}In, ^{177}Lu, and ^{90}Y and therefore may potentially be used for imaging as well as for therapy.

PSMA ligands labeled with ^{18}F (still in an experimental phase of investigation) should result in improved spatial resolution (due to the shorter positron range in tissues of ^{18}F versus ^{68}Ga) and more accurate quantitation. *N-[N-[(S)-1,3-dicarboxypropyl]carbamoyl]-4-^{18}F-fluorobenzyl-*L*-cysteine* (*^{18}F-DCFBC*) is a first-generation low-molecular-weight, urea-based inhibitor of PSMA which binds to prostate cancer cells that express high PSMA levels. The basic structure is the same as the ^{68}Ga-based agents, although labeling with ^{18}F does not require the presence of a chelator for binding the radiometal.

A novel second-generation PSMA-ligand, *^{18}F-DCFPyL*, has higher affinity and faster clearance than ^{18}F-DCFBC, thus resulting in higher tumor-to-background ratios and better detection of lower-grade or smaller-size prostate cancer compared with ^{18}F-DCFBC. Thus, ^{18}F-DCFPyL represents a highly promising alternative to ^{68}Ga-PSMA-HBED-CC for PET imaging in prostate cancer.

An additional PSMA-based agent, *EuK-Subkff-^{68}Ga-DOTAGA* (^{68}Ga-PSMA I&T) can alternatively also be labeled with ^{177}Lu for therapeutic applications.

Key Learning Points

- ^{68}Ga-labeled somatostatin analogs have been developed for PET imaging of tumor with somatostatin receptors on cell surface.
- ^{68}Ga-DOTA-TOC, ^{68}Ga-DOTA-NOC, and ^{68}Ga-DOTA-TATE are currently used in neuroendocrine cancer PET imaging; these molecular probes differ in their affinity profile for the somatostatin receptor subtypes.
- ^{18}F-Fluoroestradiol and 16-β-^{18}F-fluoro-5α-dihydrotestosterone can be used to map receptor status of tumor lesions and to predict response to hormonal therapy.
- PSMA is a tissue marker for prostate cancer and is considered an ideal target for theranostic applications. Increased PSMA expression is correlated with increased tumor grade, advanced pathological stage, biochemical recurrence, and hormonal therapy resistance.
- ^{68}Ga-labeled PSMA-ligands constitute currently the most extensively validated PET probes for clinical use in prostate cancer patients.

3.2.8 Amyloid Imaging Agents

Alzheimer's disease (AD) is characterized by the formation of insoluble aggregates of β-amyloid protein (β-amyloid plaques) and neurofibrillary tangles (NFTs), which consist of aggregates of hyper-phosphorylated tau protein. Although AD can be suspected (with variable degrees of probability) in subjects presenting with progressive impairment of memory and cognitive functions, a definitive diagnosis has traditionally been based on the post-mortem histologic demonstration of the presence of β-amyloid plaques and NFTs in the brain using either the Congo red stain or the fluorescent dye thioflavin T.

In 2004, an analog of thioflavin T labeled with ^{11}C was developed and was denominated as *^{11}C-Pittsburgh compound B* (*^{11}C-PiB*). ^{11}C-PiB binds to β-amyloid plaques with high affinity, but not to amorphous amyloid plaques nor to NFTs. Non-specific binding is seen mainly in white matter. Specific cortical binding has been reported in more than 90% of patients with a clinical diagnosis of AD, whereas healthy controls have cortical binding 1–5-fold lower than the cerebellum, which usually serves as a reference structure. However, some healthy elderly controls show higher ^{11}C-PiB binding, although the clinical implications of this amyloid deposition are not clear. The apolipoprotein E ε4 allele (APOE4) is frequently associated with β-amyloid plaques and increased uptake of ^{11}C-PiB. Subjects with mild cognitive impairment and ^{11}C-PiB PET-positive scan have a higher risk to develop manifest dementia than those with negative imaging. For several years ^{11}C-PiB has been the most employed PET radiotracer for clinical investigations on brain amyloid and AD, with sensitivities reported to range from 83% to 100% while specificities from 46% to 88%. Suboptimal specificity suggests that ^{11}C-PiB may be a biomarker of other diseases, such as mild cognitive impairment caused by vascular causes or cerebral amyloid angiopathy. Furthermore, the widespread clinical use of ^{11}C-PiB is limited by the very short physical half-life of ^{11}C (about 20 min), which requires the availability of an on-site cyclotron. In order to overcome the above limitations, novel PET radiotracers for β-amyloid plaques imaging have been developed and labeled with ^{18}F.

2-[3-^{18}F-fluoro-4-(methylamino)phenyl]-6-benzothiazolol (or *^{18}F-Flutemetamol*, approved for commercial use as Vizamyl™) is the 3-fluoro-derivative of PiB. This radiotracer has a good safety profile with high affinity to β-amyloid plaques and a good cortical-to-cerebellar uptake ratio. Amyloid imaging with ^{18}F-Flutemetamol is best performed about 90 min after i.v. injection. Cortical uptake can be

assessed qualitatively or semiquantitatively by using relative standardized uptake value ratios (SUVRs), the cerebellar cortex serving as a reference region. PET with ^{18}F-Flutemetamol can discriminate between clinically diagnosed AD or mild cognitive impairment from elderly healthy controls (sensitivity range, 91–97%; specificity range, 85–88%).

(E)-4-(2-(6-(2-(2-(2-(2-([^{18}F-fluoroethoxy)ethoxy)ethoxy)pyridin-3-yl)vinyl)-N-methyl benzenamine (or *^{18}F-Florbetapir*, approved for commercial use as Amyvid™) displays a binding pattern similar to PiB, with a high affinity for β-amyloid plaques. PET images are obtained 60 min after injection. Investigations in patients with variable cognitive status and using histopathology at autopsy as the gold standard have reported high diagnostic accuracy, with 100% specificity. Furthermore, patients who were found to be amyloid-positive at PET with ^{18}F-Florbetapir exhibited progressive worsening in cognitive and functional status compared with those who were amyloid-negative. However, as for the other β-amyloid imaging agents, differences in scan interpretation can determine significant variability in diagnostic accuracy. The use of SUVRs and semiautomated software for quantification reduces inter-reader variability in image interpretation.

4-[(E)-2-(4-{2-[2-(2-^{18}F-fluoroethoxy)ethoxy]ethoxy}phenyl)vinyl]-N-methylaniline (or *^{18}F-Florbetaben*, approved for commercial use as NeuraCeq) is a polyethylene glycol stilbene derivative with high specificity for β-amyloid plaques without binding to tau protein, to tissue from frontotemporal lobe dementia, or brain tissue from dementing patients with Lewy bodies. Phase III trials have demonstrated that ^{18}F-Florbetaben PET imaging can identify amyloid deposition in the prodromal phase of AD and has high diagnostic accuracy (comparable to that of PET with ^{11}C-PiB or [^{18}F] FDG) in the identification of AD. Interestingly, a study in patients with multiple sclerosis demonstrated decreased uptake in the white matter affected by the disease, thus opening new horizons in amyloid imaging.

In addition to the three commercially available radiopharmaceuticals described above, PET radiotracers targeting aggregated forms of tau protein have been developed. The ideal tau PET tracer should display high selectivity for tau aggregates associated with low/absent binding to β-amyloid plaques. Selective radiotracers for tau aggregates have been described, such as *7-[6-^{18}F-fluoro-3-pyridinyl]-5H-pyrido[4,3-b]indole* (or *^{18}F-flortaucipir*), ^{18}F-T807, ^{18}F-T808, and ^{18}F-THK5351. Evidence is emerging that the binding patterns observed with PET in various neurodegenerative disorders reflect the clinical and histopathological progression of the specific disease. The most widely employed ^{18}F-flortaucipir has a 25-fold greater binding affinity to tau than to β-amyloid plaques and very low white matter binding. Therefore, PET with ^{18}F-flortaucipir displays high imaging contrast between deposits of tau aggregates and background. Autoradiography studies of post-mortem tissues have consistently reported a strong binding affinity of ^{18}F-flortaucipir to tau in AD, in contrast to its much weaker binding affinity to straight filament tau in non-AD tauopathies. However, the kinetic pattern of ^{18}F-flortaucipir binding in vivo is relatively slow, thus causing the SUVR values to increase even after 60 min postinjection; this kinetic feature limits the reproducibility of quantitative estimates. ^{18}F-Flortaucipir also exhibits a high affinity for melanin-producing cells, including the substantia nigra, skin, retinal pigment epithelium, and melanomas. These distinct patterns of tau-selective radiotracer binding suggest a potential role of ^{18}F-flortaucipir as an imaging biomarker in different disease conditions, both neurodegenerative diseases and non-CNS diseases.

Key Learning Points

- ^{11}C-Pittsburgh compound B, an analog of thioflavin T, has been the first radiotracer developed for PET imaging of β-amyloid plaques.
- ^{11}C-PiB has been employed PET for clinical investigations on brain amyloid and Alzheimer's disease, with high diagnostic sensitivity.
- ^{18}F-Flutemetamol, ^{18}F-Florbetapir, and ^{18}F-Florbetaben have been recently introduced as ^{18}F-labeled radiotracers for imaging amyloid deposition.
- These radiotracers have demonstrated high diagnostic accuracy in the identification of β-amyloid brain accumulation in the prodromal phase of neurodegenerative disorders.
- ^{18}F-Flortaucipir is the most widely employed PET radiotracer for in vivo imaging of tau aggregates in the human brain and melanin-producing cells.

3.2.9 Tissue Hypoxia Imaging Agents

Besides conditions linked to insufficient blood supply to normal organs (e.g., the brain and heart), hypoxia is a common feature of solid cancers. In fact, uncontrolled growth of tumor tissue may not be mirrored by adequate vascularization, so that the core of the mass more distant from newly formed blood vessels at the growing edge of the tumor becomes hypoxic and fre-

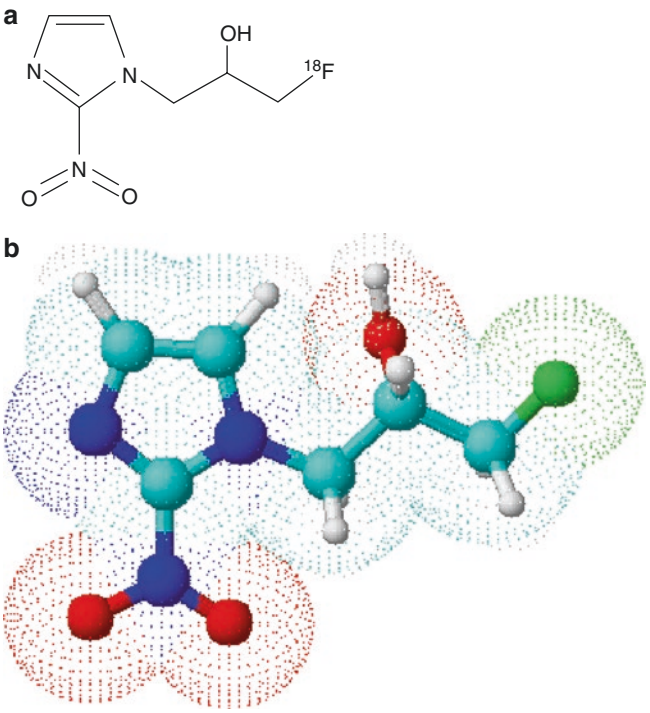

Fig. 3.27 Chemical structure (**a**) and tridimensional molecular representation (**b**) of ^{18}F-Fluoroimidazole (^{18}F-FMISO). Color codes of constituting elements: *red*, O; *gray*, H; *light blue*, C; *deep blue*, N; *green*, ^{18}F (*reproduced with permission from: Volterrani D, Erba PA, Mariani G, eds. Fondamenti di medicina nucleare – Tecniche e applicazioni. Milan: Springer; 2010*)

quently necrotic. Hypoxia induces a metabolic shift toward glucose consumption, promotes angiogenesis and cancer invasiveness, and also causes resistance to radiotherapy and chemotherapy. Although several different PET probes have been described to image tissue hypoxia, which constitutes an appealing target for molecular imaging, *^{18}F-fluoroimidazole* (*^{18}F-FMISO*; see Fig. 3.27) remains the radiotracer most extensively investigated. The other PET agents evaluated to image tissue hypoxia include the nitroimidazole family (e.g., ^{18}F-FAZA, ^{18}F-HX4-25183380, ^{18}F-EF5-112500504, ^{18}F-EF3-6918571) or compounds based on methylthiosemicarbazone incorporating a copper atom, such as copper(II)-diacetyl-bis(N^4-methylthiosemicarbazone) (ATSM) or copper-pyruvaldehyde-bis(N^4-methylthiosemicarbazone) (PTSM), that can be labeled with different positron-emitting copper radionuclides (i.e., ^{60}Cu, ^{62}Cu, or ^{64}Cu). However, most of these novel PET tracers have not progressed through all the phases of clinical validation.

Through passive transmembrane diffusion, ^{18}F-FMISO enters cells where it is reduced by nitroreductase enzymes to remain trapped in cells with reduced oxygen partial pressure. In fact, in normally oxygenated cells, the parent compound is quickly re-oxydated, and the resulting metabolites diffuse back to the extracellular compartment. Whereas, in hypoxic cells the low oxygen partial pressure prevents re-oxidation of ^{18}F-FMISO metabolites, thus resulting in tracer accumulation. Since ^{18}F-FMISO only accumulates in hypoxic cells with functioning nitroreductase enzymes, the uptake of this radiotracer can be considered an index of both tissue hypoxia and tissue viability.

Hypoxia imaging with PET can help optimize radiation therapy planning by identifying radioresistant regions of hypoxia in the tumor. Unfortunately, PET imaging with these radiotracers suffers from some important limitations. In particular, PET scanners have a spatial resolution in the order of mm, while tumor hypoxia is a cellular phenomenon with a micrometer scale. Moreover, PET probes accumulate only in viable tissue whose density may be very low in marked hypoxia. Finally, uptake of these radiotracers is due to passive transmembrane diffusion, and the blood pool activity remains high for several hours, thus reducing imaging quality and requiring delayed acquisition of PET images in order to obtain quantitative estimations. Despite these limitations, clinical studies performed in patients with head and neck or lung cancers have demonstrated the ability to quantify hypoxia and to predict patient prognosis. Thus, PET imaging remains one of the few possible strategies to investigate in vivo hypoxia and to provide comprehensive description of tumor hypoxic states and hence better guide clinical assessment and therapy design.

Key Learning Points

- ^{18}F-Fluoroimidazole is the most extensively investigated PET agent to image tissue hypoxia.
- ^{18}F-FMISO enters cells where it is reduced by nitroreductase enzymes to remain trapped in cells with reduced oxygen partial pressure.
- Hypoxia imaging with PET is highly promising for the choice of optimal treatments and therapy individualization, in particular during radiation therapy planning.

3.2.10 Neoangiogenesis Imaging Agents

In order for tumors to grow and metastasize, cancers must stimulate the development of new vasculature (neoangiogenesis). Unlike normal blood vessels, tumor blood vessels are chaotic, irregular, and leaky, which leads to irregular delivery of nutrients and therapeutic agents to the cancer mass. Tumor vasculature is emerging as an important target for anticancer therapy, and clinical trials in various malignancies are ongoing to assess the efficacy of antiangiogenic therapy with monoclonal antibodies against vascular endothelial growth factor (VEGF), a central mediator of angiogenesis. For example, HuMV833 (a humanized anti-VEGF monoclo-

nal antibody) has been labeled with ^{124}I and investigated in a phase 1 clinical trial.

After preliminary investigations in experimental animal models, another anti-VEGF antibody, bevacizumab, has been labeled with ^{89}Zr for PET imaging in patients with breast cancer, ovarian cancer, neuroendocrine tumors, renal cell carcinoma, and brain gliomas. Preliminary results suggest that *^{89}Zr-bevacizumab* PET imaging might be useful as an early predictive biomarker for anti-VEGF-directed treatment. Moreover, in small animal studies, ^{64}Cu-DOTA-VEGF121 has exhibited fast, specific uptake in highly vascularized tumors with a prominent level of VEGFR-2 expression.

Integrins constitute a superfamily of transmembrane receptors that mediate cell-to-cell adhesion. Among other functions, integrin-mediated adhesion modulates signaling cascades that control cell motility, survival, proliferation, and differentiation. Imaging based on integrin-derived agents has a great potential, as they play important roles in tumor metastasis and angiogenesis.

Currently, the most extensively studied integrin system is $\alpha_v\beta_3$, a receptor for vitronectin primarily expressed on the surface of platelets but also involved in the activation of phagocytosis by macrophages and dendritic cells. This receptor, which is also overexpressed on the activated endothelial cells of tumor neovasculature and on most tumor cells, binds to the arginine-glycine-aspartic acid (RGD)-containing components of the extracellular matrix, which are significantly upregulated in tumor vasculature. Specific PET tracer agonists to this receptor have been developed, including *^{64}Cu-DOTA-PEGEcRGDyK2* and *^{18}F-galacto-RGD*. ^{18}F-Galacto-RGD successfully imaged $\alpha_v\beta_3$ expression in human tumors, with good tumor-to-background ratio and highly promising results in patients with breast and lung cancers, sarcomas, and other solid tumors. However, the synthesis of ^{18}F-Galacto-RGD is a rather complex radiochemistry process, which has so far hampered its broad use in large clinical studies. The novel PET probe called *^{18}F-fluciclatide* (chemically defined as Ac(1)-Lys(Unk)-Cys(2)-Arg-Gly-Asp-Cys(2)-Phe-Cys(1)-Unk) contains two RGD sequences and has great potential for imaging to assess response to anti-angiogenic therapy. Promising results have been obtained with this tracer in patients with various malignancies (including breast, brain, lung, and thyroid cancers, as well as melanomas and sarcomas), and ^{18}F-fluciclatide is expected to become commercially available in the near future for PET imaging of $\alpha_v\beta_3$ expression.

Key Learning Points

- PET offers the unique possibility to image in vivo angiogenesis associated with tumor growth.
- ^{89}Zr-bevacizumab PET imaging is promising as an early predictive biomarker for anti-neoangiogenic-directed treatment.
- ^{64}Cu-DOTA-PEGEcRGDyK2 and ^{18}F-galacto-RGD are specific PET tracer agonists of $\alpha_v\beta_3$ receptor that is overexpressed on the activated endothelial cells of tumor neovasculature and on most tumor cells.
- ^{18}F-fluciclatide is a novel PET probe for $\alpha_v\beta_3$ expression that has provided promising results in various malignancies.

3.2.11 Apoptosis Imaging Agents

Cells undergoing apoptosis express phosphatidylserine on the outer leaflet of their cell membrane. Annexin V, an endogenous human protein with a high affinity for phosphatidylserine, has been radiolabeled with both single-photon and PET radionuclides (^{99m}Tc and ^{18}F). The feasibility of imaging with annexin V has been evaluated in small-sized studies in humans.

Novel small-molecule probes included in the ApoSense family (which can be defined as a novel technology for functional molecular imaging) have been designed to detect the complex cellular alterations occurring during apoptosis. Among such nuclear probes, *2-(5-^{18}F-fluoro-pentyl)-2-methyl-malonic acid* (or *^{18}F-ML-10*, Fig. 3.28) is the first PET radiopharmaceutical for molecular imaging of apoptosis that has demonstrated promising results in several small-scale clinical trials. In particular, increased uptake of ^{18}F-ML-10 has been observed on PET/CT imaging in patients with brain metastases treated with radiation therapy, although with some heterogeneity in uptake intensity within the tumor mass. Although the precise mechanism of radiotracer uptake

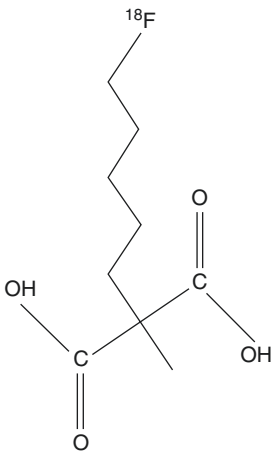

Fig. 3.28 Chemical structure of 2-(5-^{18}F-fluoro-pentyl)-2-methyl-malonic acid (^{18}F-ML-10)

remains unclear, these findings illustrate the potential of ^{18}F-ML-10 as a PET radiopharmaceutical for clinical imaging of apoptosis in tumors.

Caspases are a family of intracellular cysteine proteases that are responsible for the initiation and execution of apoptosis. In particular, caspase-3/7 is an attractive biological marker for apoptosis. Clinical trials with promising results are ongoing with the use of ^{18}*F-CP18*, the first PET radiopharmaceutical developed for imaging of apoptosis based on a substrate for caspase-3/7.

Key Learning Points

- 2-(5-^{18}F-fluoro-pentyl)-2-methyl-malonic acid is a PET radiopharmaceutical developed for molecular imaging of apoptosis that has demonstrated promising results in human cancers.
- ^{18}F-CP18 is the first radiotracer developed for PET imaging based on a substrate for caspase, a family of intracellular proteases associated with apoptosis.

Further Reading

Barthel H, Sabri O. Clinical use and utility of amyloid imaging. J Nucl Med. 2017;58:1711–7.

Barwick T, Bencherif B, Mountz JM, Avril N. Molecular PET and PET/CT imaging of tumour cell proliferation using F-18 fluoro-L-thymidine: a comprehensive evaluation. Nucl Med Commun. 2009;30:908–17.

Baum RP, Rösch F. Theranostics, gallium-68, and other radionuclides: a pathway to personalized diagnosis and treatment. Berlin: Springer Science & Business Media; 2012.

Beer AJ, Kessler H, Wester H-J, Schwaiger M. PET imaging of integrin $\alpha_v\beta_3$ expression. Theranostics. 2011;1:48–57.

Bouchelouche K, Turkbey B, Choyke PL. PSMA PET in prostate cancer – a step towards personalized medicine. Curr Opin Oncol. 2016;28:216–21.

Brown J. Effects of 2-deoxyglucose on carbohydrate metabolism: review of the literature and studies in the rat. Metabolism. 1962;11:1098–112.

Chacko A-M, Divgi CR. Radiopharmaceutical chemistry with iodine-124: a non-standard radiohalogen for positron emission tomography. Med Chem. 2011;7:395–412.

Choi Y, Ha S, Lee YS, Kim YK, Lee DS, Kim DJ. Development of tau PET imaging ligands and their utility in preclinical and clinical studies. Nucl Med Mol Imaging. 2018;52:24–30.

Chondrogiannis S, Marzola MC, Al-Nahhas A, Venkatanarayana TD, Mazza A, Opocherand G, et al. Normal biodistribution pattern and physiologic variants of F-DOPA PET imaging. Nucl Med Commun. 2013;34:1141–9.

Christensen NL, Jakobsen S, Schacht AC, Munk OL, Alstrup AKO, Tolbod LP, et al. Whole-body biodistribution, dosimetry, and metabolite correction of [^{11}C]palmitate: a PET tracer for imaging of fatty acid metabolism. Mol Imaging. 2017;16:1–9.

Croteau E, Renaud JM, Richard MA, Ruddy TD, Bénard F, et al. PET metabolic biomarkers for cancer. Biomark Cancer. 2016;8(Suppl 2):61–9.

DeGrado TR, Reiman RE, Price DT, Wang S, Coleman RE. Pharmacokinetics and radiation dosimetry of ^{18}F-fluorocholine. J Nucl Med. 2002;43:92–6.

Doss M, Kolb HC, Walsh JC, Mocharla V, Fan H, Chaudhary A, et al. Biodistribution and radiation dosimetry of ^{18}F-CP-18, a potential apoptosis imaging agent, as determined from PET/CT scans in healthy volunteers. J Nucl Med. 2013;54:2087–92.

Driessen RS, Raijmakers PG, Stuijfzand WJ, Knaapen P. Myocardial perfusion imaging with PET. Int J Cardiovasc Imaging. 2017;33:1021–31.

Eckelman WC, Boyd M, Mairs RJ. Principles of molecular targeting for radionuclide therapy. In: Strauss HW, Mariani G, Volterrani D, Larson SM, editors. Nuclear oncology – from pathophysiology to clinical applications. New York, NY: Springer; 2017. p. 35–66.

Ell PJ, Gambhir SS, editors. Nuclear medicine in clinical diagnosis and treatment. 3rd ed. New York, NY: Churchill Livingston; 2004.

Elsinga PH. Trends on the role of PET in drug development. Singapore: World Scientific; 2012.

Feinendegen LE, Shreeve WW, Eckelman WC, Bahk YW, Wagner HN Jr. Molecular nuclear medicine: the challenge of genomics and proteomics to clinical practice. Berlin: Springer Science & Business Media; 2012.

Filss CP, Cicone F, Shah NJ, Galldiks N, Langen KJ. Amino acid PET and MR perfusion imaging in brain tumours. Clin Transl Imaging. 2017;5:209–23.

Gaykema SB, Brouwers AH, Lub-de Hooge MN, Pleijhuis RG, Timmer-Bosscha H, Pot L, et al. ^{89}Zr-bevacizumab PET imaging in primary breast cancer. J Nucl Med. 2013;54:1014–8.

Grassi I, Morigi JJ, Nanni C, Fanti S. FDG and other radiopharmaceuticals in the evaluation of liver lesions. Clin Transl Imaging. 2014;2:115–27.

Hara T. ^{18}F-fluorocholine: a new oncologic PET tracer. J Nucl Med. 2001;42:1815–7.

Herbert JC, Eckelman WC, Neumann RD, editors. Nuclear medicine – diagnosis and therapy. New York, NY: Thieme Medical Publishers; 1996.

Herholz K, Ebmeier K. Clinical amyloid imaging in Alzheimer's disease. Lancet Neurol. 2011;10:667–70.

IAEA. Good practice for introducing radiopharmaceuticals for clinical use. Vienna: International Atomic Energy Agency (IAEA); 2015.

IAEA. Operational guidance on hospital radiopharmacy. Vienna: International Atomic Energy Agency (IAEA); 2008.

Ido T, Wan CN, Casella V, Fowler JS, Wolf AP, Reivich M, et al. Labeled 2-deoxy-D-glucose analogs: ^{18}F-labeled 2-deoxy-2-fluoro-D-glucose, 2-deoxy-2-fluoro-D-mannose and ^{14}C-2-deoxy-2-fluoro-D-glucose. J Labeled Compounds Radiopharm. 1978;24:174–83.

Itsenko O, Goméz-Vallejo V, Llop J, Koziorowski J. On ^{11}C chemistry reviews – surveying and filling the gaps. Curr Organ Chem. 2013;17:2067–96.

Jacobson O, Kiesewetter DO, Chen X. Fluorine-18 radiochemistry, labeling strategies and synthetic routes. Bioconjug Chem. 2015;26:1–18.

Khalil MM. Basic science of PET imaging. New York, NY: Springer; 2016.

Klingensmith WC III. The mathematics and biology of the biodistribution of radiopharmaceuticals – a clinical perspective. New York, NY: Springer; 2016.

Knaapen P, de Haan S, Hoekstra OS, Halbmeijer R, Appelman YE, Groothuis JG, et al. Cardiac PET-CT: advanced hybrid imaging for the detection of coronary artery disease. Neth Heart J. 2010;18:90–8.

Kowalsky RJ, Falen SW, editors. Radiopharmaceuticals in nuclear pharmacy and nuclear medicine. 3rd ed. Washington, DC: American Pharmacists Association; 2011.

Kuik WJ, Kema IP, Brouwers AH, Zijlma R, Neumann KD, Dierckx RAJO, et al. In vivo biodistribution of no-carrier-added 6-^{18}F-fluoro-3,4-dihydroxy-L-henylalanine (^{18}F-DOPA), produced by a new nucleophilic substitution approach, compared with carrier-added ^{18}F-DOPA, prepared by conventional electrophilic substitution. J Nucl Med. 2015;56:106–12.

Kwekkeboom DJ, Kam BL, van Essen M, Teunissen JJ, van Eijck CH, Valkema R, et al. Somatostatin-receptor-based imaging and therapy of gastroenteropancreatic neuroendocrine tumors. Endocr Relat Cancer. 2010;17:R53–73.

Lappin G, Temple S. Radiotracers in drug development. Boca Raton, FL: CRC Press; 2006.

Lütje S, Heskamp S, Cornelissen AS, Poeppel TD, van den Broek SAMW, Rosenbaum-Krumme S, et al. PSMA ligands for radionuclide imaging and therapy of prostate cancer: clinical status. Theranostics. 2015;5:1388–401.

Lyoo CH, Cho H, Choi JY, Ryu YH, Lee MS. Tau positron emission tomography imaging in degenerative parkinsonisms. J Mov Disord. 2018;11:1–12.

Mach RH. Small molecule receptor ligands for PET studies of the central nervous system — focus on G protein coupled receptor. Semin Nucl Med. 2017;47:524–35.

Maddahi J, Packard RR. Cardiac PET perfusion tracers: current status and future directions. Semin Nucl Med. 2014;44:333–43.

Martínez G, Vernooij RW, Fuentes Padilla P, Zamora J, Bonfill Cosp X, Flicker L. ^{18}F PET with florbetapir for the early diagnosis of Alzheimer's disease dementia and other dementias in people with mild cognitive impairment (MCI). Cochrane Database Syst Rev. 2017;(11):CD012216. https://doi.org/10.1002/14651858.CD012216.pub2.

Martínez G, Vernooij RW, Fuentes Padilla P, Zamora J, Flicker L, Bonfill CX. ^{18}F PET with flutemetamol for the early diagnosis of Alzheimer's disease dementia and other dementias in people with mild cognitive impairment (MCI). Cochrane Database Syst Rev. 2017;(11):CD012884. https://doi.org/10.1002/14651858.CD012884.

Martínez G, Vernooij RW, Fuentes Padilla P, Zamora J, Flicker L, Bonfill CX. ^{18}F PET with florbetaben for the early diagnosis of Alzheimer's disease dementia and other dementias in people with mild cognitive impairment (MCI). Cochrane Database Syst Rev. 2017;11:CD012883. https://doi.org/10.1002/14651858.CD012883.

Mathis CA, Mason NS, Lopresti BJ, Klunk WE. Development of positron emission tomography β-amyloid plaque imaging agents. Semin Nucl Med. 2012;42:423–32.

Mertens K, Slaets D, Lambert B, Acou M, De Vos F, Goethals I. PET with ^{18}F-labelled choline-based tracers for tumour imaging: a review of the literature. Eur J Nucl Med Mol Imaging. 2010;37:2188–93.

Molecular Imaging and Contrast Agent Database (MICAD) – NCBI – NIH. Accessible at https://www.ncbi.nlm.nih.gov/books/NBK5330/.

Morris E, Chalkidou A, Hammers A, Peacock J, Summers J, Keevil S. Diagnostic accuracy of ^{18}F amyloid PET tracers for the diagnosis of Alzheimer's disease: a systematic review and meta-analysis. Eur J Nucl Med Mol Imaging. 2016;43:374–85.

Mossine AV, Brooks AF, Jackson IM, Quesada CA, Sherman P, Cole EL, et al. Synthesis of diverse ^{11}C-labeled PET radiotracers via direct incorporation of [^{11}C]CO2. Bioconjug Chem. 2016;27:1382–9.

Nagengast WB, de Vries EG, Hospers GA, Mulder NH, de Jong JR, Hollema H, et al. In vivo VEGF imaging with radiolabeled bevacizumab in a human ovarian tumor xenograft. J Nucl Med. 2007;48:1313–9.

Núñez Miller R, Pozo MA. Non-FDG PET in oncology. Clin Transl Oncol. 2011;13:780–6.

Orsini F, Lorenzoni A, Puta E, Mariani G. Positron-emitting radiopharmaceuticals for diagnostic applications. In: Strauss HW, Mariani G, Volterrani D, Larson SM, editors. Nuclear oncology – from pathophysiology to clinical applications. New York, NY: Springer; 2017. p. 85–98.

Owunwanne A, Patel M, Sadek S, editors. The handbook of radiopharmaceuticals. New York, NY: Springer; 1995.

Pauwels EK, Ribeiro MJ, Stoot JH, McCready VR, Bourguignon M, Mazière B. FDG accumulation and tumor biology. Nucl Med Biol. 1998;25:317–22.

Price EW, Orvig C. Matching chelators to radiometals for radiopharmaceuticals. Chem Soc Rev. 2014;43:260–90.

Price TW, Greenman J, Stasiuk GJ. Current advances in ligand design for inorganic positron emission tomography tracers ^{68}Ga, ^{64}Cu, ^{89}Zr and ^{44}Sc. Dalton Trans. 2016;45:157092–724.

Reivich M, Kuhl D, Wolf A, Greenberg J, Phelps M, Ido T, et al. Measurement of local cerebral glucose metabolism in man with ^{18}F-2-fluoro-2-deoxy-D-glucose. Acta Neurol Scand Suppl. 1977;64:190–1.

Rice SL, Roney CA, Daumar P, Lewis JS. The next generation of positron emission tomography radiopharmaceuticals in oncology. Semin Nucl Med. 2011;41:265–82.

Sandström M, Velikyan I, Garske-Román U, Sörensen J, Eriksson B, Granberg D, et al. Comparative biodistribution and radiation dosimetry of ^{68}Ga-DOTATOC and ^{68}Ga-DOTATATE in patients with neuroendocrine tumors. J Nucl Med. 2013;54:204–10.

Sarparanta M, Demoin DW, Cook BE, Lewis JS, Zeglis BM. Novel positron-emitting radiopharmaceuticals. In: Strauss HW, Mariani G, Volterrani D, Larson SM, editors. Nuclear oncology – from pathophysiology to clinical applications. New York, NY: Springer; 2017. p. 129–72.

Schelhaas S, Heinzmann K, Bollineni VR, Kramer GM, Liu Y, Waterton JC, et al. Preclinical applications of 3′-deoxy-3′-[^{18}F]fluorothymidine in oncology – a systematic review. Theranostics. 2017;7:40–50.

Schuster DM, Nanni C, Fanti S. PET tracers beyond FDG in prostate cancer. Semin Nucl Med. 2016;46:507–21.

Sols A, Crane RK. Substrate specificity of brain hexokinase. J Biol Chem. 1954;210:581–95.

Som P, Atkins HL, Bandoypadhyay D, Fowler JS, MacGregor RR, Matsui K, et al. A fluorinated glucose analog, 2-fluoro-2-deoxy-D-glucose (F-18): nontoxic tracer for rapid tumor detection. J Nucl Med. 1980;21:670–5.

Strauss HW, Mariani G, Volterrani D, Larson SM, editors. Nuclear oncology – from pathophysiology to clinical applications. New York, NY: Springer; 2017.

Subramanian G, Rhodes BA, Cooper JF, Sodd VJ. Radiopharmaceuticals. Society of Nuclear Medicine: New York, NY; 1975.

Theobald T, editor. Sampson's textbook of radiopharmacy. 4th ed. London: Pharmaceutical Press; 2010.

Trembath L, Newell M, Devous MD Sr. Technical considerations in brain amyloid PET imaging with ^{18}F-Florbetapir. J Nucl Med Technol. 2015;43:175–84.

Podoloff DA, et al. NCCN task force: clinical utility of PET in a variety of tumor types. J Natl Compr Canc Netw. 2009;7(Suppl 2):S1–S26.

Vallabhajosula S. Molecular imaging – radiopharmaceuticals for PET and SPECT. Berlin-Heidelberg: Springer; 2009.

van Asselt SJ, Oosting SF, Brouwers AH, Bongaerts AH, de Jong JR, Lub-de Hooge MN, et al. Everolimus reduces ^{89}Zr-bevacizumab tumor uptake in patients with neuroendocrine tumors. J Nucl Med. 2014;55:1087–92.

Varrone A, Asenbaum S, Vander Borght T, Booij J, Nobili F, Någren K, et al. EANM procedure guidelines for PET brain imaging using [^{18}F]FDG, version 2. Eur J Nucl Med Mol Imaging. 2009;36:2103–10.

Villemagne VL, Doré V, Burnham SC, Masters CL, Rowe CC. Imaging tau and amyloid-β proteinopathies in Alzheimer disease and other conditions. Nat Rev Neurol. 2018;14:225. https://doi.org/10.1038/nrneurol.2018.9.

Wang X, Feng H, Zhao S, Xu J, Wu X, Cui J, et al. SPECT and PET radiopharmaceuticals for molecular imaging of apoptosis: from bench to clinic. Oncotarget. 2017;8:20476–95.

Warburg O, Wind F, Negelein E. The metabolism of tumors in the body. J Gen Physiol. 1927;8:519–30.

Waxman AD, Herholz K, Lewis DH, Herscovitch P, Minoshima S, Ichise M, et al. Society of nuclear medicine procedure guideline for FDG PET brain imaging. Version 1.0, approved February 8, 2009. Accessed at www.snmmi.org.

Welch MJ, Redvanly CS, editors. Handbook of radiopharmaceuticals: radiochemistry and applications. Hoboken, NJ: Wiley; 2003.

Wick AN, Drury DR, Nakada HI, Wolfe JB. Localization of the primary metabolic block produced by 2-deoxyglucose. J Biol Chem. 1957;224:963–9.

Wild D, Bomanji JB, Benkert P, Maecke H, Ell PJ, Reubi JC, Caplin ME. Comparison of ^{68}Ga-DOTANOC and ^{68}Ga-DOTATATE PET/CT within patients with gastroenteropancreatic neuroendocrine tumors. J Nucl Med. 2013;54:364–72.

Xia C, Dickerson BC. Multimodal PET imaging of amyloid and tau pathology in Alzheimer disease and non-Alzheimer disease dementias. PET Clin. 2017;12:351–9.

Xu Z, Li XF, Zou H, Sun X, Shen B. ^{18}F-Fluoromisonidazole in tumor hypoxia imaging. Oncotarget. 2017;8:94969–79.